5-2022

Wetland Uranium Transport via Iron-Organic Matter Flocs and Hyporheic Exchange

Connor J. Parker
cparke4@clemson.edu

WETLAND URANIUM TRANSPORT VIA IRON-ORGANIC MATTER FLOCS AND HYPORHEIC EXCHANGE

A Dissertation
Presented to
the Graduate School of
Clemson University

In Partial Fulfillment
of the Requirements for the Degree
Doctor of Philosophy
Environmental Engineering & Earth Sciences

---

by
Connor Joseph Parker
May 2022

Accepted by:
Brian A. Powell, Committee Chair
Daniel I. Kaplan
Nicole E. Martinez
Lawrence Murdoch

ABSTRACT

Uranium (U) released from the M-Area at the Department of Energy Savannah River Site into Tims Branch, a seasonal wetland and braided stream system, is estimated to be 43,500 kg between 1965 and 1984. The motivation for this work is the uranium's persistence in the wetland for decades, where it is estimated that 80% of the U currently remains in the Tims Branch wetland. U has begun to incorporate into wetland iron (Fe) and carbon cycles, associating with local Fe mineralogy and deposits of rich wetland organic matter (OM). The objective of this work is to characterize the chemical phases responsible for sequestration or mobilization of U, Fe, and C in a riparian wetland system and to understand the partitioning and lability of uranium incorporated into natural Fe and C cycles. Born from the observation of Fe-OM flocs under specific hydrologic conditions, it is hypothesized that the mobilization of Fe-OM flocs drive U transport from the wetland as U incorporates into the wetland cycles. This work first investigates the lateral distribution of U within the wetland and identifies key hotspots where U has accumulated due to hydrologic and geochemical controls. With knowledge of these hotspots, work sought to identify relationships of U to Fe and OM throughout the wetland in the water column and as a function of depth at the hotspots. Next, these relationships to Fe and OM were investigated further via parallel extraction of redox-preserved cores in oxic and anoxic atmospheres. This study determined that OM concentrations coupled with OM compound diversity heavily impact metal sequestration and availability in wetland sediments. Deep sediment layers with relatively non-labile OM accumulate metals naturally, as isotopic ratio evidence indicates that sequestration of natural U is occurring in addition to accumulation of anthropogenic depleted U. With an improved understanding of the metal inventories in the wetland, a seasonal study of metal transport allowed for initial estimates of seasonal U and Ni

transport associated with Fe-OM flocs. Fluxes of U in Fe-OM flocs can be conservatively estimated to be of minimal risk to water quality, as worst-case assumptions and measurements pre- and post-storm determine that flocs would have mobilized only 132 kg U over the last 60 years. Currently, stream sediments are now hypothesized to be the primary driver of U transport from the wetland, but these U fluxes only amount to roughly 20 kg per year, based on stream flowrate data collection and stream water sampling.

ACKNOWLEDGMENTS

Thank you first and foremost to my advisor, Dr. Brian A. Powell. You have shaped me into the researcher I am today, and your support and confidence in me helped me pursue my passion for the environment. Thank you to my committee—Drs. Kaplan, Martinez, and Murdoch—for challenging me, helping me produce the best work possible and grow along the way. Thank you to Dr. Kathryn Peruski, whose support as a mentor and as a friend helped me make the most of graduate school.

I would also like to acknowledge the various offices that have funded the projects that I have worked on, including U.S. Department of Energy Office of Science, Office of Basic Energy Sciences and Office of Biological and Environmental Research, and Savannah River Remediation.

TABLE OF CONTENTS

Page

LIST OF TABLES

Page

LIST OF FIGURES

Page

I. INTRODUCTION

The goal of this work is to narrow knowledge gaps surrounding the nexus of uranium (U), iron (Fe), and organic matter (OM) in wetlands, specifically the Tims Branch wetland at the DOE Savannah River Site (SRS). Broadly speaking, this work aims to better 1) quantify the current inventory of U in the wetland, 2) identify the chemical speciation of U at key hydrologic interfaces where both transport and accumulation may be occurring, and 3) the relationship and interactions between U and OM on a molecular scale. Wetlands commonly immobilize and sequester metals, behaving as the geochemical "kidneys of the earth" and remediating waters passing through a wetland ecosystem. Currently, we see this occurring with the U process waste released in the mid- to late-20th century, which remains relatively consolidated, but a strong association between Fe, U, and OM has become apparent in preliminary studies (Parker et al 2022, Kaplan, et al 2020). Redox gradients present in wetlands influence U mobility by dictating the aqueous and solid phases U speciation. Investigating the transport vectors that move these three constituents—especially iron-rich flocs observed readily in Tims Branch exclusively in oxidizing conditions—helps inform our understanding of how these reservoirs evolve over decadal scales.

Uranium geochemical behavior and environmental mobility is of paramount importance in understanding its role as a risk driver at geologic waste repositories and behavior at contaminated sites. Wetlands provide a unique canvas for investigating U mobility, as U from natural minerals, process wastes, and nuclear production waste streams commonly end up in wetlands. As a naturally occurring element, U has always been present in our geosphere but became an innovation focal point during the nuclear revolution of the mid-20th century and the development of the atomic bomb. As such, the EPA tolerates a 30 ppb (U.S. EPA) maximum

contamination level for drinking water, compared to a lower tolerance for some other anthropogenic contaminants. As a heavy metal toxin and an alpha emitter, U poses the greatest risk to human health when inside the body, which leads to risk assessment of U contaminations to focus on pathways which could introduce U into the body. This work investigates U geochemical transport behaviors in surface and subsurface waters of a tributary to the Savannah River, a major surface water pathway in the Southeastern United States.

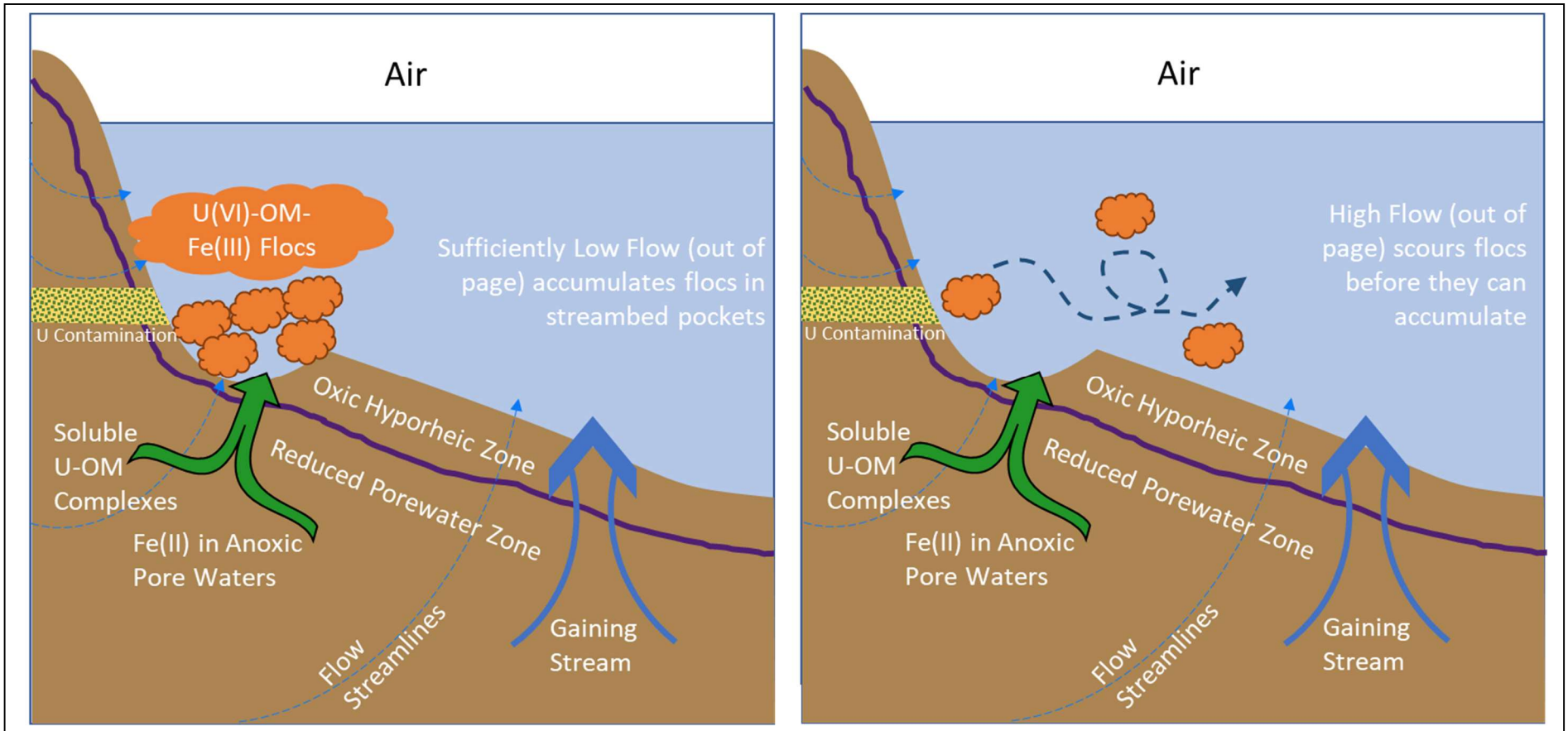

Figure 1 - 1: Conceptual model for floc formation in the Steed Pond reaches of Tims Branch, with the low stream velocity case on the left and the high stream velocity case on the right.

Process waste release events between 1965 and 1988 introduced U and other metals to the wetland while the 1984 Steed Pond dam failure exposed former pond sediments to streamwaters leaving the watershed (Evans, et al. 1992). As such, this system behaves as both a primary and secondary source, continually releasing material from the original deposition zone downgradient as well as exposing material formerly settled in the pond to downgradient transport. Prior studies (Szalay, 1964, Yang, et. al., 2012, Yang, et. al., 2013) have posited interactions between U and naturally occurring OM, noting uranium's high binding affinity for OM and the potential uses of wetland OM as a reductant to encourage immobilization by sorption or precipitation. Additionally, Fe is an essential component of biogeochemical cycling, and microbes and local flora produce siderophores for extracting Fe from mobile or immobile phases. The complex nature of OM—particularly wetland soil OM—results in a void in literature regarding the association of metals with soluble soil OM and aggregate stabilization in stream systems. The proposed work, while still merely providing an empirical categorization of OM and any metal-OM complexes, seeks to determine how U and Fe are reacting with particular categories of OM and refine the conceptual model for vectors of U transport in the wetland. Figure 1 - 1 shows how these processes change as a function of high and low flowrate in the stream. Flow from the subsurface brings porewaters from the anoxic, reduced zone into the oxic hyporheic zone and ultimately into the stream, where flocs formed when Fe(II) oxidizes into Fe(III) either settle in pockets of the streambed or are scoured away in high flow before the opportunity to settle.

The three projects encompassed in this work aim to sequentially investigate smaller spatial scales and make rough estimates of temporal transport of U from the Tims Branch

wetland. Figure 1 - 2 uses concentric boxes to highlight the ways the studies expand on one another and continue to improve the community's understanding of U sequestration in Tims Branch. The main priorities of this work are to create an updated inventory of U in the wetland since the initial release events, characterize the incorporation of U into Fe and OM pools in redox-preserved soil cores, and understand the interactions of U, Fe, and OM in U transport downgradient over the course of a year. While U is not currently a primary risk driver for water quality surrounding the Savannah River, investigating these knowledge gaps will ultimately inform risk assessors as current U deposits are accounted and future U releases can be monitored and understood more effectively.

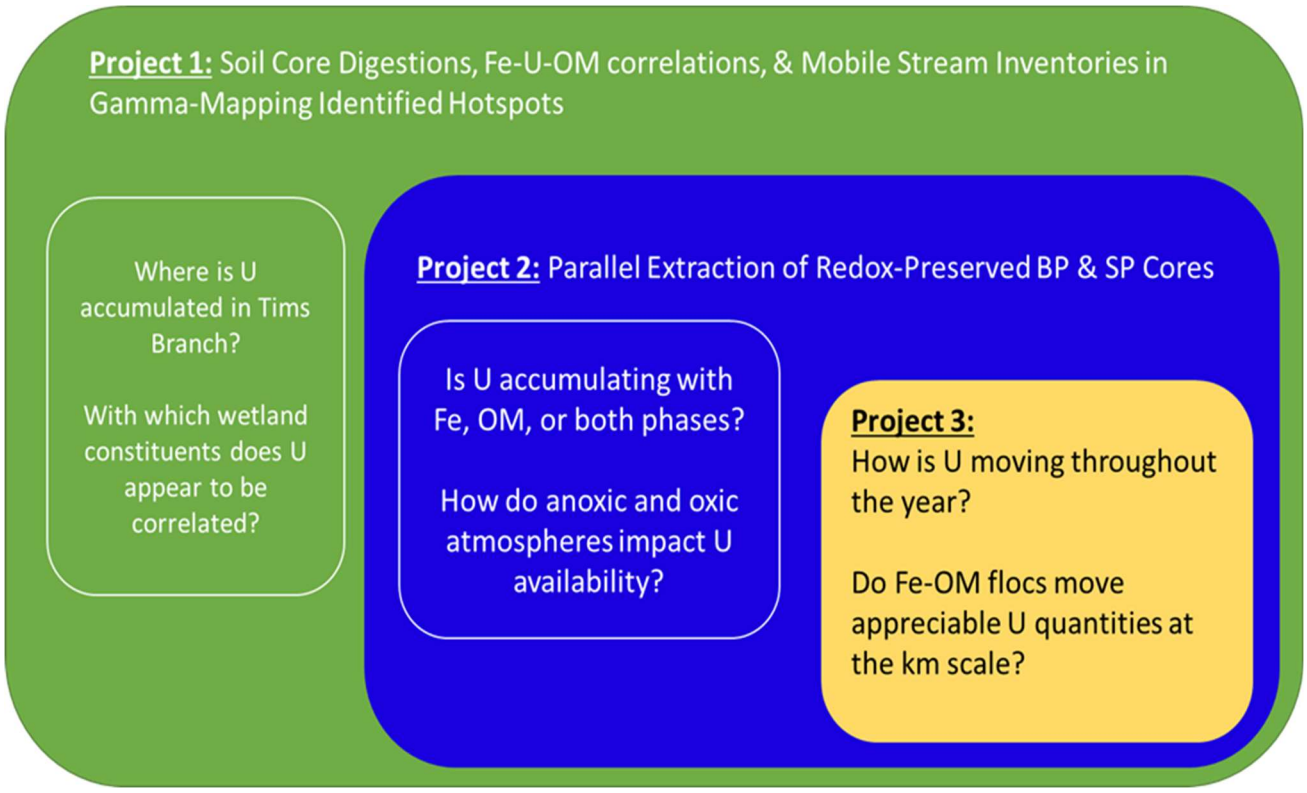

Figure 1 - 2: Concentric boxes that depict the roles of each project related to one another. Project 1 aims to identify where U has accumulated in Tims Branch. Project 2 will investigate impacts of redox speciation and selective extractants on pools of U in preserved sediment cores collected from Steed Pond (SP) and Beaver Pond (BP). Project 3 will study U transport over the course of a year and identify the associations of U with Fe and OM in the flocs observed at Steed Pond.

II. BACKGROUND

Actinides

Uranium (U) is a naturally occurring radioactive element used both in the nuclear fuel and weapons production industries. Following use in these sectors, U and other actinides like neptunium (Np) and plutonium (Pu) must be stored as high-level radioactive waste; in lieu of reprocessing, the United States currently stores its waste in either vadose zone storage tanks or subsurface disposal sites (like WIPP, New Mexico's Waste Isolation Pilot Plant). Alternatively, the ultimate goal of a centralized geologic repository for geologic and engineered storage controls could sequester nuclear waste for thousands of years if approved and constructed. To effectively and safely store these waste products, the scientific community must sufficiently understand environmental actinide mobility and reactivity to accurately model risk to ecosystems and human health, ensuring that waste storage facilities will not pose significant damages and danger following the lifetime of its creators. From a radiation detection perspective, the four dominant isotopes of U are ^{238}U, ^{235}U, ^{234}U, in order of abundance with ^{233}U being an anthropogenic decay daughter (Allard, et al., 1984). While each isotope has a characteristic alpha decay emission, the common method of detecting enrichment and percent compositions in environmental samples is to detect the daughter products of each isotope, as these are distinguishable and have gamma emission energies more easily detected than the alpha emissions unless samples are purified and prepared for alpha spectroscopy. Efficient detection of U in the environment allows researchers to analyze U from both a chemical and radiological perspective, where one method may better suit a sampling scheme or field site. For example, in this work field based gamma spectroscopy will be used to map the distribution of uranium in the Tims Branch wetland at the SRS.

Oxidation states govern the environmental reactivity and mobility of the actinides, with the complexation affinity of each state increasing with increasing effective charge on the central atom. Actinides in the An(V) and An(VI) oxidation states are ordinarily coordinated by two axial oxygens to form the AnO_2^+ and AnO_2^{+2} cations, respectively. This leads to the trend:

$$An(IV)>An(VI)\sim An(III)>An(V)$$

With An(IV) having the greatest ligand and sorption affinity and An(V) having the lowest affinity (Silva and Nitsche, 1995). Conversely, the trend reverses for environmental mobility, with An(V) species being most labile and An(IV) being least mobile. An(VI) and An(V) each have an average coordination of 3.2 and 2.2, respectively, when the axial oxygens are accounted for, leading to their positions in this trend (Silva and Nitsche, 1995). While Pu readily forms all four of these oxidation states in environmentally relevant E_H and pH values (Kim, 1986), U only forms the U(IV) and U(VI) species, as the U(V) species is unstable and rapidly disproportionates in aqueous solutions (Morse and Choppin, 1991). As such, U(IV) is often immobile as a sorbed or precipitated species and U(VI) is mobile as the uranyl aquo ion or in a mobile aqueous complex (Silva and Nitsche, 1995).

Uranium minerals are relatively insoluble in circumneutral pH values observed in natural waters. Mobilization of aqueous U complexed by various ligands is of more concern than U oxide or oxyhydroxide minerals behaving as a source term. The precipitation of uranium minerals is one approach in remediation efforts, as alkaline reducing conditions precipitate amorphous U(IV) hydroxides (Neck and Kim, 2001). When conditions are reducing and slightly acidic, U^{+4} ions readily sorb to mineral surfaces as the tetravalent species or as a subsequent hydrolysis product when pH approaches neutral to alkaline conditions (Silva and Nitsche, 1995). Likewise, alkaline oxidizing conditions with high carbonate concentrations induce mobile

uranyl-carbonate complexes (Silva and Nitsche, 1995), but this scenario is more relevant to carbonate-rich systems like the Rifle Site in CO where the goal is to precipitate $CaCO_3$ to remove nearly all carbonate by allowing microbes to produce increased pH and oxidizing conditions (Yabusaki, et. al., 2011). The U plume at the Rifle Site currently consists of U bound in fine-grained naturally reducing zones with rich sulfur mineralogy, so removing the main mobile ligand—the local carbonate—reduces U mobility (Janot et al., 2016). Thus, environmental conditions that are of highest concern are systems with low or high pH, as sorption is strongest at midrange pH values. At SRS, U transport is often characterized by transport on colloidal or suspended particle surfaces in a surface water pathway rather than a flow of uranyl ion (Batson et al., 1996).

Hydrologic Transport

The two main environmental compartments that are most relevant to this work are surface waters such as streams and standing bodies of water (ponds, lakes) and groundwater, predominantly the porewater saturating portions of the wetland. Currently focusing on streams as primary surface water compartments, exchange between groundwater and surface water occurs in the hyporheic zone, the saturated mixing zone between the subsurface and a stream. The hyporheic zone includes the stream floor and all streambanks saturated with water (Jolly et al., 2008). The equivalent mixing zone between groundwater and the atmosphere is the vadose zone, where unsaturated soil above the water table is subject to percolation from the surface, presence of air in soil pores, and fluctuations of the groundwater table. The relevant "hill" when discussing groundwater-surface water interactions is the hydraulic gradient, which is the flow of water induced by head differences. When a stream is under losing stream conditions, the groundwater is subject to recharge, where the stream feeds into the subsurface via hyporheic

exchange; the stream stage is higher than the water table, so the pressure gradient resolves by flowing from the stream into the subsurface (Jolly et al., 2008). Inversely, a stream is under gaining conditions when the water table is higher than the stream stage and groundwater discharges via the hyporheic zone. While some studies may aim to quantify these fluxes with seepage meters, strategically placed piezometers, and tracer tests (Kalbus et al., 2006), this work will investigate some of these flow measurements with respect to the adjacent hyporheic cross-sections, not necessarily for the entire wetland.

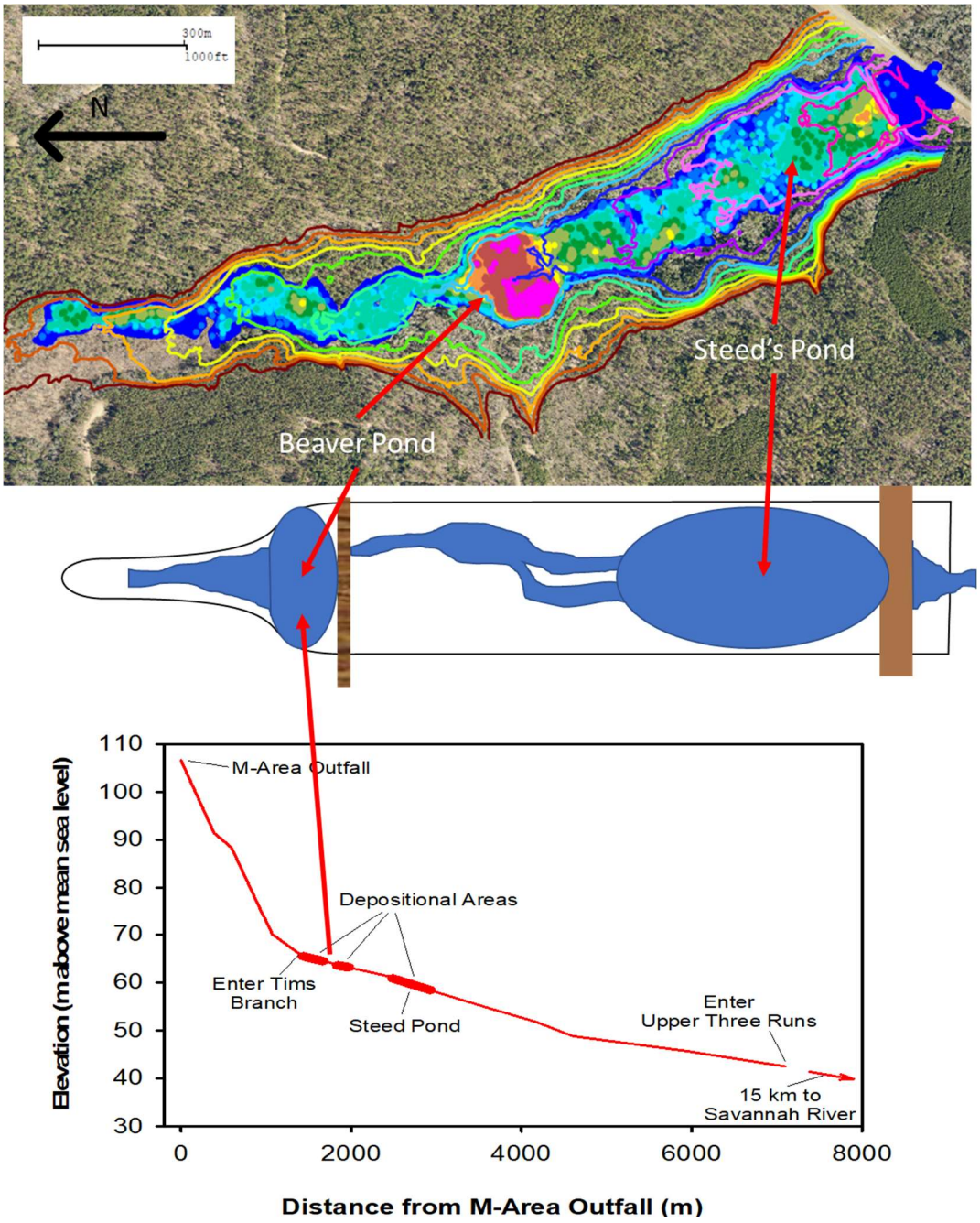

Figure 2-1: Gamma count rate heat map corresponding to Uranium activity, including LIDAR 1-m lines (top), corresponding to the conceptual model schematic (middle), and elevation as a function of distance from the A-014 Outfall (bottom).

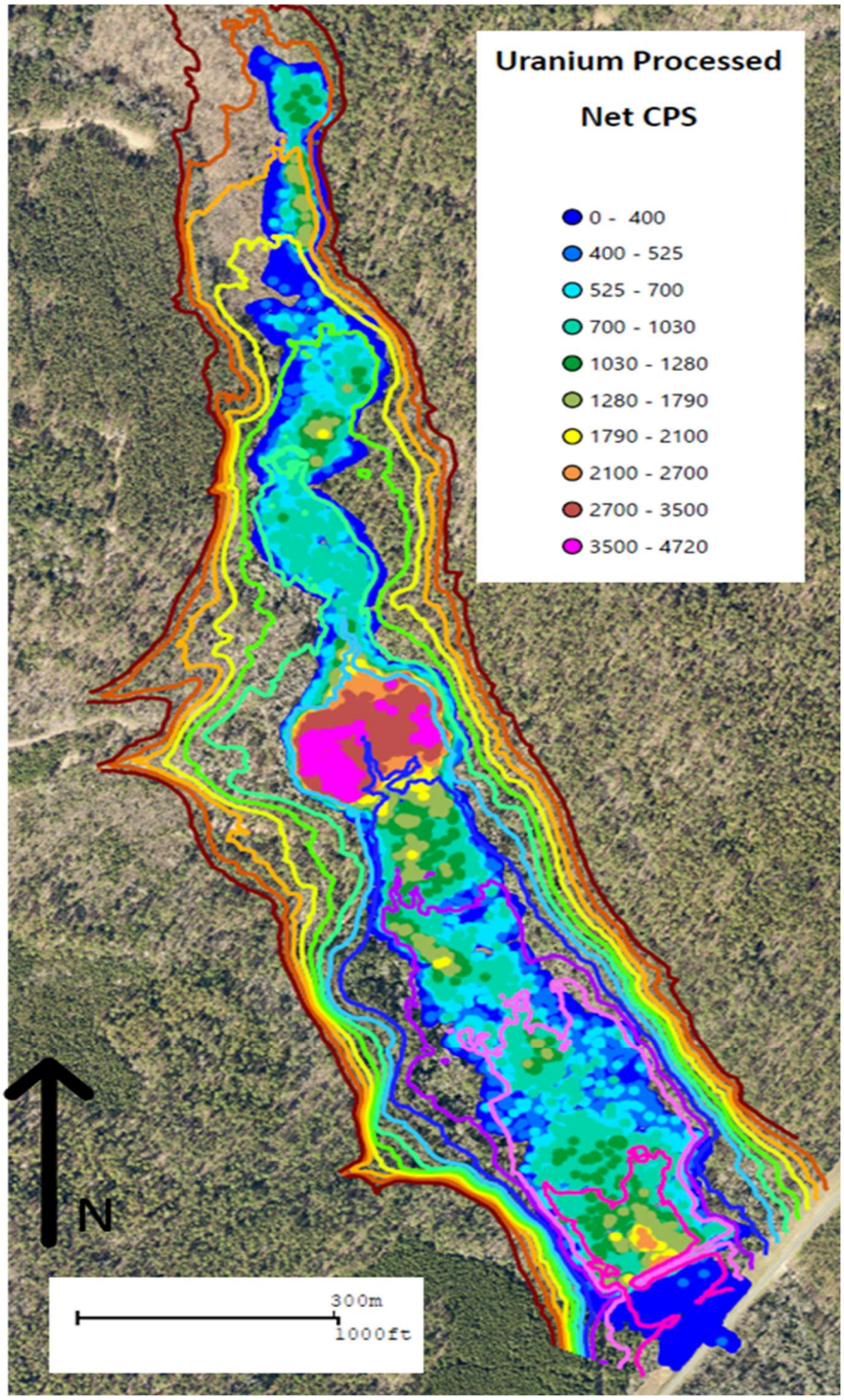

Figure 2-2: LIDAR map of 1-m elevation topographic lines for the Tims Branch wetland, and gamma countrate heatmap.

The Rifle Site in Colorado remains a testbed for U remediation research in an aquifer with well-characterized groundwater flow and conductivity (Janot et al., 2016; Yabusaki et al., 2011). However, while it is well-characterized, the subsurface still displays a significant degree of heterogeneity. At the Rifle Site, researchers have studied the predominance of "hotspots," sections of the aquifer that have high concentrations of U and increased microbial activity, leading to heterogenous sections of the aquifer where concentrations deviate from the surrounding matrix. Capturing hotspots accurately in models is critical, as coarse sampling or modeling grids may entirely miss these and misrepresent the local concentration profile, while fine sampling and modeling grids are inefficient to sample and computationally expensive to model. Studying field sites with contaminations is an important platform to move between two distinct spatial scales. Laboratory experiments often study high concentration sources in highly controlled systems. Meanwhile, in field experiments there are fewer controlled variables and more hotspots—either "hot" in concentration or "hot" in hydraulic conductivity—that can render large scale hydrogeochemical transport unpredictable.

The DOE Site vital to this work is the Savannah River Site, most notably the Tims Branch braided stream system and seasonal wetland. From 1965 to 1988, the M-Area Fuel Fabrication Facility released process waste from the A-014 outfall, which joins the Tims Branch system after flowing through a narrow, steep channel. Figure 2-1 shows how the stream opens up into the flat wetland floodplain after the channel widens and the slope reduces, while Figure 2-2 shows just the LIDAR topographic data and the gamma countrate heatmap with the intensity legend. Nearly 43,500 kg of U were released from this outfall during this time period, and most material remained in the initial deposition area derived from a combination of effluent, and other suspended solids. With the reduced velocity at the entrance to the wetland, the increased reaction

time and settling velocity created accumulation conditions with the reactive Fe and OM present. However, downstream was Steed's Pond, a defunct farming pond preceding DOE custody of the land, which contained much of the transported U; sediments and particulates settled here with an approximate 3-day hydraulic residence time (Evans et al., 1992). However, in 1984, the dam broke, allowing both the U bound to settled particles and any U transported from upgradient to leave the watershed. Prior characterization of the aquifer and the surrounding SRS geology has helped refine the relevant local geochemistry and potentially reactive mineral surfaces, expected local soil pH values, and anticipated redox conditions that play a role in the transport of Fe, U, and OM. The entire timeline of Tims Branch processes and the relevant conceptual diagrams for each period of the wetland's history are highlighted in Figure 2-3. Tims Branch and the rest of SRS are located in the Upper Coastal Plains in a sandy-clay, clayey-sand aquifer (Kaplan et al., 1994), resulting in relatively high hydraulic conductivities, iron-rich sediments, and reactive mineral surfaces. Understanding the coupled transport of OM, Fe, and U in Tims Branch is the focal point of this work, as the accumulation of U associated with Fe and OM can help fill knowledge gaps in interaction processes and the transport of these constituents throughout a watershed.

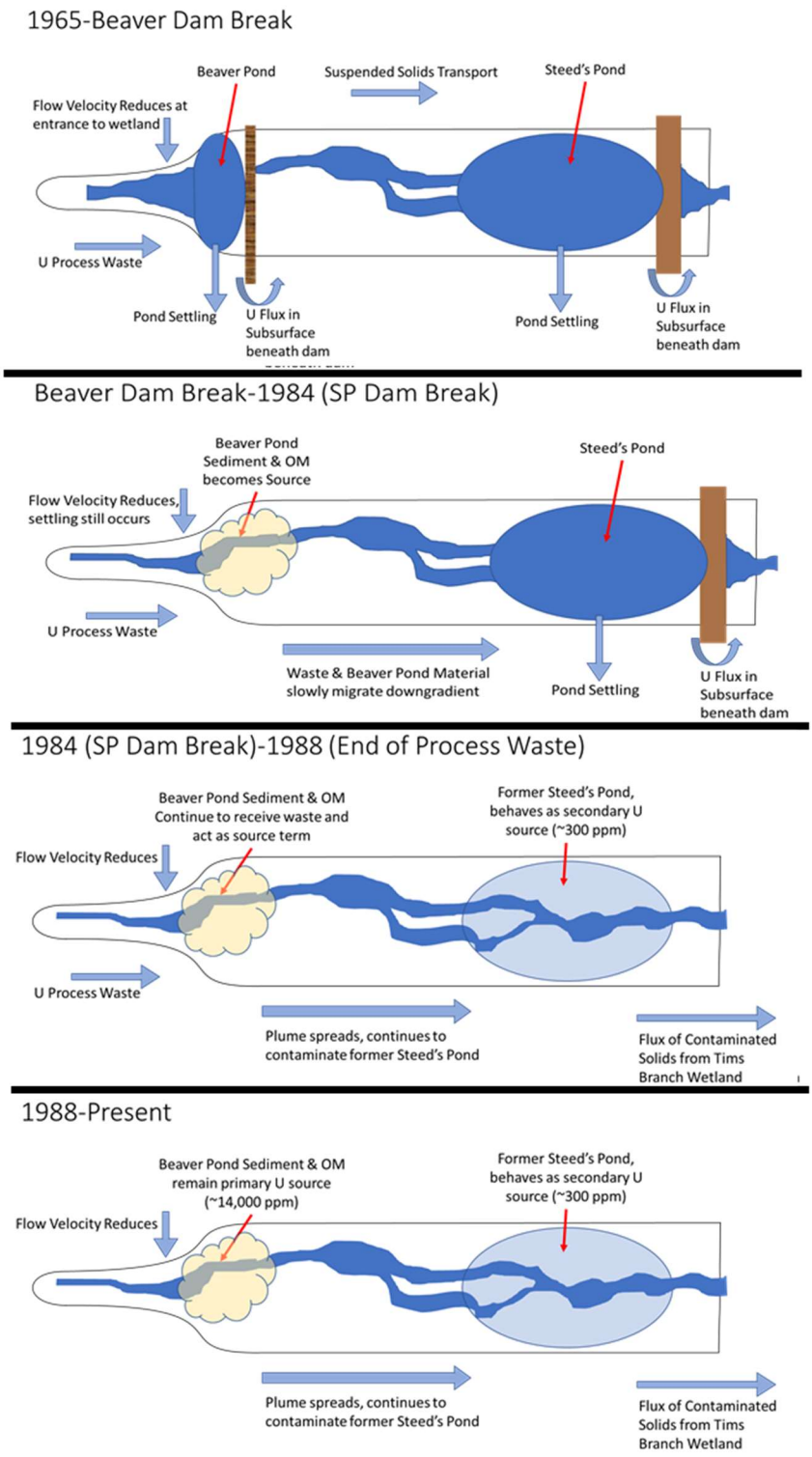

Figure 2-3: Conceptual model for the chronology of Tims Branch and the relevant hydrogeochemical processes.

In both surface water transport and wastewater treatment, settling and sedimentation are key fluxes responsible for the removal of constituents from the water flow (Brown and Lawler, 2003). Meanwhile, in both subsurface transport and wastewater treatment, residence time governs the degree of reaction between constituents and the surrounding matrix (Conn and Fiedler, 2006). While not being applied to wastewater in this work, many of the principles of sedimentation and residence time associated with wastewater treatment relate to the flow characteristics of this system. Applied to wetlands, these three processes heavily impact the mobility of dissolved constituents and suspended particulate matter in transport pathways. As a corollary to wastewater treatment, wetlands are often described as "the kidneys of the earth," and understanding how metals accumulate and are immobilized is an important aspect of the hydrologic transport. Settling and sedimentation refer to the settling of suspended particles in low-flow regimes, and Steed's Pond accumulated appreciable sediment during its lifetime (Dixon et al., 1996). Suspended sediment grains, organic colloidal species, and particulate metals from the process waste are three noteworthy categories comprising the suspended solid pathway for U in the wetland (Evans et al., 1992). U can potentially adhere to suspended sediments or organic colloids and be mobilized downgradient in the surface water; this results in accelerated surface water U transport as the primary transport vector in the wetland.

Wetlands

Wetlands are operationally partially defined as ecosystems where the soil is saturated for at least two weeks during the region's growing season each year. This definition leads to varied site-specific wetland characteristics around the country, as a wetland in Maine could be hydrogeochemically different from a wetland in South Carolina, but both are still considered wetlands. However, what remains is that wetlands are ecosystems where the earth is saturated

amidst the year's highest flux of water into plants; the precipitation and subsurface can sustain this water-use demand. The seasonality—or permanence—of saturation in wetlands dictates how active microbes can be and what geochemical conditions will be present as metals flow through the wetland. A slow flowing, constantly saturated wetland would likely exhibit relatively more acidic, reducing characteristics, while a wetland that meets the minimum requirement to be a hydric wetland soil would demonstrate more frequent fluctuations between oxidizing and reducing conditions in the vadose zone. While the subsurface saturation and hydric soils may define a wetland, the presence of stream channels introduces oxygen via hyporheic exchange where oxygen otherwise would not be present, and these streams allow for the transport of geochemical species—both aqueous and sorbed to suspended solids—at a rate often faster than subsurface flow.

Heavy metal accumulation in wetlands has led to the use of constructed wetlands as a remediation technique; while Tims Branch is not a constructed wetland, constructed wetlands are a testament to the ability of wetlands to sequester and accumulate metals without significant harm to the surrounding ecosystem (Conn and Fiedler, 2006; Persson et al., 1999). Commonly, wetlands begin to remediate contaminations of metals including Pb, Ni, Co, and Cr, all of which are relatively redox active in the environment (Masscheleyn et al., 1992). As is observed in the Tims Branch wetland, U has accumulated here, and the surface water channels have rendered subsurface U flow negligible: while there is a dominant hydraulic gradient in the wetland, surface flow represents most of the hydrologic flux through the wetland, and U in the sediment and porewaters remains relatively immobile except for hyporheic exchange. Redox-active U falls under the umbrella of metals often remediated in wetlands and impacted by reactivity of OM, and, while U is not an essential micronutrient like Fe, U and Fe remain subject to the redox

potentials induced by microbial communities and the sorption processes occurring in OM deposits. As a parallel to the wetland redox activity of U, chromium can be remediated by wetlands and demonstrates how microbes and Fe-oxide minerals can reduce soluble Cr(VI) to insoluble, immobile Cr(III), rendering waters downstream of the wetland clean and wholly remediated (Masscheleyn et al., 1992). The coupling of Fe geochemistry and microbial activity in wetlands allows for the remediation and immobilization of metals at many sites; preliminary data indicates that U has followed suit in the Tims Branch wetland but still releases some U downgradient in surface waters.

Focusing on the interactions between U and wetland constituents, U mobility is reduced by both OM and Fe in wetlands. Szalay reports findings of U accumulation in peat sediments rich in characteristic humic substances (Szalay, 1964); while it is an isolated sorption experiment, the experimental conditions appear sound and reproduceable, and there is marked accumulation of U onto the humics, yielding an accumulation factor of up to 10,000x. This accumulation is in line with other literature (Yang et al., 2012), as humics have been observed as a primary carrier of wetland contaminant metals Pb, Cr, U, and other rare-earth elements in a study of wetland metal release that aimed to differentiate effects of Fe(III) mineral reduction and OM deposits on metal mobility (Grybos et al., 2007). Cumberland, et. al., provide a thorough review of the geochemical processes involved in U transport with respect to OM deposits (Cumberland et al., 2016), biomineralization and incorporation of U, and relevant solubilities of mineral categories either including U in their structure or providing constituents necessary to mobilize or immobilize U in subsurface pathways. Yang, Saiers, and Barnett (Yang et al., 2013) demonstrate the coupling of U sorption with pure intrinsic metal-oxide colloids and humic acid colloids, highlighting that carboxyl functional groups of humic acid colloids played a significant

role in interactions between heterogenous Fe-oxide colloids and U introduced to the system. While these studies indicate the affinity for interactions between U, OM, and Fe, no single study answers this complex question, and the body of literature requires further research to fill this knowledge gap.

Organic Matter

Wetlands are rich in a wide variety of organic molecules as byproducts of microbial processes, decay of leaflitter, and release of plant exudates, but characterizing and labeling all organic products in wetlands would be an insurmountable task. Humus, the soil constituent responsible for the addition of geochemically available organics, is broken down over time to form humic acid and other reactive organics defined operationally by their molecular size and environmental reactivity (Sutton and Sposito, 2005). Humification refers to the systematic breakdown of cellulose and other macromolecule "building blocks" that make up the organic matter observable in the field, and microbial and fungal enzymes facilitate humification (Lehmann and Kleber, 2015). While many of these enzymes and their digestive mechanisms have been characterized, the wide variety of macromolecules present are all subject to these processes, and the enzymes can interact with molecules multiple times and at multiple stages of the breakdown process (Schmidt et al., 2011). Due to the nature of enzyme-catalyzed hydrolysis, a parcel of OM can contain stable cellulose, mobile organic acids, and all interstitial degradation products; the coexistence of these organic moieties results in myriad reactive sites in soil OM (Schmidt et al., 2011).

Humic acid, humus, and fulvic acids are all defined operationally, where humic acid is the fraction of organic matter that can be extracted in alkaline conditions, humus represents the overall total solids that derive humic acids, and fulvic acid comprises the remaining dissolved,

mobile extractable organics. Currently, this operationally defined humification process focuses on properties of the classes of molecules present in the humus; Schmidt, et al, posit that humification should be a function of the ecosystem, not the resulting molecules (Schmidt et al., 2011). Considering this approach, humification is no longer classified by precise soil conditions and generalizations about site conditions; rather, it can be assumed that all decay processes are capable of occurring when the right inputs are available from leaflitter, rhizosphere exudates, and microbial metabolic byproducts and the right conditions exist. Applying this perspective to the OM in Tims Branch, there may be macromolecules present that are resistant to decay and decomposition solely because the necessary enzymes are not present, rendering them available as a reactive "surface site" for metal contaminants but wholly immobile. Likewise, conditions created in upper layers of the topsoil may produce redox conditions below 30 cm for microbial communities to produce enzymes necessary for the creation of mobile, fragmented organic molecules, but applying wholesale "decay rates" to the entire body of wetland soil would be inappropriate given that these rates may fluctuate based on conditions of other layers. While not a particularly satisfying explanation, the synthesis of this notion with the perspective on OM posed by Sutton and Sposito (Sutton and Sposito, 2005) and the Soil Continuum Model (Lehmann and Kleber, 2015; Schmidt et al., 2011) leads researchers to approach OM holistically, treating each site differently and assuming any humification pathways are possible when the correct reactants are present. The Soil Continuum Model addresses soil OM as a spectrum, where larger macromolecules are constantly degrading into smaller products that partition to mineral surfaces and other geochemically relevant reactive sites (Lehmann and Kleber, 2015; Schmidt et al., 2011). Considering the Soil Continuum Model explains why Tims Branch exhibits such a diversity of immobile OM species and dissolved, mobile OM species with no correlation

between geochemical conditions, depth, and soil composition; all of them are achieving constantly shifting equilibria as geochemical conditions change on a local (i.e. centimeter) scale.

Focusing more on organics that represent common behaviors across the many organics found in humus, generic ligands and siderophores include basic organic building blocks such as acetate and oxalate, up to the larger chain synthetic polymers such as polyaspartic acid (PAA). When comparing the utility of various organic ligands as chelating agents and agents of mineral dissolution like siderophores, the general size and functional groups of molecules are most important, rather than the ecosystem conditions posited above. Polydentate ligands, such as citric acid, have multiple binding sites by which to complex a metal, while monodentate ligands simply have one site. Thus, binding simultaneously to multiple sites decreases the likelihood of a metal leaving the ligand altogether; applying this principle to long-chain, macromolecular complexes explains why a large fraction of semidecayed humus would retain metals well. Likewise, metals bound to a bidentate or higher order chelating agent that fragments from a larger macromolecule during humification would be labile in porewaters and available for hyporheic exchange to surface water pathways.

Synthesizing all four categories of literature review, organic colloids, hereby referred to as “flocs,” represent an important transport pathway in the Tims Branch wetland and other hyporheic exchange zones between oxic and anoxic compartments. Flocs typically refer to the coagulated, amorphous particulates during water treatment processes, where alum is added to catalyze the settling of unwanted aqueous constituents via coprecipitation with amorphous aluminum oxides. However, this flocculation process is not exclusive to water treatment, as it is observed in environmental field sites with different geochemical constituents and catalysts as well. Lapworth and Stolpe (Lapworth et al., 2013) characterize groundwater Fe-OM colloids in

both oxic and anoxic sampling systems as well as observing aggregation of colloids upon oxidation with an atomic force micrograph. Further, Pokrovsky and Schott (Pokrovsky and Schott, 2002) study the incorporation of contaminant metals into colloidal field samples at various surface water bodies and the associated filterable/filtered fractions of metals in each compartment; smaller metals more prone to existing as a cationic aqueous species were less likely to incorporate, but larger ions and trace elements demonstrated a high propensity for coprecipitating with iron oxides in the midst of colloidal OM species. Finally, Wang (Wang et al., 2013) characterizes U(IV) mobility and incorporation with both inorganic and organic colloids, the latter being composed of Fe and OM and representing a significant fraction of the U mobilizing from the porewater into the wetland braided stream and ultimately out of the wetland. While U(IV) is not directly observed in flocs in the Tims Branch system, understanding mechanisms by which U can incorporate into OM colloids alongside Fe helps build the literature knowledge surrounding U transport via hyporheic exchange.

References

Allard, B., U. Olofsson, and B. Torstenfelt, *Environmental Actinide Chemistry.* Inorganica Chimica Acta-F-Block Elements Articles and Letters, 1984. **94**(4): p. 205-221.

Batson, V.L., Bertsch, P.M. and Herbert, B.E. (1996) Transport of Anthropogenic Uranium from Sediments to Surface Waters During Episodic Storm Events. Journal of Environmental Quality 25, 1129-1137.

Brown, P.P. and Lawler, D.F. (2003) Sphere Drag and Settling Velocity Revisited. Journal of Environmental Engineering 129, 222-231.

Conn, R.M. and Fiedler, F.R. (2006) Increasing Hydraulic Residence Time in Constructed Stormwater Treatment Wetlands with Designed Bottom Topography. Water Environment Research 78, 2514-2523.

Cumberland, S.A., Douglas, G., Grice, K. and Moreau, J.W. (2016) Uranium mobility in organic matter-rich sediments: A review of geological and geochemical processes. Earth-Science Reviews 159, 160-185.

Dixon, K.L., Rogers, V.A., Conner, S.P., Cummings, C.L., Gladden, J.B. and Weber, J.M. (1996) Geochemical and physical properties of wetland soils at the Savannah River site. Savannah River Site (SRS), Aiken, SC.

Evans, A.G., Bauer, L.R., Haselow, J.S., Hayes, D.W., Martin, H.L., McDowell, W.L. and Pickett, J.B. (1992) Uranium in the Savannah River Site Environment, Aiken, SC, pp. WSRC-RP-92-315.

Fritz, B.G., Kohn, N.P., Gilmore, T.J., McFarland, D., Arntzen, E.V., Mackley, R.D., Patton, G.W., Mendoza, D.P. and Bunn, A.L. (2007) Investigation of the hyporheic zone at the

300 Area, Hanford Site. Pacific Northwest National Lab.(PNNL), Richland, WA (United States).

Grybos, M., Davranche, M., Gruau, G. and Petitjean, P. (2007) Is trace metal release in wetland soils controlled by organic matter mobility or Fe-oxyhydroxides reduction? Journal of Colloid and Interface Science 314, 490-501.

Janot, N., Lezama Pacheco, J.S., Pham, D.Q., O'Brien, T.M., Hausladen, D., Noël, V., Lallier, F., Maher, K., Fendorf, S., Williams, K.H., Long, P.E. and Bargar, J.R. (2016) Physico-Chemical Heterogeneity of Organic-Rich Sediments in the Rifle Aquifer, CO: Impact on Uranium Biogeochemistry. Environmental Science and Technology 50, 46-53.

Jolly, I.D., McEwan, K.L. and Holland, K.L. (2008) A review of groundwater-surface water interactions in arid/semi-arid wetlands and the consequences of salinity for wetland ecology. Ecohydrology 1, 43-58.

Kalbus, E., Reinstorf, F. and Schirmer, M. (2006) Measuring methods for groundwater - Surface water interactions: A review. Hydrology and Earth System Sciences 10, 873-887.

Kaplan, D.I., Bertsch, P.M., Adriano, D.C. and Orlandini, K.A. (1994) Actinide association with groundwater colloids in a Coastal Plain aquifer. Radiochimica Acta 66-67, 181-187.

Kim, J.I., *Chemical behaviour of transuranic elements in natural aquatic systems*, in *Handbook on the Physics of the Actinides*, A.J. Freeman and C. Keller, Editors. 1986, Elsevier Science Publishers B. p. 413-455.

Lapworth, D.J., Stolpe, B., Williams, P.J., Gooddy, D.C. and Lead, J.R. (2013) Characterization of suboxic groundwater colloids using a multi-method approach. Environmental Science and Technology 47, 2554-2561.

Lehmann, J. and Kleber, M. (2015) The contentious nature of soil organic matter. Nature 528, 60-68.

Masscheleyn, P.H., Pardue, J.H., DeLaune, R.D. and Patrick, J.W.H. (1992) Chromium redox chemistry in a lower Mississippi Valley bottomland hardwood wetland. Environmental Science & Technology 26, 1217-1226.

Morse, J.W. and G.R. Choppin, *The Chemistry of Transuranic Elements in Natural-Waters.* Reviews in Aquatic Sciences, 1991. **4**(1): p. 1-22.

Neck, V. and Kim, J.I. (2001) Solubility and hydrolysis of tetravalent actinides. Radiochimica Acta 89, 1-16.

Persson, J., Somes, N.L.G. and Wong, T.H.F. (1999) Hydraulics Efficiency of Constructed Wetlands and Ponds. Water Science and Technology 40, 291-300.

Pokrovsky, O.S. and Schott, J. (2002) Iron colloids/organic matter associated transport of major and trace elements in small boreal rivers and their estuaries (NW Russia). Chemical Geology 190, 141-179.

Schmidt, M.W.I., Torn, M.S., Abiven, S., Dittmar, T., Guggenberger, G., Janssens, I.A., Kleber, M., Kögel-Knabner, I., Lehmann, J. and Manning, D.A.C. (2011) Persistence of soil organic matter as an ecosystem property. Nature 478, 49-56.

Silva, R.J. and Nitsche, H. (1995) Actinide Environmental Chemistry. Radiochimica Acta 70-71, 377-396.

Sutton, R. and Sposito, G. (2005) Molecular structure in soil humic substances: The new view. Environmental Science and Technology 39, 9009-9015.

Szalay, A. (1964) Cation exchange properties of humic acids and their importance in the geochemical enrichment of UO2++ and other cations. Geochimica et Cosmochimica Acta 28, 1605-1614.

Wang, Y., Frutschi, M., Suvorova, E., Phrommavanh, V., Descostes, M., Osman, A.A.A., Geipel, G. and Bernier-Latmani, R. (2013) Mobile uranium(IV)-bearing colloids in a mining-impacted wetland. Nature Communications 4, 1-9.

Yabusaki, S.B., Fang, Y., Williams, K.H., Murray, C.J., Ward, A.L., Dayvault, R.D., Waichler, S.R., Newcomer, D.R., Spane, F.A. and Long, P.E. (2011) Variably saturated flow and multicomponent biogeochemical reactive transport modeling of a uranium bioremediation field experiment. Journal of Contaminant Hydrology 126, 271-290.

Yang, Y., Saiers, J.E. and Barnett, M.O. (2013) Impact of interactions between natural organic matter and metal oxides on the desorption kinetics of uranium from heterogeneous colloidal suspensions. Environmental Science and Technology 47, 2661-2669.

Yang, Y., Saiers, J.E., Xu, N., Minasian, S.G., Tyliszczak, T., Kozimor, S.A., Shuh, D.K. and Barnett, M.O. (2012) Impact of natural organic matter on uranium transport through saturated geologic materials: From molecular to column scale. Environmental Science and Technology 46, 5931-5938.

III. OBJECTIVES, HYPOTHESES, & RESEARCH OUTCOMES

In order to address these knowledge gaps, some research questions must be developed to formulate objectives and testing hypotheses. Study 1 looks to determine the present-day distribution of U in the wetland for comparison with historical data. Literature provides a generic idea of wetland controls on metals, but Study 1 narrows this to a site-specific demonstration of U profiles in the wetland. Study 2 utilizes laboratory characterization of core samples to investigate the influence of U speciation on U distribution between the porewater and mineral surfaces, isolating what causes desorption from solid phases and potential migration. Study 3 further enriches the work by studying the field site biweekly over 9 months to investigate how geochemical gradients could influence mobilization and immobilization, specifically with regards to U associated with flocs. These three studies collectively identify geochemical processes that control U in the subsurface and at the hyporheic interface, acknowledging that sediment transport during overland flow is a potential option but is not within the scope of this work.

Study 1 focuses on the current inventory of U within the Tims Branch wetland. The objective of this study is to quantify the present-day distribution of U throughout the wetland. A revised qualitative conceptual model of U mobility will be developed based on comparison of the present-day U distribution with 1) the sparse amount of historical U data available and 2) the present-day concentrations of Fe and OM. These data will:

1. Identify regions where high U concentrations merit further sampling in future studies
2. Determine correlations between U, Fe, and OM concentrations to help inform a revised conceptual model of U migration in the wetland

It is hypothesized that U and Fe will be more concentrated where OM is most prevalent, whether this is a reservoir of long-accumulated immobile OM or dynamic, mobile, dissolved OM. Work will include radiation mapping of U deposits in the wetland and measurement of Fe, U and OM concentrations in soil cores retrieved from areas with elevated U concentrations. These data will be used to determine the total present-day inventory of U in the wetland and identify the relationship between U and key wetland constituents.

Study 2 focuses on core characterization from chemical speciation and soil property standpoints. The objective of Study 2 is to identify specific chemical phases with which U associates in the soil and identify conductive sediment beds within the core. Data resulting from these analyses will refine the conceptual model describing U distribution between the porewater and the mineral surfaces. Sampled from the same location of Study 3 field analyses, the Study 2 core will inform where potential high U concentration zones may be and their relationship to any conductive soil layers near the hyporheic interface. It is hypothesized that U will closely associate with the organic phase, where immobile OM solids retain U and segments of high water-extractable [U] also contain high dissolved OM. Further, it is hypothesized that there will be beds of sediments that are rich in water-extractable U. Specific geochemical experiments include a parallel variation on the redox-preserved sequential extraction outlined in Schultz 1998, while the main hydrologic experiment uses particle size analysis and localized hydraulic conductivity measurements to determine conductivity in all layers. These data will identify conductive soil layers and sections of high [U]. When conductive layers correspond to high [U] segments, these relationships will inform the ongoing development of the conceptual model for U reservoirs in the wetland. Research outcomes will be an extensive characterization of redox-preserved U speciation with depth in a soil core and the characterization of hydrologic soil

properties of each segment. These can be compared with future Study 3 data when further in situ field data are collected, as conductive bands through elevated U concentration zones may increase U-bearing floc formation at the hyporheic interface.

Study 3 is field-centric, studying sources of dissolved U entering the stream and becoming a part of the colloidal fraction in the Fe-OM flocs. The main question being answered with Study 3 and the accumulated work is "How is this colloidal floc fraction contributing to the overall transport of U?" and acknowledges that eroded sediment transport is likely also occurring but is not the focus of this study. It is hypothesized that all water-extractable U from Study 2 will be equivalently concentrated in the porewaters, and the flocs sampled from the stream will have incorporated nearly all porewater U. Additionally, it is hypothesized that the stream will be gaining, and conductive bands will dominate the flow of subsurface water through the hyporheic interface. Experiments in a meter-scale transect will include 1) the use of porewater sipper samplers to measure concentrations of wetland constituents in porewaters, 2) water column floc sampling to determine concentrations of U and Fe in flocs and stream solids, and 3) slug tests, piezometer measurements, and long-term stream flow monitoring to characterize the water flow at the specific field sampling site and begin to understand seasonal fluxes of U from the wetland. The primary expected research outcome is a confirmation that gaining stream conditions produce flocs in the stream and to what degree U incorporates into these flocs, thereby improving the community's understanding of one of the potential transport pathways by which U continues to move through the wetland.

IV. URANIUM PARTITIONING FROM CONTAMINATED WETLAND SOIL TO AQUEOUS AND SUSPENDED IRON-FLOC PHASES: IMPLICATIONS OF DYNAMIC HYDROLOGIC CONDITIONS ON CONTAMINANT RELEASE

Publication Status: Published in *Geochimica et Cosmochimca Acta*, 2022 (https://doi.org/10.1016/j.gca.2021.11.034)

Introduction

Wetland ecosystems host diverse geochemical redox gradients, dynamic biological activity, and a variety of hydrologic flow regimes. These factors create ideal conditions for heavy metal contamination remediation (Dean et al., 2013). Constructed wetlands often behave as idealized reactors for settling contaminated solids or using natural and imposed redox gradients to change the chemical form of heavy metals (Persson et al., 1999; Conn and Fiedler, 2006). Natural wetlands achieve the same result with anthropogenic releases, as the rich organic matter (OM) pool inherent to wetlands provides myriad reactive sorption sites, complexing agents, and ligands (Schmidt et al., 2011). Wetlands have demonstrated the ability to accumulate and immobilize many heavy metal contaminants including those that form surface reactive species under reducing conditions, such as Pb, Ni, Co, and Cr (Masscheleyn et al., 1992). Redox-active U has been shown to be immobilized in wetlands and impacted by OM reactivity (Sowder et al., 2003; Kaplan et al., 2017). Wetland OM is vital to metal cycling, as redox potentials induced by microbial activity and the sorption processes occurring in OM deposits both contribute to metal cycling (Powell et al., 1996; Yang et al., 2012; Wang et al., 2013; Pan et al., 2017). This work investigates the Tims Branch wetland at the Department of Energy (DOE) Savannah River Site (SRS) and the U contamination in and around former natural and man-made ponds.

Releases of U into Tims Branch began in 1965 when M-Area's Fuel Fabrication Facility manufactured target assemblies (Reed and Swanson, 2006). Effluent releases consisted primarily

of dissolved, colloidal, and particulate U phases from uranium fuel and target assembly activities (Evans et al., 1992). Effluents from the facility went to the A-14 tributary and then concentrated in Tims Branch, a riparian wetland downgradient of the facility. A steep grade change and widened stream channel going from the A-14 tributary to Tims Branch promoted settling in what has been named the Beaver Pond, a former pond created by beaver activity at the top of the wetland study site. Steed Pond, a now defunct former farm pond which predated the Savannah River Site, was dammed along the Tims Branch wetland from the 1930's until dam failure in 1984. The topography and hydrologic barriers created two settling basins; thus, much of the released U that passed through the Beaver Pond area would likely accumulate in Steed Pond. Of the 43.5 Mg of uranium released into Tims Branch, an estimated 61% was released between 1968-1971 and a recent study has demonstrated that 36.2 Mg remains in the wetland as of 2020 (Kaplan et al., 2020).

Uranium deposits in Tims Branch have been studied intermittently over the past 30 years (Bertsch et al., 1994; Hunter and Bertsch, 1998; Arey et al., 1999; Sowder et al., 2003; Jackson et al., 2005; Li et al., 2014). Following the suite of soil cores analyzed by Evans et al. (1992), a team led by Batson studied U transport during episodic storm events and determined that as much as 2.2 kg of U left the wetland during a single storm event (Evans et al., 1992; Batson et al., 1996). This mobile U was associated with stream solids liberated from sediments exposed when Steed Pond was drained, as negligible amounts of U were associated with the <0.45 μm size fraction. Newly formed Fe microprecipitates or eroded soil grains were identified to be the contributing transport vector. Though 2.2 kg of U per storm event may appear large, it represents only a small fraction of the total U inventory, estimated presently to be about 36,000 kg U (Kaplan et al., 2020). The apparently strong sequestration of U was demonstrated by Sowder, et

al., (2003) using sequential extractions and 1-to-1 soil-water extractions to show a strong correlation between U and dissolved organic carbon (Sowder et al., 2003). Another key result of this work was the observation of stronger U association with immobile solid soil phases, when compared to other heavy metals, including Ni, Pb, and Cr, in Tims Branch originating from M-Area releases (Seaman et al., 2001; Sowder et al., 2003). These previous results (Seaman et al., 2001; Sowder et al., 2003) are from samples collected exclusively at the former Steed Pond floor. The current work expands our understanding of U migration through Tims Branch by comparing the formerly unknown Beaver Pond U deposits to the Steed Pond soils. Areal overflight data and in situ gamma surveys identified elevated U concentrations in the upgradient Beaver Pond site (Kaplan et al., 2020). From this mapping work, 80% of the released U is estimated to remain in the wetland, with more than 60% of the released U remaining in Beaver Pond (Kaplan et al., 2020). Identification of key hotspots informed collection for our field samples (Kaplan et al., 2020).

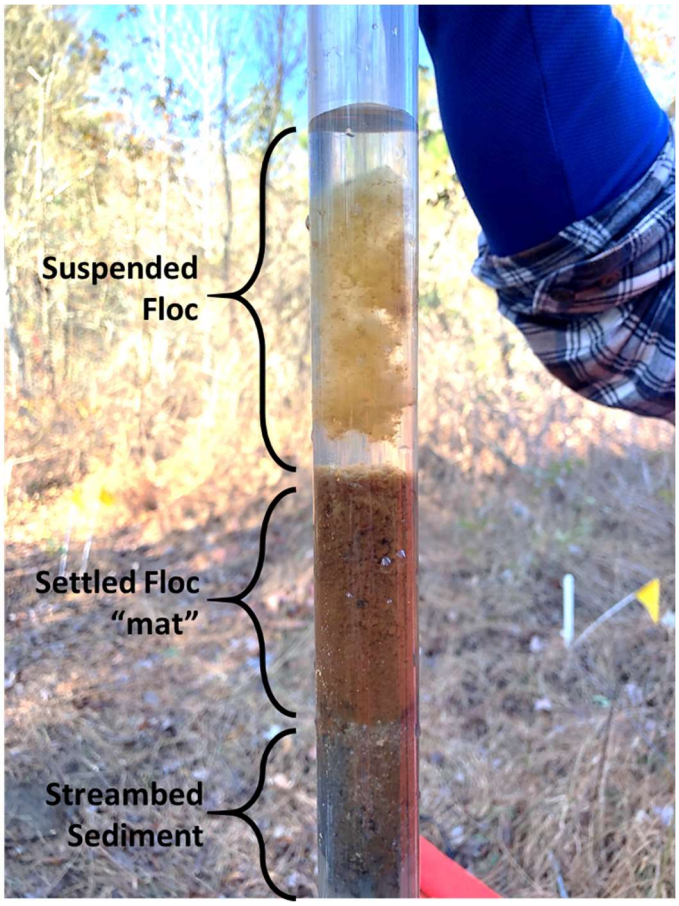

Figure 4-1: Photo of preserved water column and streambed. The upper section of the water column includes readily mobile floc, while the settled floc "mat" has been observed to accumulate along streambank crevices and depressions during low flow. Ordinary streambed sediment here resembles the solids that are often collected in Beaver Pond, as no floc has been observed there.

Iron (Fe) and OM colloids are a potential transport vector for heavy metals in wetland environments, forming through hyporheic exchange at surface water interfaces (Liao et al., 2017, 2020). These colloids, known as flocs, form at oxic-anoxic boundaries in wetlands and riverine environments (Lapworth et al., 2013). Shallow groundwater environments promote rapid aggregation of flocs upon oxidation, often at the hyporheic interface, where oxidizing surface

water and reducing groundwater interact (Lapworth et al., 2013). While Fe(III) colloids and OM colloids may aggregate at the hyporheic interface at other sites, the Fe and OM concentrations present at Steeds Pond produce the Fe-OM flocs in Figure 4-1 which will be referred to as "flocs" in this work. Large metal ions have a high propensity for incorporation into flocs, while smaller ions prone to cation exchange are generally less likely to incorporate (Lapworth et al., 2013). The rapid oxidation of Fe(II) to Fe(III) promotes precipitation of amorphous Fe(III) hydroxides, often ferrihydrite microprecipitates (Philippe and Schaumann, 2014). These microprecipitates are either encompassed by or stabilized by hyporheic OM, but precise characterization of floc structure and the effects of oxidation on organic matter's role in floc formation are topics outside the scope of this work. Mobilization of reduced Fe(II) from the subsurface to streams occurs during hyporheic exchange, when gaining stream conditions move anoxic, Fe(II)-bearing subsurface water into the stream. Gaining stream conditions occur when the local groundwater table exerts pressure on the lower stream stage, resulting in a flux of water from the wetland to the stream (Jolly et al., 2008). Inversely, losing stream conditions occur when the stream stage exerts a higher head pressure than the local groundwater table, moving water from the stream into the bank porewater and into the subsurface (Jolly et al., 2008). This hydrologic couple can be constant in an ecosystem or can vary temporally along a given reach of the stream, depending on rainfall and topography.

Primary objectives of this study were to 1) determine relationships between total U, Fe, and OM within contaminated wetland soils, 2) determine the water-extractable soil U, Fe, and OM concentrations as an estimate of the labile fraction, and 3) compare U and Fe partitioning between filterable (>0.1 um) and nonfilterable stream water fractions following two storm events of differing magnitude. Particular attention was directed at quantifying and understand the

partitioning of U in stream water between filterable and unfilterable fractions along a stream segment that passed through both gaining and losing portions of Tims Branch.

Methods

Site Description and Field Observations

Sampling locations in the wetland were informed by the U maps reported in Kaplan et al. (2020) (Figure 4-2). Groundwater and surface water samples were first collected from six sampling locations in August 2020 and another three locations were added in a second sampling campaign in September 2020. Locations were selected to have one sample upgradient of the Beaver Pond deposition area (which corresponds to 0 km in the data), two within this hotspot, one in the middle of the wetland, and two more approaching the former Steed Pond Dam, with the additions in September providing improved spatial resolution. The blue heatmap ends at the former Steed Pond dam. Two soil cores were collected from the two depositional areas (Beaver Pond and Steed Pond in Figure 4-2) and analyzed for total U, Fe, and OM as described below.

Flocs are frequently observed in Steed Pond, never observed in Beaver Pond, and intermittently observed between the two former ponds. While I have not determined a minimum threshold Fe and OM concentration necessary to create flocs, gaining conditions must be present to facilitate migration of Fe from the pore waters to the stream. Thus, I will generally refer to these three reaches along Tims Branch as gaining, losing, and intermittently gaining or losing hydrological stream conditions, consistent with present understanding of the role of hydrology on floc formation (Figure 4-2) (Knorr, 2013).

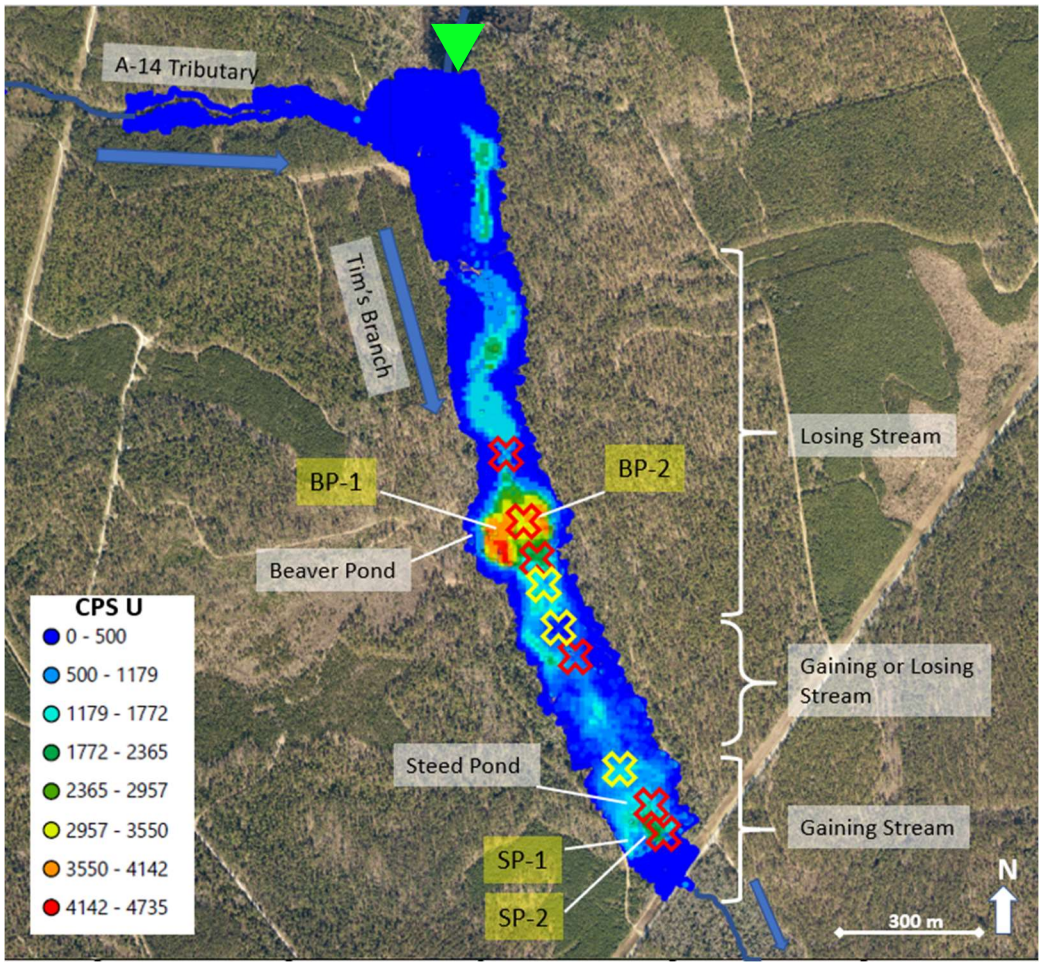

Figure 4-2: Sample locations of soil cores recovered from Beaver Pond (BP-1 and BP-2) and Steed Pond (SP-1 and SP-2) and stream sampling locations from the August 2020 sampling campaign (red crosses) and additional September 2020 sampling campaign (yellow crosses). Gamma heatmap of U counts (more specifically ^{234m}Pa counts, a ^{238}U daughter product) is adapted from Kaplan, et al. (2020). The green triangle marks where background soil samples were collected (upgradient from confluence with the contaminating A-14 Tributary). The M-Area releases originated upgradient on the A-14 Tributary, outside the area of this map.

The U distribution in the gamma mapping study (Kaplan et al., 2020) can be generally explained by the topography and historical hydrologic conditions in Tims Branch (Figure 4-2).

The dominant hydraulic gradient runs from north to south, that is, from Beaver Pond to Steed Pond, and it encompasses both subsurface flow and overland surface water flow. The wetland opens from a small, steep channel upgradient at the A-14 outfall to a wider, flat stream channel, resulting in reduced streamflow velocity that allowed sufficient time for aqueous and suspended constituents to settle or react in this deposition basin (Baba and Komar, 1981; Tang et al., 2002). Likewise, the Steed Pond Dam created ideal conditions for another settling reach of the stream, where all flow rates were reduced in the Pond, allowing for greater particle settling before making confluence with the Upper Three Runs Creek and eventually the Savannah River. This depositional history resulted in the unexpected immobilization of U, up to 80% of the total released mass, according to Kaplan, et al. (2020).

For the September 2020 sampling event, the specific sampling locations exhibited evidence of stormwater flow when compared to the sampling one month earlier. Especially in the Steed Pond area, streambank erosion and crushed streambank grasses indicate that flow had recently exceeded the current height by more than a meter. The flat middle reach of the wetland, where gaining and losing conditions fluctuate, was inundated and had such a slow flow velocity that flow direction was nearly indistinguishable, and there was no stream channel present. When perturbed, sediments and flocs here quickly resettled, indicating that particle settling is achievable and probable within this wide reach approaching the former Steed Pond area.

Sample Collection, Preparation, and Analysis

Water Samples

Stream water columns and the adjacent hyporheic porewaters were sampled and analyzed for U, Fe, and OM in the losing, mixed, and gaining reaches of the wetland (Figure 4-2). At locations depicted as "Xs" in Figure 4-2, stream water samples were collected from the top and bottom of the stream water column, as the stream was too shallow to illicit sampling of any greater resolution. Stream samples were collected in 50 mL centrifuge tubes from the top of the water column (3-5 cm from surface, center of the channel) and bottom of the water column (3-5 cm from streambed, center of channel). Samples were placed on ice and returned to the laboratory that day. The following day, these were vacuum filtered through a 0.1 μm PTFE filter, and the resulting filtrate was acidified to 2% HNO_3. Filters were weighed (Mettler Toledo MX-5 Ultra Microbalance, Mettler Toledo) before use and again after 48 hours of drying at 50°C to determine total dry mass of filtered solids collected. Filters were rehydrated in a centrifuge tube before sonication to reconstitute solids in DDI water. Cleaned filters were again dried at 50°C for 48 hours before a final dry clean mass was measured, to determine mass of solids digested by difference. The reconstituted solids from the filters were dissolved in 1 mL aliquots of concentrated HNO_3 until no solids remained visible and the solution was pale yellow or transparent. Only samples with visible floc material required heavier digestion beyond 5 mL acid added in total. These solutions were initially dark brown, and, as organic material reacted with the HNO_3, the solution turned to a pale yellow color. Upon digestion completion, a 0.1 mL aliquot was collected and added to 10 mL of 2% HNO_3 to match the analysis matrix.

All aqueous samples were analyzed via ICP-MS in 2% HNO_3. In September, samples were collected from three additional locations. For all September samples, pH (PCTSTestr 50,

Oakton Instruments), oxidation-reduction potential (ORP, ORPTestr 50, Oakton Instruments) and dissolved oxygen (DO, Hanna Instruments HI 4192) were measured in each water sample (porewaters and stream waters) immediately upon collection, and subsamples were collected specifically for TOC analysis. However, no correlations of stream and porewater constituents with pH, ORP, and DO appeared in the data. Additionally, porewater concentrations are not reported here, as the focus was on stream water conditions and trends in porewaters were similar to those observed in the stream waters.

The total concentration of analytes in both the stream aqueous filtrates and the digested solids in each top and bottom stream water column sample was determined using Equation 1.

$$[Me]_{Tota} = \frac{\sum_{i=1,2}([Me]_{SS,i} * SS_i * V_i + [Me]_{aq,i} * V_i)}{\sum_{i=1,2} V_i} \quad \text{Eq. 4.1}$$

Where [*Me*] can be either U or Fe, indices 1 and 2 represent the top and bottom water column samples, $[Me]_{SS}$ is the concentration in the stream solids (µg/g, dry), $[Me]_{aq}$ is the aqueous stream water concentration (µg/L), *V* is the volume of water collected for that sample (L), *SS* is the suspended solids loading in the stream (g/L) for all stream solids collected by a 0.1 µm filter. The $[Fe]_{Total}$ and $[U]_{Total}$ inventories calculated at each location represent the entire mass concentration passing through the system during the sampling interval and can be considered an integrated mass for reactive transport modeling efforts.

Soil Cores

Four ~70-cm long cores were collected on April 10, 2019: two from the most contaminated section of the Beaver Pond (samples BP-1 and BP-2) and two from the former Steed Pond floor, near the damaged retaining dam (samples SP-1 and SP-2) (Figure 4-2). The

cores were cut into segments of approximately 5 cm, recording precise lengths for creation of a depth profile. The convention for recording depth is that measured values are associated with the midpoint of the soil segment (i.e., the concentration listed at 2.5 cm represents the soil analyzed for 0-5 cm). Soils were dried at 50 °C until a stable weight was reached (~5 days), from which water content was calculated by gravimetric loss. A 1-2 g subsample of the dried, homogenized soil was heated at 450°C for 4 hours to determine total organic matter (TOM) after loss on ignition prior to HNO_3 digestion by EPA method 3050 (EPA, 1996). No pre-treatment was necessary to account for carbonate mineral volatilization because there are negligible amounts of carbonate minerals in these acidic soils. This value of TOM was converted to total soil organic carbon (TSOC) by multiplying TOM by 0.526 (Sparks et al., 1996). An aliquot of this digestate was diluted to 2% HNO_3 and analyzed via ICP-MS (Thermo X-Series 2) to determine total U and Fe concentrations in the soil.

Extractable U, Fe, and organic carbon (OC) were quantified as the dissolved aqueous concentrations released after mixing a second subsample of soil (1–2 g) with 45 mL of ultrapure water (≥18 MΩ cm) for 12 days. Dissolved organic carbon (DOC) was measured using a Shimadzu TOC-V, after filtration through a 0.45 μm PTFE filter. These digestions and extractions included a blank sample, measuring the metals present in topsoil upstream from where the A-14 outfall meets the Tims Branch stream; this blank represents our background concentration for anthropogenic U compared to naturally-occurring U, but it does not adequately provide a background value for Fe or OM, as the topsoil does not accurately represent these constituents as a function of depth.

Results

Soil Concentration Profiles

Soil concentration profiles of U, Fe, and OM with depth from Beaver Pond and Steed Pond indicate significant differences between the two wetland deposition zones (Figure 4-3). Above 30-cm depth, the soil cores from Beaver Pond had greater U concentrations than Steed Pond, consistent with the U mapping conducted by Kaplan et al. (2020). The soil cores from Beaver Pond had maximum U concentrations at a depth of 5 to 10 cm, compared to Steed Pond where the soil cores had maximum concentrations at the surface 0 to 5 cm segment (Figure 4-3). There have been no additional U inputs into Tims Branch since the M-Area facility was closed in 1988. As such, it is likely the Beaver Pond profiles are a result of stream sediment depositions resulting in decreased surficial U concentrations, while U in Steed Pond was subjected to greater erosion after removal of the dam. Fe, OM, and U depth profiles for all four cores changed in similar patterns (Figure 4-3). Linear regression calculations were conducted between the Fe-OM, Fe-U, and U-OM soil concentration data presented in Figure 4-3 (Table 4-1). As expected, highly significant correlations ($p < 0.01$) were observed between Fe and OM concentrations. These constituents have a strong affinity for each other (Spirakis, 1996; Cumberland et al., 2016), and they have been geochemically cycling for decades or longer. The significant correlation between Fe and U may stem from different processes, including the high affinity of U in the +6 or +4 oxidation state for iron oxyhydroxide surfaces, especially in conditions where pH values are greater than 6 (Waite et al., 1994; Barnett et al., 2002; Davis et al., 2004), and the coprecipitation of U into iron oxyhydroxide minerals under oscillating redox conditions (Duff et al., 2002; Pidchenko et al., 2017).

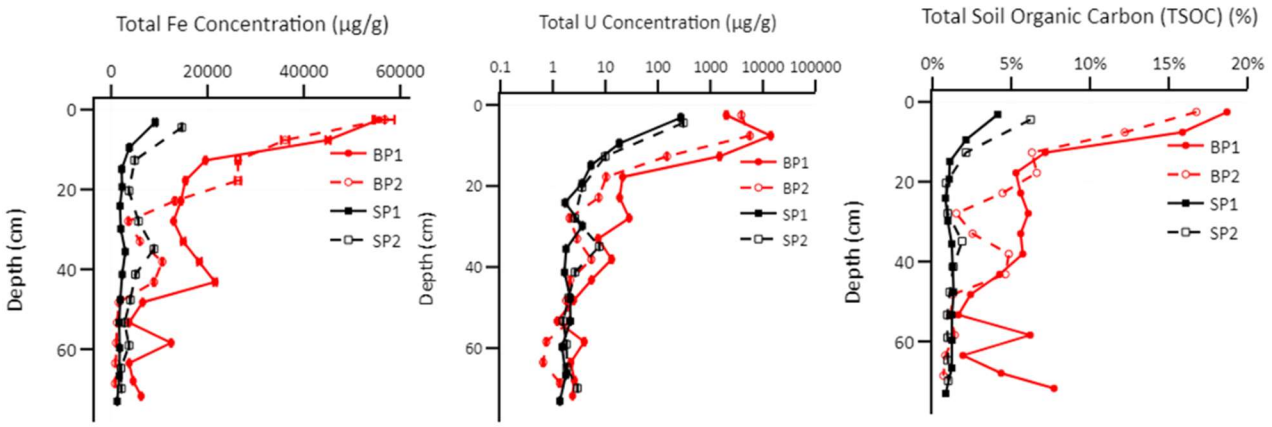

Figure 4-3: Concentrations of Fe (µg/g soil, dry) (left), U (µg/g soil, dry) (center), and Total Soil Organic Carbon (g C/g soil, dry) (right) in soil cores recovered from Beaver Pond (BP-1 and BP-2) and Steed Pond (SP-1 and SP-2). Lines are not data, they are present to guide the reader. Error bars represent analytical error and may be hidden by symbol.

Table 4-1: Coefficient of determination (R^2) for correlations between Fe-OM, Fe-U, and U-OM in BP-1, BP-2, SP-1, and SP-2 soil cores.

Soil Core	Fe-U	Fe-OM	U-OM
BP-1	0.40*	0.86**	0.42**
BP-2	0.59**	0.96**	0.69**
SP-1	0.92**	0.94**	0.90**
SP-2	0.69**	0.79**	0.94**

* and ** represent significant correlations at $p \leq 0.05$ and $p \leq 0.01$, respectively, for 11 to 15 observations.

Comparing the depth profiles for total concentration of each analyte to the water extractable profiles provides a measure of the labile phase, defined here as the tendency of the analyte to desorb from the solid phase and enter the aqueous mobile phase (Figure 4-4). These data can be interpreted as the reciprocal of a soil-water distribution coefficient (K_d, the commonly used ratio for solid-to-aqueous phase concentrations in geochemical transport models). A lower ratio here indicates that a smaller proportion of the total analyte concentration is labile.

Lability ratios increased with depth for Fe, U, and OM (Figure 4-4). The greater U lability ratios may be the result of generally lower total Fe and OM concentrations at depth (Figure 4-3), the two soil components that are especially effective at binding U. These ratios also tended to be many times greater in Steed Pond soils than in Beaver Pond soils. The water extractable dissolved organic carbon (DOC) appears to be relatively constant with depth (Figure A - 3). With a decreasing total U concentration and constant water extractable DOC, the fraction of total U that could be leached by a finite amount of water extractable DOC may increase with depth.

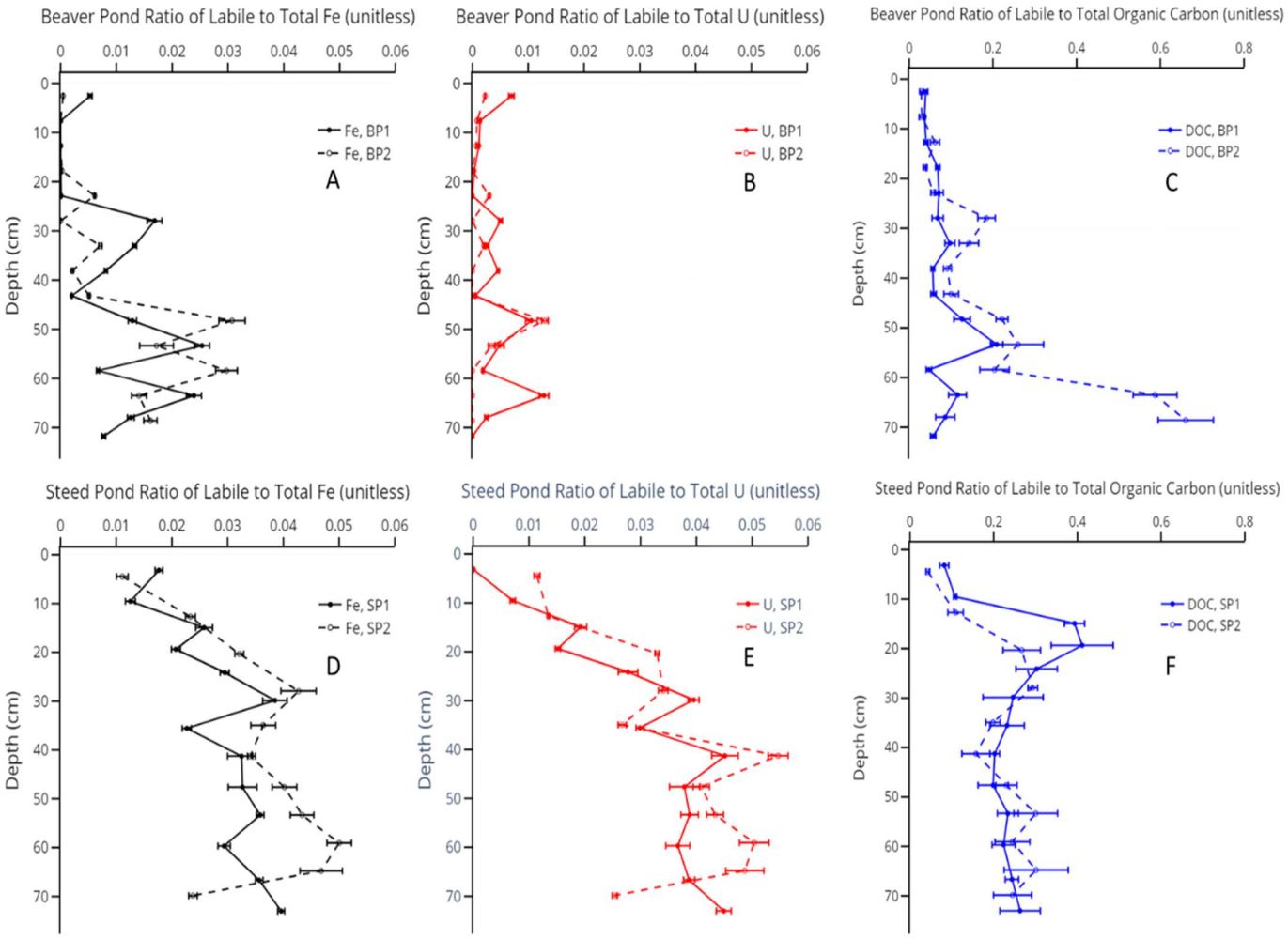

Figure 4-4: Ratios of water extractable (labile) to total concentrations of analytes in Beaver Pond soil cores (BP-1 and BP-2) (A, B, and C) and Steed Pond soil cores (SP-1 and SP-2) (D, E, and F). Lines are not data, they are present to guide the reader. Error bars represent analytical error and may be hidden by symbol.

Rainfall and Stream Height Data

Rainfall and stream height data preceding each event provide context for the stream-sampling data collected in August and September 2020. The rainfall data comes from a weather station located 1.1 km from the study site, and the stream height data is from a stream gauge just downstream of Steed Pond. These are hydrologic data for each sampling event in Figure 4-5, and

the complete plot can be found in Figure A - 2. Three key differences exist between August and September rainfall (Figure 4-5). The August rain event was a less intense and a shorter duration storm than the September rain event (9.87 mm over 5.0 hours and 100.81 mm over 3.0 hours, respectively). Sampling occurred 24 hours after the August storm and five days after the September storm. The August storm did not perturb the system from relative baseflow conditions, while the September storm continued to drain from the wetland for a week before the stream returned to baseflow conditions. These hydrologic data confirm our physical observations from each sampling date. In August, the wetland was relatively dry except for a single stream channel, and there was no evidence of flooding. In September, flooding had crushed many streambank plants and scoured many loose banks, and the stream was comprised of several braided channels. Furthermore, the middle reach of Tims Branch between Beaver Pond and Steed Pond was dry in August but in September was inundated with standing water. Sampling in different conditions was intentional, as I hypothesized that there would be variation between the floc geochemistry in each scenario, hence sampling before baseflow was reached in September 2020. Investigating specific timescales for floc formation, scouring, and transport relative to recent rainfall events will be addressed in future studies.

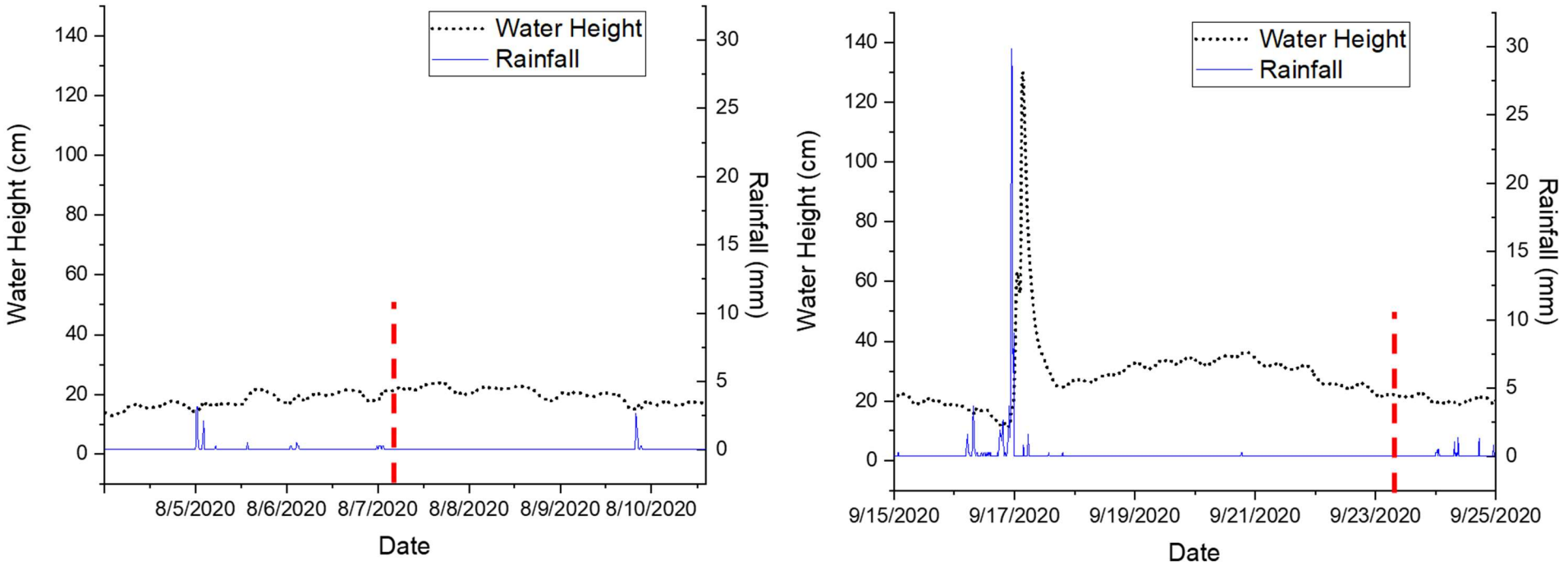

Figure 4-5: Rainfall (mm) and stream depth (cm, 100 m downstream of Steed Pond dam debris) around the period of the August and September 2020 sampling events (red lines).

Concentrations in Stream

Suspended solid samples in Tims Branch were collected at 9 locations (Figure 4-2) from the upper (5-10 cm depth) and lower (5-10 cm above the streambed) portion of the stream. No significant differences in Fe and U concentrations in the solids were noted between these two depths; consequently, the two values were averaged together (Figure 4-6A). The upgradient Beaver Pond area commonly exhibits losing conditions, the middle of the wetland exhibits mixed gaining or losing conditions, and the Steed Pond area predominantly exhibits gaining conditions. Gaining hydrologic conditions facilitate floc formation and U incorporation into flocs at Steed Pond, where the Tims Branch floodplain narrows. Both sampling events had flocs visibly deposited on streambanks within the Steed Pond (gaining) reach but not the Beaver Pond (losing) reach or mixed reaches. Photos of the floc-covered Steed Pond banks and sandy Beaver Pond banks are available in Figure A - 1. The Fe ($[Fe]_{SS}$) and U ($[U]_{SS}$) concentrations in the stream filterable (>0.1 μm) solids (in units of μg/g, dry) collected throughout the wetland remained constant along the sampling transect within both sampling events. While the $[Fe]_{SS}$ profile is also constant between sampling events, the $[U]_{SS}$ profile highlights the consistency of U-loading through the wetland during a given event but order of magnitude differences between sampling events.

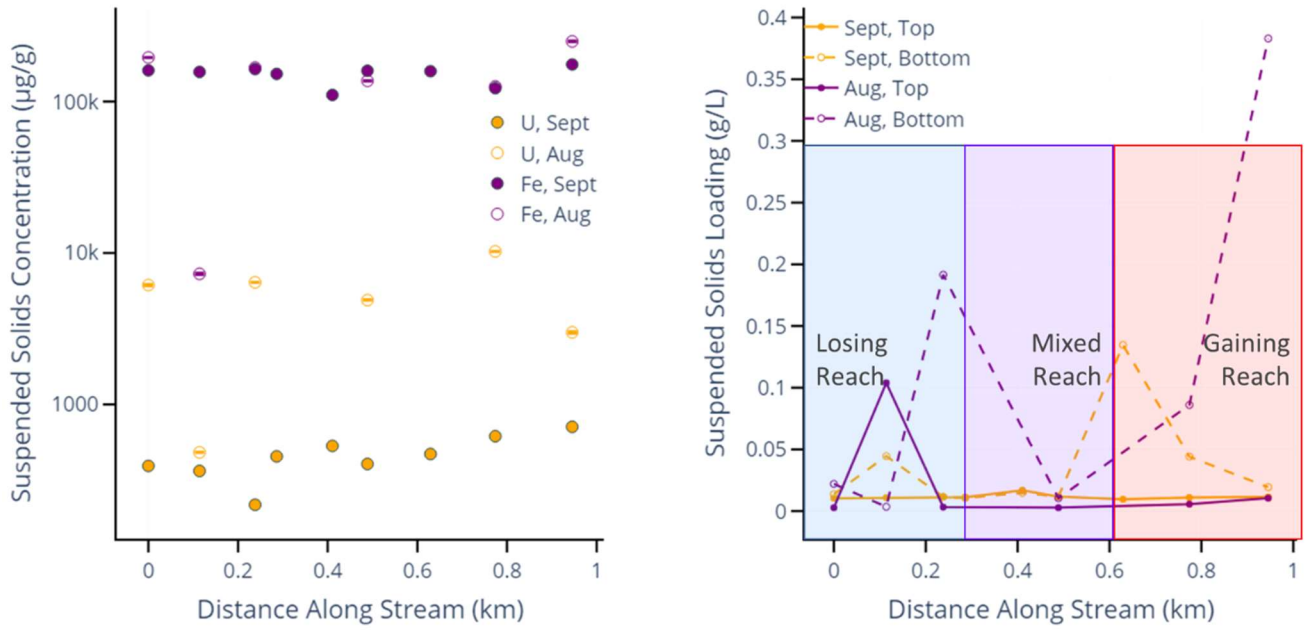

Figure 4-6: Average Fe and U suspended solids concentrations, $[Fe]_{SS}$ and $[U]_{SS}$ (µg/g, dry), respectively, for August and September sampling events (A). A logarithmic scale of (A) is available in Figure A - 5. Map of sample locations is presented in Figure 4-2 and Distance Along Stream starts at the northernmost location. Each value is an average of 2 measurements, the top of water column (5-10 cm below water surface) and bottom of water column (5-10 cm above streambed). Suspended solids loading (g/L) for the top and bottom of water column during August and September sampling events (B).

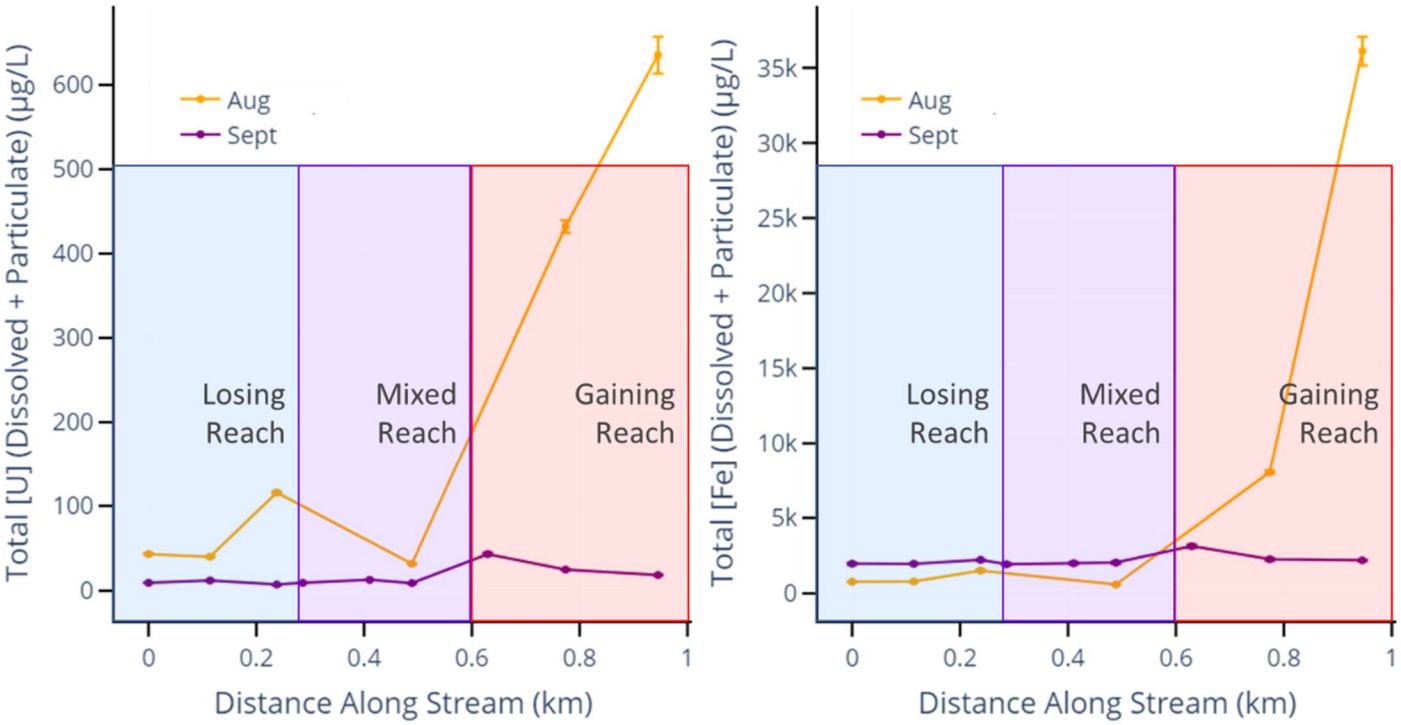

Figure 4-7: Total U (left) and total Fe (right) in the stream at each sampling location, where 0 km is the most northern point of the 1-km-long sampling region along Tims Branch (Figure 4-2). Colored boxes indicate the local hydrology in each segment of the wetland. The total concentration was calculated via Eq. 4.1. Each value is an average of 2 measurements, the top of water column (5-10 cm below water surface) and bottom of water column (5-10 cm above streambed). Aqueous contributions to Total U and Total Fe do not exceed 3% of solid phase contributions for any sample, and plots of aqueous contributions are available in Figure A - 6. Lines are present for clarity and do not represent data or a simulation.

The total U and Fe inventory profiles in Figure 4-7 represent the summation of the aqueous and solid phase metal inventories in both the top and bottom of the water column, calculated by using Eq. 4.1. Suspended solids loading (g/L) values can be found in Figure 4-6B. Flocs only form in gaining reaches of the stream, and there is more U in the mobile stream phase in this gaining reach of Tims Branch. Increased solid loading at Steed Pond is further supported by field observations: flocs were exclusively seen in Steed Pond during both sampling events, and, in September, they were exclusively on streambanks and not flowing in the main stream channel.

Discussion

Geochemical and depositional patterns emerged in three distinct categories for comparison: gaining versus losing stream reaches, temporal differences following storms in August and September, and Beaver Pond versus Steed Pond. These data provide further insights into assertions made by key studies since the 1990's, including the relationships between U and stream solids, U and Fe, and U and OM (Batson et al., 1996; Sowder et al., 2003; Jackson et al., 2005; Li et al., 2014; Kaplan et al., 2017). However, the primary conclusion from the data is that, at the kilometer wetland scale and meter soil-core scale, geochemical analysis needs to be coupled with an understanding of site hydrology to improve predictions of U, Fe and OM cycling. Depositional history, recent storm events, and distance from source must all be considered in conjunction with local geochemistry when analyzing the Tims Branch U inventory and transport from the wetland.

Gaining and Losing Stream Reaches

Gaining reaches provide conditions favorable for floc formation, as reduced Fe(II) in porewater near the hyporheic zone flows through streambanks and encounters oxidizing conditions to yield Fe(III)-OM colloids and microprecipitates (Lapworth et al., 2013). Both Fe(II) and U must be dissolved in porewaters in order for U to become incorporated into or onto the Fe flocs for stream transport. Gaining reaches in Tims Branch experience increased Fe and U stream concentrations, while mixed and losing stream reaches do not (Figure 4-7). Conversely, relatively low total Fe and U concentrations are present in the stream from 0 to 0.2 km, the Beaver Pond U hotspot, where iron flocs were not formed (Figure 4-7). However, some U is moving through the wetland in a solid phase with low Fe content; the increase in Total U available at 0.25 km is not accompanied by an equivalent increase in Fe. This indicates that U may be associated with stream solids other than flocs, such as the streambed sands and sediments in Figure 4-1. An increase in Fe proportional to 0.95 km-Steed Pond-August would be expected if the U was mobilized by Fe-OM flocs instead of contaminated streambed sediments. Photos in Figure A - 1 show the difference between the floc-filled Steed Pond streambed and the sandy, clear Beaver Pond streambed. Although core data in Figure 4-3 and the U mapping data in Figure 4-2 show total U concentration higher in Beaver Pond than Steed Pond, there was more labile U, Fe, and OM (Figure 4-4) in the Steed Pond sediment available to incorporate into flocs during hyporheic exchange (Figure 4-7). Under losing conditions, migration of U into the stream is not expected because it could only occur if the rate of transport due to U diffusion is faster than the advective flow into the groundwater. The infrequency of gaining conditions at Beaver Pond render this U pool less labile than the Steed Pond inventory. To this end, the apparent elevated U concentrations in Beaver Pond may in part be attributed to the depositional

environment (i.e., flat topography) as well as to the minimal release over time into Tims Branch due to its frequent losing stream conditions.

Regional topography and observations suggest that the middle of the wetlands, and especially the broader reaches of the stream between Beaver Pond and Steed Pond, would be conducive for settling of suspended solids. Tims Branch had relatively uniform total U stream water concentrations during a given sampling event (Figure 4-7A). A linearly decreasing stream water U concentration gradient as a function of distance downgradient from Beaver Pond but before Steed Pond would indicate consistent and progressing release from the primary U source as samples near the hotspot would be expected to have high U concentrations and as you move farther from the hotspot, concentrations decrease as the material has progressively released over time. Considering thermodynamic equilibria between aqueous and solid phases, it would be expected for soil concentrations to be relatively proportional to whatever is in the stream, as deposition of upheaved solids in the wetland on a decadal scale is a primary driver of wetland cycling. Instead of a linearly decreasing trend, consistent U soil concentrations from the gamma heatmap are relatively homogenous in the middle of the wetland (Figure 4-2), indicating that storms distribute solids laterally from the primary stream channel, except where small deviations at lower energy stream reaches induce particle settling in the main stream channel itself. The prolonged return to baseflow (Figure 4-5 and more completely in Figure A - 2), appears to spread contaminated solids beyond the extent of ordinary baseflow stream channels and flow paths, rendering these solids inaccessible to transport in the primary stream channel. While water levels were not above the banks during stream sampling, depth profiles in Figure 4-3 indicate that Steed Pond continues to receive U, Fe, and OM inputs to the surface.

August and September Sampling Events

The final calculated inventories of mobilized U from September were negligible compared to August's concentrations (Figure 4-7A). Uranium concentrations in suspended solids varied greatly between the August and September sampling campaigns (Figure 4-6A). A key finding in this study was that U concentrations in suspended solids were consistent within sampling events but varied 10x between sampling events. Suspended solid Fe concentrations reached a maximum at 0.95 km during August, one of two samples (the other being 0.8 km, August) that contained visible floc. The $[U]_{SS}$ value at 0.95 km in August drops slightly, when floc material increases and Fe becomes more prevalent (average of 18%, up to 25% at 0.95 km, August) in the floc composition. The increase in suspended solids observed in Figure 4-6B leads to the increased U and Fe inventories observed in Figure 4-7. Equation 4-1 accounts for both the aqueous and solid components of the total U or Fe being transported, but these C_{Total} values were dominated by the solid component, with the aqueous phase of the inventory being orders of magnitude lower and only accounting for 1-3% of the total inventory (Figure A - 6).

Consistent with the findings of Batson et al. (1996), solids remain the primary transport vector for U in riparian wetlands, but the current conditions controlling U transport differ. Batson et al. (1996) concluded that stream flow intensity was responsible for controlling the amount of U remobilized from the wetland. It is noteworthy that, during the timeframe of their 1993 sampling, Steed Pond was only recently drained, and the pond floor was largely unvegetated. Additionally, stream flow was much greater due to upstream releases of water from industry and a large-scale environmental pump-and-treat project. Together, the higher stream flow rates and the unvegetated stream banks were conducive to the Tims Branch wetland being appreciably

more prone to stream bank erosion and stream resuspension of contaminated sediment particles than it is today. Almost 30 years later, Steed Pond is largely vegetated, and surface water flow is restricted to a well-formed stream channel. While suspended solids undoubtedly continue to play an important role in contaminant export from this contaminated wetland, these data suggest that the antecedent conditions prior to a storm event may also be important. Climatic conditions conducive to the creation of gaining stream floc-forming conditions may also be especially important. This work suggests that certain storms create conditions primed for floc formation, which influences current U, Fe, and OM migration throughout the wetland. The importance of these temporal variations is highlighted by the 10x variation in $[U]_{SS}$ between August and September sampling events (Figure 4-6A). Additional rain event sampling is required to identify and to quantify the importance of antecedent wetland conditions on U-bearing solids formation.

Beaver Pond and Steed Pond

Beaver Pond has the highest total U concentrations of the wetland but has the poorest relationship between Fe-U and U-OM. The 14,000 µg/g U peak seen in Figure 4-3B is at the 5-10 cm depth interval, while the Fe and OM maxima are found in the 0-5 cm surface sample. The U concentrations are approximately 10 µg/g near 10 cm in the soil columns from Steed Pond (Figure 4-3B). The U background from upgradient of the A-14 outfall junction (representing background U in soil preceding anthropogenic releases) is 2.53 ± 0.06 µg/g (n=12). In the top 10 cm in Steed Pond, 4x this background concentration is present and indicates some of the U may have been deposited during the periods when U was being released from M-Area. Further inputs of U have occurred over the past decades from the incorporation of U into the natural wetland metal cycle, which releases Fe, OM, and now ug/L-levels of U from upgradient at Beaver Pond.

Steed Pond exhibited major U transport in the 1990's due to heavy erosion of the exposed pond floor sediments, sparse vegetation, and few central stream channels (Evans et al., 1992; Batson et al., 1996; Sowder et al., 2003). Today, widespread vegetation, designated stream channels, and removal of the less-compacted soil layers by erosion has created a system that experiences more natural decadal wetland nutrient and metal cycling than the raw, exposed pond floor of the 1990's. As such, comparisons of studies between then and now require hydrologic contextualization, but the retention of heavy metals in the wetland due to decadal wetland cycling appears to be a predominant influence in the attenuation of U within Tims Branch and the prevention of U release offsite in downgradient channels (Powell et al., 1996; Yang et al., 2012; Wang et al., 2013; Pan et al., 2017).

The OM and Fe maxima in all soil cores are at the surface (Figure 4-3A) and the Fe and OM concentrations are highly correlated (Table 4-1). A strong relationship between Fe and OM results from continual geochemical cycling of these two abundant and reactive wetland constituents (Riedel et al., 2013). However, U has a weaker linear relationship with Fe and OM as a function of depth in the Beaver Pond cores than in the Steed Pond cores. The difference in correlations is hypothesized to be related to differences between the chemical and physical processes causing the initial deposition of U within the Beaver Pond and those controlling migration downgradient to Steed Pond. Physical processes include the release of U from M-Area as a combination of dissolved, colloidal, and particulate phases which accumulated in the Beaver Pond primarily through physical straining and accumulation in surface OM/Fe layers. Any U released that was not attenuated here was likely retained and settled in Steed Pond. Thus, U associated with stream solids settled at Steed Pond upstream of the dam, yielding a stronger correlation between U and Fe-OM than the initial depositional band at Beaver Pond (Table 4-1).

Geochemically, this is consistent with wetland cycling, as metals that are present in wetlands in many chemical forms have the opportunity to react with the constituents that are physically filtering them—in this case, the organic-rich leaflitter layer that formed the bottom of Beaver Pond and the iron-rich local geology. This Fe and OM behavior contrasts with Beaver Pond, where no U has been released into Tims Branch since 1988, yet fresh inputs of Fe and OM are naturally occurring as OM and sediment move through the wetland. Uranium was introduced approximately 60 years ago, while Fe and OM have been cycling for the entire life of the wetland, yielding poorer U relationships at Beaver Pond.

Considering all possible transport mechanisms and the complex hydrologic history of Tims Branch, Steed Pond's history demonstrates that particle settling is a driving mechanism for the composition of the current soil column that once comprised the pond floor. Demonstration that U mobility appears to be driven by transport of wetland solids (e.g., flocs and suspended particles) decades after similar observations were made provides an important assessment of the stability of this system and the long-term controls of U mobility (Evans et al., 1992; Batson et al., 1996; Sowder et al., 2003). The U maxima for Steed Pond cores in Figure 4-3B are at the surface, just as they were for Fe and OM in Beaver Pond, discussed above. Steed Pond simultaneously acts as a sink and a source for U transport in Tims Branch. Surface U concentration maxima and strong linear proportionality with Fe and OM concentration profiles indicate an incorporation into wetland nutrient-metal cycles (i.e., "sink" behavior), receiving U from Beaver Pond associated with solids that settled in the Steed Pond surface water prior to the dam breaking in 1984. This accumulated U then becomes a source of mobile U. The Fe and OM that comprise the soil column prime the soil for floc formation during hyporheic exchange and gaining stream conditions.

Results of the water extraction from soil cores indicate that, while the inventory of U, Fe, and OM is orders of magnitude higher at Beaver Pond, all three constituents are more labile in the Steed Pond soils, leading to ideal conditions for both floc formation and U incorporation into flocs. While suspended solids may appear throughout the wetland, U incorporation into the flocs must occur in gaining reaches to transport U downgradient. Thus, U must be leached into the subsurface porewaters to be available for transport to the stream surface water under gaining stream conditions. From this initial source, transport may occur through erosion of large soil grains as it did throughout the 1990's in the exposed pond floor sediments. Now that Steed Pond is vegetated and erosion is presumably less prevalent, a high and consistent throughput of fresh porewater is required to leach U into porewaters, potentially as soluble U(VI) or as U(IV/VI) complexes with soluble OM. Further speciation studies are required to determine the specific species involved in leaching U into pore waters. With more labile OM and Fe pools at Steed Pond, higher releases of total U and Fe are observed in Figure 4-7. This hypothesized behavior of OM acting as both a sink for the accumulation of U and a source of mobile U is consistent with a revised conceptual model of OM serving as a diverse mixture of relatively low molecular weight components associated by hydrophobic and hydrophilic interactions (Sutton and Sposito, 2005). Further work will be necessary to elucidate the role of Fe and OM in transport and whether one induces mobility of the other. However, the clear difference in U-loading into solids in Figure 4-6A further supports the hypothesis that U-incorporation is a vital component of U cycling. When precise hydrologic conditions do not encourage U migration into the stream waters and association with suspended solids, less total U is found in the water column.

Broader Implications

Previous gamma mapping (Kaplan, et. al., 2020) and other studies (Evans et al., 1992; Batson et al., 1996; Sowder et al., 2003) have demonstrated that U concentrations leaving Steed Pond are sufficiently low to not impact downstream water quality. However, the underlying mechanisms attenuating U in the wetland are not fully understood. Stream water measurements of U throughout Tims Branch demonstrate that U is becoming more highly correlated with Fe and OM as U integrates into the natural wetland metal cycling. This incorporation into the wetland metal cycle provides some initial explanation for why the majority of U appears to remain attenuated within SRS. The continued accumulation of uranium is particularly interesting given the drastic changes that have occurred within Steed Pond since the 1980's; it was a small pond, became an open sediment bed after the Steed Pond dam collapse, and now is heavily vegetated and is composed of hydric soils resulting in a dynamic wetland system. The current distribution of U, with major accumulations in the Beaver Pond and Steed Pond areas, is proposed to be due to the initial deposition. Subsequently, the small amounts of U (relative to the total amount of U in the wetland) have migrated downstream were initially driven by erosion soon after the Steed Pond dam failure and have now become incorporated into the iron/carbon biogeochemical cycle. Key conclusions emerge from this work and improve our understanding of metal cycling in the Tims Branch wetland:

- At the kilometer and meter scales, geochemical analysis requires contextual hydrologic analysis to describe contaminant transport, as Fe and OM have been cycling and settling in Tims Branch for longer times than U has.

- Storm intensity and duration do not appear to be directly proportional to U release from Tims Branch. Antecedent hydrologic conditions (weeks- to months-time scale) influence the formation of Fe flocs that appear to impact U mobility.
- The mass of solids (i.e., floc and suspended sediment) present in a stream reach is often correlated to how much U is moving.
- The tendency for soil U to release into the labile fraction may be influenced not only by local geochemical (e.g., redox) and hydrological conditions (e.g., gaining and losing), but also by whether the U originates from the original source (M-Area) or a secondary U source (U originally from Beaver Pond now present in Steed Pond due to incorporation into trace metal cycling).

Planning for future work, redox preservation of soil cores, coupled with more detailed hydrologic data at the exact sampling location, will provide a more mechanistic conceptual model in future studies. Geochemical speciation and redox preservation will aid in understanding of whether Fe, OM, or both wetland constituents induce U mobility here. Current wetland conditions do not favor significant U movement, but changes in local and regional hydrology may alter this delicate biogeochemical balance.

Acknowledgements

This research was supported by the U.S. Department of Energy (DOE) Office of Science, Office of Basic Energy Sciences and Office of Biological and Environmental Research under Award Number DE-SC-0012530 and the Savannah River National Laboratory's Laboratory Directed Research and Development program (LDRD-2021-00263). Work was conducted at the

Savannah River National Laboratory under the U.S. Department of Energy Contract DE-AC09-96SR18500.

References

Arey J. S., Seaman J. C. and Bertsch P. M. (1999) Immobilization of uranium in contaminated sediments by hydroxyapatite addition. *Environ. Sci. Technol.* **33**, 337–342.

Baba, J. and Komar P. D. (1981) Measurements and analysis of setting velocities of natural quartz sand grains. *J. Sed. Res.* **52(2)**, 631-640.

Barnett M. O., Jardine P. M. and Brooks S. C. (2002) U(VI) adsorption to heterogeneous subsurface media: Application of a surface complexation model. *Environ. Sci. Technol.* **36**, 937–942.

Batson V. L., Bertsch P. M. and Herbert B. E. (1996) Transport of Anthropogenic Uranium from Sediments to Surface Waters During Episodic Storm Events. *J. Environ. Qual.* **25**, 1129–1137.

Bertsch P. M., Hunter D. B., Sutton S. R., Bajt S. and Rivers M. L. (1994) In Situ Chemical Speciation of Uranium in Soils and Sediments by Micro X-ray Absorption Spectroscopy. *Environ. Sci. Technol.* **28**, 980–984.

Conn R. M. and Fiedler F. R. (2006) Increasing Hydraulic Residence Time in Constructed Stormwater Treatment Wetlands with Designed Bottom Topography. *Water Environ. Res.* **78**, 2514–2523.

Cumberland S. A., Douglas G., Grice K. and Moreau J. W. (2016) Uranium mobility in organic matter-rich sediments: A review of geological and geochemical processes. *Earth-Science Rev.* **159**, 160–185.

Davis J. A., Meece D. E., Kohler M. and Curtis G. P. (2004) Approaches to surface complexation modeling of Uranium(VI) adsorption on aquifer sediments. *Geochim. Cosmochim. Acta* **68**, 3621–3641.

Dean A. P., Lynch S., Rowland P., Toft B. D., Pittman J. K. and White K. N. (2013) Natural wetlands are efficient at providing long-term metal remediation of freshwater systems polluted by acid mine drainage. *Environ. Sci. Technol.* **47**, 12029–12036.

Duff M. C., Coughlin J. U. and Hunter D. B. (2002) Uranium co-precipitation with iron oxide minerals. *Geochim. Cosmochim. Acta* **66**, 3533–3547.

Evans A., Bauer L., Haselow J. and Hayes D. (1992) *Uranium in the Savannah River Site Environment.* WSRC-RP-92-315, Westinghouse Savannah River Company, Aiken, SC.

Hunter D. B. and Bertsch P. M. (1998) In situ examination of uranium contaminated soil particles by micro-X-ray absorption and micro-fluorescence spectroscopies. *J. Radioanal. Nucl. Chem.* **234**, 237–242.

Jackson B. P., Ranville J. F., Bertsch P. M. and Sowder A. G. (2005) Characterization of colloidal and humic-bound Ni and U in the "dissolved" fraction of contaminated sediment extracts. *Environ. Sci. Technol.* **39**, 2478–2485.

Jolly I. D., McEwan K. L. and Holland K. L. (2008) A review of groundwater-surface water interactions in arid/semi-arid wetlands and the consequences of salinity for wetland ecology. *Ecohydrology* **1**, 43–58.

Kaplan D. I., Buettner S. W., Li D., Huang S., Koster van Groos P. G., Jaffé P. R. and Seaman J. C. (2017) In situ porewater uranium concentrations in a contaminated wetland: Effect of seasons and sediment depth. *Appl. Geochemistry* **85**, 128–136.

Kaplan D. I., Smith R., Parker C. J., Baker M., Cabrera T., Ferguson B. O., Kemner K. M., Laird M., Logan C., Lott J., Manglass L., Martinez N. E., Montgomery D., Seaman J. C., Shapiro M. and Powell B. A. (2020) Uranium Attenuated by a Wetland 50 Years after Release into a Stream. *ACS Earth Sp. Chem* **2020**, 1360–1366.

Knorr K. H. (2013) DOC-dynamics in a small headwater catchment as driven by redox fluctuations and hydrological flow paths - Are DOC exports mediated by iron reduction/oxidation cycles? *Biogeosciences* **10**, 891–904.

Lapworth D. J., Stolpe B., Williams P. J., Gooddy D. C. and Lead J. R. (2013) Characterization of suboxic groundwater colloids using a multi-method approach. *Environ. Sci. Technol.* **47**, 2554–2561.

Li D., Seaman J. C., Chang H. S., Jaffe P. R., Koster van Groos P. G., Jiang D. T., Chen N., Lin J., Arthur Z., Pan Y., Scheckel K. G., Newville M., Lanzirotti A. and Kaplan D. I. (2014) Retention and chemical speciation of uranium in an oxidized wetland sediment from the Savannah River Site. *J. Environ. Radioact.* **131**, 40–46.

Liao P., Li W., Jiang Y., Wu J., Yuan S., Fortner J. D. and Giammar D. E. (2017) Formation, aggregation, and deposition dynamics of nom-iron colloids at anoxic-oxic interfaces. *Environ. Sci. Technol.* **51**, 12235–12245.

Liao P., Pan C., Ding W., Li W., Yuan S., Fortner J. D. and Giammar D. E. (2020) Formation and Transport of Cr(III)-NOM-Fe Colloids upon Reaction of Cr(VI) with NOM-Fe(II) Colloids at Anoxic-Oxic Interfaces. *Environ. Sci. Technol.* **54**, 4256–4266.

Masscheleyn P. H., Pardue J. H., Delaune R. D. and Patrick W. H. (1992) Chromium Redox Chemistry in a Lower Mississippi Valley Bottomland Hardwood Wetland. *Environ. Sci. Technol.* **26(6)**, 1217-1226.

Pan C., Troyer L. D., Liao P., Catalano J. G., Li W. and Giammar D. E. (2017) Effect of Humic Acid on the Removal of Chromium(VI) and the Production of Solids in Iron Electrocoagulation. *Environ. Sci. Technol.* **51**, 6308–6318.

Persson J., Somes N. L. G. and Wong T. H. F. (1999) Hydraulics Efficiency of Constructed Wetlands and Ponds. *Water Sci. Technol.* **40**, 291–300.

Philippe A. and Schaumann G. E. (2014) Interactions of Dissolved Organic Matter with Natural and Engineered Inorganic Colloids: A Review. *Environ. Sci. Technol.* **48**, 8946–8962.

Pidchenko I., Kvashnina K. O., Yokosawa T., Finck N., Bahl S., Schild D., Polly R., Bohnert E., Rossberg A., Göttlicher J., Dardenne K., Rothe J., Schäfer T., Geckeis H. and Vitova T. (2017) Uranium Redox Transformations after U(VI) Coprecipitation with Magnetite Nanoparticles. *Environ. Sci. Technol.* **51**, 2217–2225.

Powell R. T., Landing W. M. and Bauer J. E. (1996) Colloidal trace metals, organic carbon and nitrogen in a southeastern U.S. estuary. *Mar. Chem.* **55**, 165–176.

Reed M. B. and Swanson M. T. (2006) *300/M-Area-Fuel and Target Fabrication*., 1189, Stone Mountain, GA.

Riedel T., Zak D., Biester H. and Dittmar T. (2013) Iron traps terrestrially derived dissolved organic matter at redox interfaces. *Proc. Natl. Acad. Sci. U. S. A.* **110**, 10101–10105.

Schmidt M. W. I., Torn M. S., Abiven S., Dittmar T., Guggenberger G., Janssens I. A., Kleber M., Kögel-Knabner I., Lehmann J., Manning D. A. C., Nannipieri P., Rasse D. P., Weiner S. and Trumbore S. E. (2011) Persistence of soil organic matter as an ecosystem property. *Nature* **478**, 49–56.

Seaman J. C., Arey J. S. and Bertsch P. M. (2001) Immobilization of nickel and other metals in contaminated sediments by hydroxyapatite addition. *J. Environ. Qual.* **30**, 460–469.

Sowder A. G., Bertsch P. M. and Morris P. J. (2003) Partitioning and availability of uranium and nickel in contaminated riparian sediments. *J. Environ. Qual.* **32**, 885–898.

Sparks D. L., Page A. L., Helmke P. A. and Loeppert R. H. (1996) *Methods of Soil Analysis, Part 3 - Chemical Methods*., Soil Science Society of America, Inc., Madison, WI.

Spirakis C. S. (1996) The roles of organic matter in the formation of uranium deposits in sedimentary rocks. *Ore Geol. Rev.* **11**, 53–69.

Sutton R. and Sposito G. (2005) Molecular structure in soil humic substances: The new view. *Environ. Sci. Technol.* **39**, 9009–9015.

Tang P., Greenwood J. and Raper J. A. (2002) A model to describe the settling behavior of fractal aggregates. *J. Colloid Interface Sci.* **247**, 210–219.

U.S. EPA (1996) *Method 3050B: Acid Digestion of Sediments, Sludges, and Soils*., Washington, DC.

Waite T. D., Davis J. A., Payne T. E., Waychunas G. A. and Xu N. (1994) Uranium(VI) adsorption to ferrihydrite: Application of a surface complexation model. *Geochim. Cosmochim. Acta* **58**, 5465–5478.

Wang Y., Frutschi M., Suvorova E., Phrommavanh V., Descostes M., Osman A. A. A., Geipel G. and Bernier-Latmani R. (2013) Mobile uranium(IV)-bearing colloids in a mining-impacted wetland. *Nat. Commun.* **4**, 1–9.

Yang Y., Saiers J. E. and Barnett M. O. (2013) Impact of interactions between natural organic matter and metal oxides on the desorption kinetics of uranium from heterogeneous colloidal suspensions. *Environ. Sci. Technol.* **47**, 2661–2669.

V. LEACHING OF URANIUM & NICKEL FROM ANTHROPOGENICALLY CONTAMINATED WETLAND SEDIMENTS UNDER OXIC & ANOXIC CONDITIONS: INFLUENCE OF IRON AND ORGANIC MATTER SPECIATION

Introduction

Metallurgy processes resulted in the release of 43,500 kg U to the Tims Branch wetland at the Department of Energy (DOE) Savannah River Site (SRS). Fuel fabrication and target assembly began in 1964 at DOE's M-Area at SRS, where process waste effluents were released until 1984 and consisted of dissolved, colloidal, and particulate U phases (Evans et al., 1992; Reed and Swanson, 2006). Predominantly depleted U was released concurrently with Ni, Pb, Cr, and other heavy metals (Evans, et al., 1992). Facility effluents entered the A-14 tributary and concentrated in Tims Branch, a riparian wetland that ultimately makes confluence with the Savannah River via Upper Three Runs Creek roughly 20 km downgradient. Hydrologic conditions, beaver activity, and a former farm pond resulted in the retention of U and other metals in a beaver pond at the opening of the wetland and behind the farm pond dam roughly 1 km downgradient. In 1984, M-Area ceased production, and U releases ended. In the same year, the beaver dams and former farm pond (Steed Pond) dam collapsed, resulting in exposure of contaminated sediments to the atmosphere and local hydrologic fluxes.

Studies of Tims Branch in the late 1990's identified Steed Pond as a primary hotspot where U had accumulated during M-Area releases and was being mobilized by erosion of contaminated sediments during and after storm events (Batson et al., 1996; Evans et al., 1992; Sowder et al., 2003). While estimates of U fluxes from the wetland were made (Batson et al., 1996) and initial depth profiles were taken within the exposed pond floor (Sowder et al., 2003), no extensive work had been done to identify the extent of contamination nor to estimate how much of the 43.5 Mg U still remained in Tims Branch. In addition to identifying the degree of

contamination in Steed Pond, work by Kaplan, et al., (2020) determined that 36.2 Mg U (83% of original releases) still remains in Tims Branch and that 26.1 Mg (60%) of the U remains upgradient in a previously unidentified former beaver pond, referred to in the literature as Beaver Pond. Steed Pond was believed to bear the majority of the U, but Kaplan's study determined it only held roughly 23% of all U released since 1964 (Kaplan, et al., 2020).

The study by Kaplan, et al., (2020) improved the scientific community's understanding of where primary U deposits persist by determining the lateral extent of U contamination, but only coarse data from the late 1990's (Batson et al., 1996; Evans et al., 1992; Sowder et al., 2003) existed to highlight how deep the contamination is. Further, these studies had only identified Steed Pond as a contamination zone. Using this newly developed lateral heatmap as guidance for sampling (Kaplan, et al, 2020), cores were taken in both Steed Pond and Beaver Pond and digested to identify correlations between U, Fe, and OM as a function of depth and in finer resolution than previous studies (Parker et al., 2022). Strong correlations between U, Fe, and OM in Steed Pond indicate that natural wetland Fe and C cycling appears to have incorporated U into decadal fluxes (Parker, et al., 2022). Meanwhile, Beaver Pond sediments are rich in U but lack a strong correlation with Fe and OM, as inputs of these wetland constituents continue naturally while U releases into Tims Branch ended in 1984 (Parker, et al., 2022). The current work aims to understand how redox activity impacts geochemical inventories in both Beaver Pond and Steed Pond, and it more deeply investigates how OM reactivity and diversity impact metal retention in both Tims Branch hotspots.

High concentrations of OM and rich OM diversity create conditions conducive to wetland metal retention, as OM reactivity with heavy metals has been observed in field survey studies of riparian wetlands (Sobolewski, 1999). Field samples and long-term water quality monitoring in

various North American wetlands indicate that OM is central to the retention of contaminant metals and accumulation of natural trace concentrations of influent metals (Sobolewski, 1999). Metals are retained as wetlands remediate contaminated influents and release effluents with significantly lower metal concentrations (Masscheleyn et al., 1992; Sobolewski, 1999). Plant-derived residues in soil OM may degrade into smaller biopolymers in 20-30 years for lignin and up to 160 years for long-chain *n*-alkanes, based on ^{13}C-labelled studies of over 20 field sites and up to 23 years in length (Lehmann et al., 2020; Schmidt et al., 2011b). However, dissolved OM often accounts for less than 2% of total OM in wetland soils (von Lützow et al., 2007), and plant-derived lignin contributes heavily to metal reactivity and retention within the soil solution (Guo et al., 2008; Jones, 1998). With long residence times in wetlands, lignin and other metal-binding constituents are able to remain immobilized in soils for decades before biotic degradation processes cleave smaller, mobile biopolymers—and the metals bound to them—from these structures (Lehmann et al., 2020; Lehmann and Kleber, 2015).

Oxidation in soils can release metals via oxidation of the metal itself or through the oxidation of the organic complexes that are binding metals. Reducing conditions increase the solubility of Fe minerals, while hydrolysis effects rapidly precipitate and immobilize Fe(III) species in oxidizing conditions (Schwertmann, 1991; Stefánsson, 2007). However, Fe(II)/Fe(III)-OM complexes experience increased solubility in many systems, and if Fe is present as Fe(III) in solution, it is likely complexed by OM (Chen et al., 2020; LaRowe and Van Cappellen, 2011). These OM complexes provide a mechanism for Fe(III) dissolution in oxidizing conditions by direct oxidation and solubilization of the OM ligands (Liang et al., 1993), contrary to the common convention that Fe(III) is consistently insoluble in soil solutions. Vadose zone oxygen diffuses only a few centimeters before being consumed by aerobes, resulting in pools of reduced

OM that persist in soils within anaerobic micropores that are sensitive to aeration if perturbed (Keiluweit et al., 2017). In the absence of anthropogenic perturbations, these reduced organic carbon pools are expected to remain stable. Likewise, any anthropogenic or hydrologic aerobic perturbations of regularly anoxic soils can oxidize the soil carbon and release Fe and other metals into solution if porewaters are present.

In this work, I digest subsamples of redox-preserved cores in parallel—in an inert, anoxic atmosphere and in atmospheric conditions after oxidizing for three days—to compare metal inventories extractable in each oxygen regime. This builds upon current literature—lateral deposition of anthropogenic U (Kaplan, et al., 2020) and U concentrations as a function of depth in previously identified hotspots (Parker, et al., 2022)—by identifying processes within natural wetland cycles (Schlesinger and Bernhardt, 2013) that are accumulating metals, most notably U remaining in Tims Branch from M-Area releases between 1964 and 1984. Our primary objective is to identify correlations between metal inventory changes, changes within the OM pool in each atmosphere, and the diversity of OM at key metal-retaining depths. I hypothesize that more metals will be available in more phases in the anoxic atmosphere when compared to the oxic atmosphere. Further, I hypothesize that the OM will retain a sizable fraction of the total metals in the soil column when comparing values of the NaPP- and HF-extractable metal concentrations.

Methods

Sample Collection

Two soil cores were collected from the Tims Branch wetland in the DOE Savannah River Site in Aiken, South Carolina (Figure 5-1). One core was from the Beaver Pond (BP) and the other was collected from the former Steed Pond (SP) floor. Cores were 5 cm in diameter and the BP core was 30 cm long while the SP core was only 21 cm long. Upon removal from the earth,

each core was capped and placed inside a sealed aluminized mylar bag filled with 100 commercial oxygen-removing packets and placed on dry ice before collecting the next core. In the laboratory, cores were placed into the 95% N_2/5% H_2 atmosphere glovebox for preservation and only unsealed in this anoxic atmosphere. Cores were sectioned into 3-cm segments (n_{BP} = 10, n_{SP} = 7), soils were homogenized in each sample, and soil masses were recorded. A blank soil from Tims Branch upgradient of confluence with the A-14 outfall was included as a background for metals released from the outfall. Soils were weighed into reaction vessels for the series of digestions, and the remaining soil was kept in sealed bottles in the glovebox until all digestions were complete and digestates analyzed. The soil subsamples designated for oxic analysis were portioned and weighed in the glovebox and then removed to the atmosphere for exposure to natural levels of O_2 for three days.

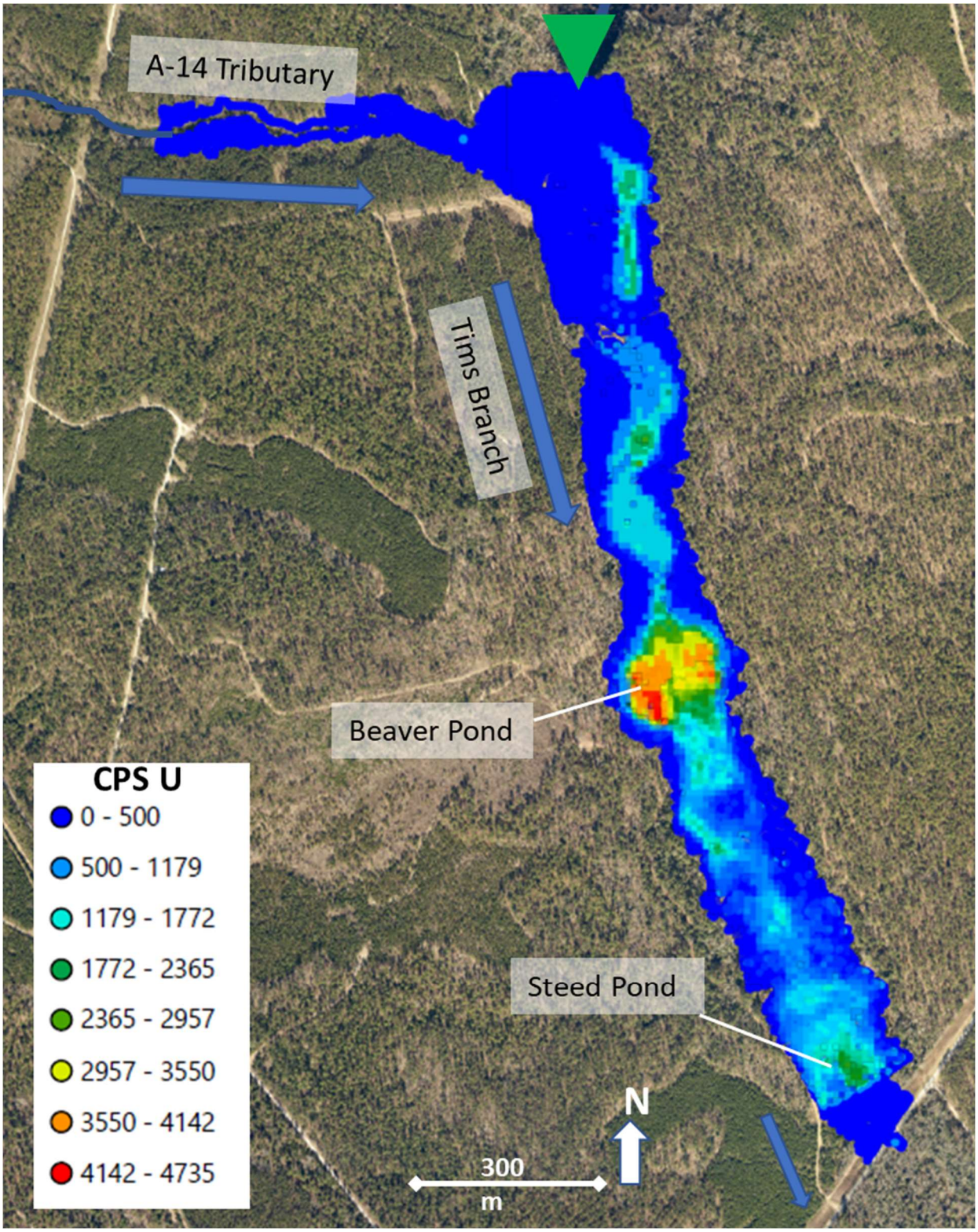

Figure 5-1: Map of sampling site, where the dominant hydraulic gradient is denoted by the blue arrows, the green triangle marks the location of the upgradient background soil sample, and the heatmap is based on U daughter counts per second (CPS), all adapted from Kaplan, et. al., 2020.

Sample Analysis

The soils were analyzed using what we call a parallel extraction. This differs from the sequential extraction (Schultz et al., 1998) in that the cores are still redox-preserved and analyzed for various heavy metal fraction associations in the soil, but here the analyses were performed on separate subsamples and not in sequence. Thus, extractions cannot be considered exclusive to a certain phase, but rather represent a comparison of each phase between samples anoxically preserved and those exposed to the atmosphere for three days. All subsamples were between 1-3 g mass, depending on the compaction and density of the wet soil. After all chemical analyses were performed, the remaining soil was dried at 50°C to a constant weight then heated in a furnace for 6 hours at 450°C to determine organic matter content via loss on ignition. All analyses were procedurally identical for the oxic and anoxic samples, except for the atmosphere. Reagents were ACS Reagent grade, and all solutions were made using DDI (>18mΩ) H_2O. However, those used in the anoxic glovebox were made with degassed DDI (>18mΩ) H_2O. Degassing was achieved by boiling the water in a flask for 1 hour at a full rolling boil and then cooling to 25°C while $Ar_{(g)}$ was bubbled to the bottom of the flask. Once cooled, this vessel was sealed and immediately moved to the anoxic glovebox for solution preparation. All digestates were analyzed in a 2% HNO_3 matrix by inductively coupled plasma mass spectrometry (ICPMS, Thermo RQ) unless otherwise noted.

Water Extractable Cation Exchange: Extraction of the water extractable phase is adapted from the water extractions of Schultz (1998) and Sowder (2003). Three working solutions were prepared in 0.4 M $MgCl_2$ and leached for 24 hours, 48 hours, and 72 hours. The background solution 0.4 M $MgCl_2$ was chosen to match the water extractable, cation exchangeable fraction of both the Schultz (1998) and Sowder (2003) studies. The high ionic strength, while not

representative of Tims Branch porewaters, does allow for a flooding of Mg^{+2} ions to exchange any simple cationic species of U, Fe, Ni, and other metals present on the soil surface. Reactor vessels rotated end over end for the 24 hours of reaction. Collected solution masses were recorded, as well as the initial vial mass and sample mass, so a quantitative mass balance can be performed on the solid remaining in the vial as well as residual water that remained after decanting but before the recharge solution was added.

Acid Leachable and Oxidation State Analysis: An acid leachable fraction was removed by reacting a soil subsample with 0.1 M HCl for 15 minutes. Performed in triplicates, these subsamples rotated end over end before an aliquot was removed. The aliquot was syringe-filtered through 0.45 μm polyethersulfone filters (Whatman). From this 2.5 mL aliquot, 1.0 mL was then removed and placed in a vial with 0.5 mL 0.01M $La_2(NO_3)_3$ then amended with 15 μL of 15.8 M (concentrated) HF. This amendment results in a precipitation of LaF_3 and co-precipitation of trivalent and tetravalent actinides (Kobashi et al., 1988). The aliquot with the microprecipitate was centrifuged and an aliquot of the supernatant was diluted in 2% HNO_3 for analysis. Any uranium removed following LaF_3 co-precipitation was assumed to be in the tetravalent state. Furthermore, any uranium which was not initially leached from the soil as assumed to be tetravalent uranium, consistent with previous studies (Powell et al., 2004, 2005; Powell et al., 2008). Though there are no studies to evaluate the efficacy of the LaF_3 co-precipitation of tri and tetravalent actinides in the presence of organic ligands, it is assumed that the high concentration of fluoride in the procedure minimizes any perturbance from the organic ligands in the oxidation state analysis technique.

Citrate, Dithionite, & Bicarbonate: Adapted from Mehra and Jackson (1958), the citrate, dithionite, bicarbonate (CDB) extraction targets Fe-oxides in the soil (Mehra and Jackson, 1958).

Reaction vessels were prepared by amending soil samples with 40 mL of 0.3 M $NaHCO_3$/0.2 M Na-Citrate, and the extraction was initiated by adding 1 g of $Na_2S_2O_{4(s)}$, producing rapid, vigorous effervescence. These were heated at 50°C for 30 minutes then centrifuged, and the supernatant was decanted and collected. An aliquot of the supernatant was diluted in 2% HNO_3 for ICPMS analysis.

Sodium Pyrophosphate: To extract organic matter from the soil surfaces, reaction vessels were amended with 15 mL of 0.1 M $Na_2P_2O_7$ and rotated end over end for 24 hours (Hall et al., 1996). Upon centrifugation, the supernatant was decanted, collected, and an aliquot was diluted to 2% HNO_3 for ICPMS analysis. The alkaline extraction results in a supernatant pH of roughly 10. As such, the tar black, viscous solution was confirmed to consist of soluble material when filtered through an 0.45 μm filter and the solution remained colored.

Residual Fraction via HF-HNO_3 Total Digestion: Total concentrations in the soil were determined by HF-HNO_3 microwave digestion (EPA, 1996). In PTFE digestion vessels, 2 mL of soil slurry DDI (>18mΩ) H_2O, 7 mL concentrated HNO3, and 3 mL concentrated HF reacted with the soil at 175°C for 15 minutes. Preceding these digestions, the soil subsamples were heated at 450°C for 6 hours to remove any soil organic matter that could produce volatile reaction byproducts with the digestion matrix.

Soil Texture Characterization

Soils were suspended in 100 mL of 50 g/L Na-HMP and shaken overnight before analysis, to disperse any clay aggregates. The suspensions of 10-30 g of soil in 50 g/L Na-HMP were then diluted to 500 mL with DDI (>18mΩ) H_2O in 500 mL graduated cylinders. Using the hydrometer method adapted from Day (1965), blank measurements were taken in a 500 mL graduated cylinder with 400 mL DDI (>18mΩ) H_2O and 100 mL 50g/L Na-HMP, to account for

differences in water viscosity and density with slight changes in temperature (laboratories ranging between 22-26°C during analysis) (Day, 1965). These blank measurements were subtracted from the sample reading, to yield the net difference in specific gravity of the solution above a background water solution. Additionally, based on time of measurement, size fraction cumulatively settled, and temperature of water at time of measurement, adjustments were made for the effective settling depth of the hydrometer. Although calculated individually at measurement times, the sand fraction (>2000 μm) was entirely settled after roughly 75 seconds, and the silt fraction (50-2000 μm) was settled at 12 hours. The clay fraction (2-50μm) was assumed to remain in solution past this time.

$$F_{Sand} = 1 - \frac{[R_{75sec} - R'_{75sec}] * V}{M} \quad \text{Eq. 5.1}$$

$$F_{Clay} = \frac{[R_{12hr} - R'_{12hr}] * V}{M} \quad \text{Eq. 5.2}$$

$$F_{Silt} = 1 - [F_{Sand} + F_{Clay}] \quad \text{Eq. 5.3}$$

Where F is the fraction as sand, clay, or silt, M is the total mass of soil analyzed (g), V is the volume of the suspension (cm^3), R is the hydrometer reading (g/cm^3) at specified times, and R' is the blank hydrometer reading (g/cm^3) at corresponding time of measurement. These conventions for particle fractionation were developed by Day (1965) and are operationally applied for simple soil fraction analysis.

To take the hydrometer measurement, the soil suspensions were brought to 500 mL in the graduated cylinder and then stopped at the top and turned smoothly end over end for 1 minute. Minimizing turbulence when setting the cylinder on the benchtop, the hydrometer was gently inserted into the solution and the timer immediately started. For consistency, all measurements in suspensions and water blanks were read at the upper meniscus of the hydrometer, and cylinders were sufficiently wide to avoid any capillary effects at the vessel walls.

Organic Matter Characterization

After geochemical analysis, further analysis of organic matter composition became necessary. Aliquots from the NaPP extractions were filtered through 0.45 μm polyethersulfone filters and analyzed for total organic carbon using a Shimadzu TOC-V. Samples from the oxic and anoxic NaPP extractions were measured, to identify any differences in total removable carbon between oxic and anoxic regimes. This measurement is not intended to represent native soil dissolved organic carbon values but, instead, is intended to represent a total of potentially mobile carbon under harshest extraction conditions; it can be thought of as all carbon that is not structural or strongly bound to mineral surfaces. Any differences between oxic and anoxic regimes are likely due to oxidation of the organic matter.

Diversity of Organic Compounds

A measurement of the diversity of organic compounds was performed on key soil samples whose relevance emerged in the total OM and geochemical profiles. Samples analyzed included surface samples (BP-1 and SP-1), lowest depth samples (BP-10 and SP-7), and samples with inexplicably high peaks in certain metal profiles or total OM (BP-4, SP-2, SP-6). These seven samples underwent 0.1 M NaOH extraction for 24 hours while mixing, centrifugation, and collection of the supernatant. This supernatant solution was acidified to pH = 2 using HCl, and a 2 mL aliquot of this OM-precipitated slurry was filtered through an Agilent Bond ElutPPL column and eluted with 100% methanol. After evaporation via $N_{2\,(g)}$ purging, the OM solids were resuspended in 100 μL methanol and analyzed via Liquid Chromatography Mass Spectrometry (LC-MS/MS, Thermo Orbitrap FusionTribrid Mass Spectrometer) to identify the total number of unique organic compounds present and to classify these compounds into relevant statistically significant categories based on metal reactivity, structure, and functional groups.

Results and Discussion

Higher concentrations of U, Fe, and Ni are present in Beaver Pond than in SP, and it acts as a source term for transport into Steed Pond via erosion of contaminated sediments and natural wetland cycling of Fe and OM. As such, a natural split emerged in the data analysis and discussion: Beaver Pond extraction treatments and profiles were grouped together (*i.e.,* comparing U profiles for all five treatments alongside one another to the five for Fe), while each treatment was studied for all of the elements in Steed Pond (*i.e.,* comparing the Fe, U, and Ni profiles for the NaPP treatment). As such, all extraction treatments are discussed together for Beaver Pond, but metals are compared to one another within treatments for Steed Pond, to contextualize the geochemical implications of trends between oxygen regimes and between the metals in each extraction treatment.

Beaver Pond

The concentration and diversity of organic matter compounds was found to vary widely with depth in both BP and SP cores. These variations are discussed through this work to gain a more detailed understanding of Fe, Ni, and U incorporation into wetland OM cycling. The NaPP-extractable OC (Figure 5-2A) varies proportionally with Total OM (Figure 5-2C) as a function of depth in both the oxic and anoxic phases. Similarly, Total S content (Figure 5-2B) in the soil follows this trend, which is to be expected in Fe-rich wetland sediments, where S often follows Fe-mineralogy, OM content, or both (Schwertmann et al., 2005).

Phytochemicals are plant-derived secondary metabolites with a high affinity for metal binding and tannins that contain multiple phenolic compounds to increase metal binding. Lignin is comprised of longer chain, more complex macromolecules that still maintain a degree of metal reactivity. Carboxylic rich allocylic moieties (CRAM) are mobile, cyclic, compounds with high

metal affinity, and carboxyl-containing aliphatic moieties (CCAM) resemble CRAM except they are chains instead of cyclic compounds (Jones, 1998; Kaplan et al., 2016; Wen et al., 2018). Of these compounds, all are considered to have strong metal-binding capacity (Jones, 1998; Kaplan et al., 2016; Wen et al., 2018), but lignin is wholly immobile in the soil column and requires further degradation before lignin decomposition products can become labile (Guo et al., 2008; Lehmann and Kleber, 2015). The remaining classifications more easily become labile in natural porewaters (Lehmann and Kleber, 2015), but the treatments in this work focus on Total OM via loss on ignition and the oxidized or reduced pools of NaPP-removable carbon. While the latter pools are more likely to be aerated in the vadose zone and mobilized, the NaPP extractant in this work is not a proxy for the natural porewaters.

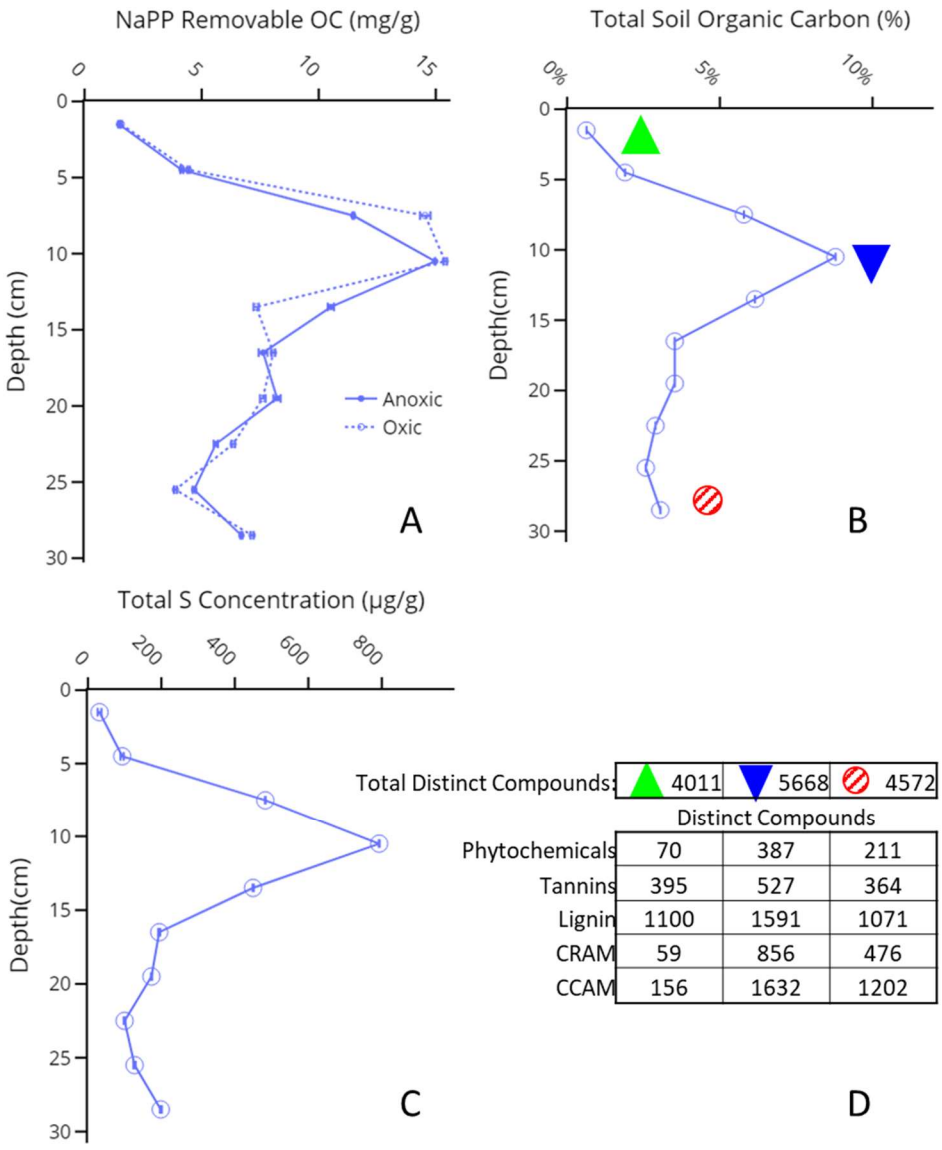

Figure 5-2: Beaver Pond NaPP removable organic carbon in oxic and anoxic phases (A). Total soil organic carbon (TSOC) as determined by 0.5206 times the total OM via loss on ignition in BP core (B). Total sulfur from HF digestion of residual in BP (C). Organic matter diversity (number of distinct compounds in each class) for the three BP sediments identified in plot C (D). Error bars originate from the instrumental analytical error.

In conjunction with the higher Total OM content and most NaPP-extractable OC, the diversity of organic compounds (Figure 5-2D) exhibits a wide range of compound classes with

strong metal binding affinity and thus presents the potential for metal accumulation in Beaver Pond when coupled with the high OM content in these layers. This occurs because of the increased diversity of metal-binding compounds *and* increased OM content, as there is more OM present and more diverse OM present.

The most critical data supporting metal accumulation over time in BP are both the concentration (TSOC, Figure 5-2C) and the diversity of organic compounds (Diversity Analysis, Figure 5-2D) at each layer. Soil at 10 cm has the highest total abundance of compounds and, most notably, the highest diversity of lignin compounds. Further, 10 cm has the highest overall OM content in the column, meaning that the soil here has both a high amount of OM and a high diversity of metal-binding organic compounds, especially lignin. Meanwhile, the surface sample has the lowest total OM, lowest NaPP-extractable OC (supported by the 10x lower diversity of mobile CRAM/CCAM compounds at the surface compared to 10 cm deep), and lowest overall OM diversity in the core. The rich diversity and high concentration of organic carbon present at the 10 cm depth create excellent conditions for metals to bind to OM and accumulate. The lignin diversity is capable of retaining metals while persisting for decades in the soil (Jones, 1998; Kaplan et al., 2016; Wen et al., 2018). The OM that is present in the BP core is suited to accumulate metals, including the U that was released in the 1960's and has been mapped within the lateral extent of the former Beaver Pond (Kaplan et al., 2020).

Total concentration profiles (rightmost panels of Figure 5-3; Fe, Ni, and U, respectively) in the BP cores closely resemble the shape of the OM and S total profiles (Figure 5-2B and 2C). Iron present at BP is minimally water soluble (Figure 5-3), as a three-day cycle of daily recharge of the reaction vessel's water removed approximately 50 μg/g Fe from the soil, 0.125% of the maximum total Fe as determined from total digestion of the soil. As expected based on trends in

Fe(II)/Fe(III) solubility, Fe was more available in water in the anoxic phase (Schwertmann, 1991; Stefánsson, 2007).

Uranium and nickel core profiles also resemble the OM profile shown in Figure 5-2B. Uranium appears to be more reactive with OM at BP, as 50% of the Total U was removed in the NaPP extraction, while roughly 10% of the Ni and Fe maxima were removed via NaPP extraction. Another important relationship between OM, U, and Ni in the BP core is the differences in U and Ni removal between oxic and anoxic phases. At depths 7 cm, 10 cm, and 13 cm, when carbon was more available in the oxic phase (Figure 5-2A), U and Ni were more available in the oxic phase. Likewise, when carbon was more available in the anoxic phase, U and Ni were more available in the anoxic phase. This relationship between U, Ni, and NaPP extractable OM indicates a coupling to OM rather than sorption to reactive sites in local Fe mineralogy present in Tims Branch and much of SRS (Dixon et al., 1996). If Fe was driving the release of these metals and the OM, a comparable change in Fe in the NaPP extraction at those depths would have been expected; thus, the absence of these proportional changes in the Fe profile indicates that U and Ni at these upper surface depths are governed by OM release and changes in OM mobility due to oxidation or reduction in the upper vadose zone. Sample depth 10 cm includes the highest diversity of immobile lignin as well as potentially mobilizable phytochemicals, tannins, CRAM, and CCAM (Figure 5-2D). Coupling this diversity of compounds to the total OM present in the soil at this depth (Figure 5-2C), organic-rich soils drive both the accumulation of metals introduced to this wetland and their slow release over time.

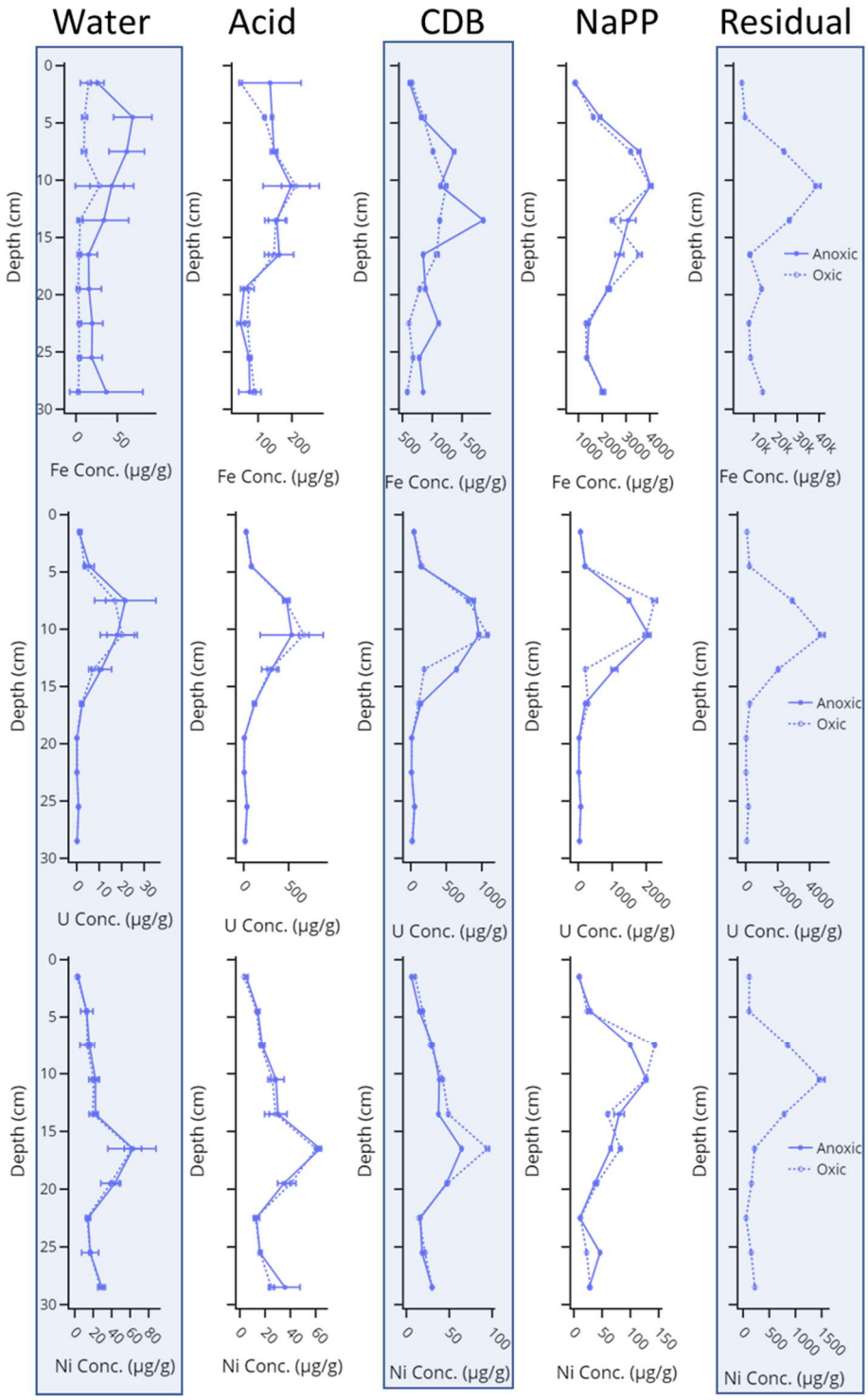

Figure 5-3: Beaver Pond extraction profiles for Fe (top), U (middle), and Ni (bottom) for all five treatments and both oxic and anoxic conditions. Treatments are described in the figure header and were conducted in parallel, as opposed to sequentially. Error bars are derived from instrumental analytical error.

Finally, the changes in the Ni profiles as a function of more harshly targeted extraction treatment (from left to right in Figure 5-3) provides evidence for an organic-based accumulation of Ni in the wetland over time and as decadal wetland cycling decomposes large, reactive organic compounds into smaller, more mobile compounds (Lehmann and Kleber, 2015; Schmidt et al., 2011a). Depths shallower than 10 cm likely contain the anthropogenic Ni released concurrently with U during M-Area process waste releases, highlighted by the similarly shaped Residual-U and Residual-Ni concentration profiles (Figure 5-3; correlation coefficient $R^2 = 0.98$, significant at $\alpha = 0.05$). However, the weaker treatments show greater Ni lability (e.g., greater propensity of Ni to partition to the aqueous phase) at deeper soil depths, indicating either an accumulation via natural wetland cycling and then a subsequent release from more weathered sediments by these extractions or a vertical migration of mobile Ni from the deposited anthropogenic pool. While there is no extensive characterization of OM other than the depth of 28 cm, the characterization of this sample and the surface samples suggest that organic compounds here are diversely mobile compounds and have lower immobile lignin content, further indicating that as OM pools degrade over time in decadal wetland cycles, the residual pool of OM has the potential to create more labile pools of trace metal ions (Lehmann et al., 2020; Lehmann and Kleber, 2015; Sutton and Sposito, 2005). The aged and degraded OM likely present at these lower depths could be more easily removed, in addition to the natural Ni that accumulated in the OM earlier in the wetland's history.

Steed Pond

Organic matter in Steed Pond sediments is more susceptible to oxidative mobilization at the surface than at depths lower than 15 cm. Noting the increase in oxic NaPP-extractable C at 5 cm (Figure 5-4A), this difference between oxygen regimes is twice as large as the gap between oxygen regimes at the most different sample in BP (Figure 5-2A). Further, the removable C fractions in SP (Figure 5-4A) are less variable as a function of depth when compared to the BP profile (Figure 5-2A). When compared to the BP surface OM, surface SP sediment has a higher diversity of lignin compounds (Figure 5-4D), a higher total OM content (Figure 5-4C), and a higher relative abundance of tannins and CCAM (Figure 5-4D). The SP reach of Tims Branch is frequently a gaining stream (Parker et al., 2022), so porewaters flowing into the stream have long resided in the subsurface and are likely reducing rather than oxidizing. Thus, these mobile carbon moieties (Figure 5-4D) could be mobilized more effectively by oxidizing solutions (Figure 5-4A) different from the native anoxic porewaters present at SP.

In the deeper soil samples, high OM content presents an opportunity to accumulate nutrients and contaminants per natural wetland cycling (Sobolewski, 1999). The layer of OM-rich soil at 16 cm (Figure 5-4B) has accumulated more S (Figure 5-4C) than any other layer in the SP core and has significantly higher (Figure 5-4D, significant at $\alpha = 0.05$) lignin than any other SP sample. The coupled higher organic content and higher lignin diversity presents conditions conducive to metal accumulation in this OM-rich soil layer. Contrasted with the oxidizable and potentially removable OM at 5 cm, this immobile layer that is diverse in lignin compounds efficiently accumulates material similar to the metal-binding observed in Tims Branch and other similar wetlands (Masscheleyn et al., 1992; Sowder et al., 2003).

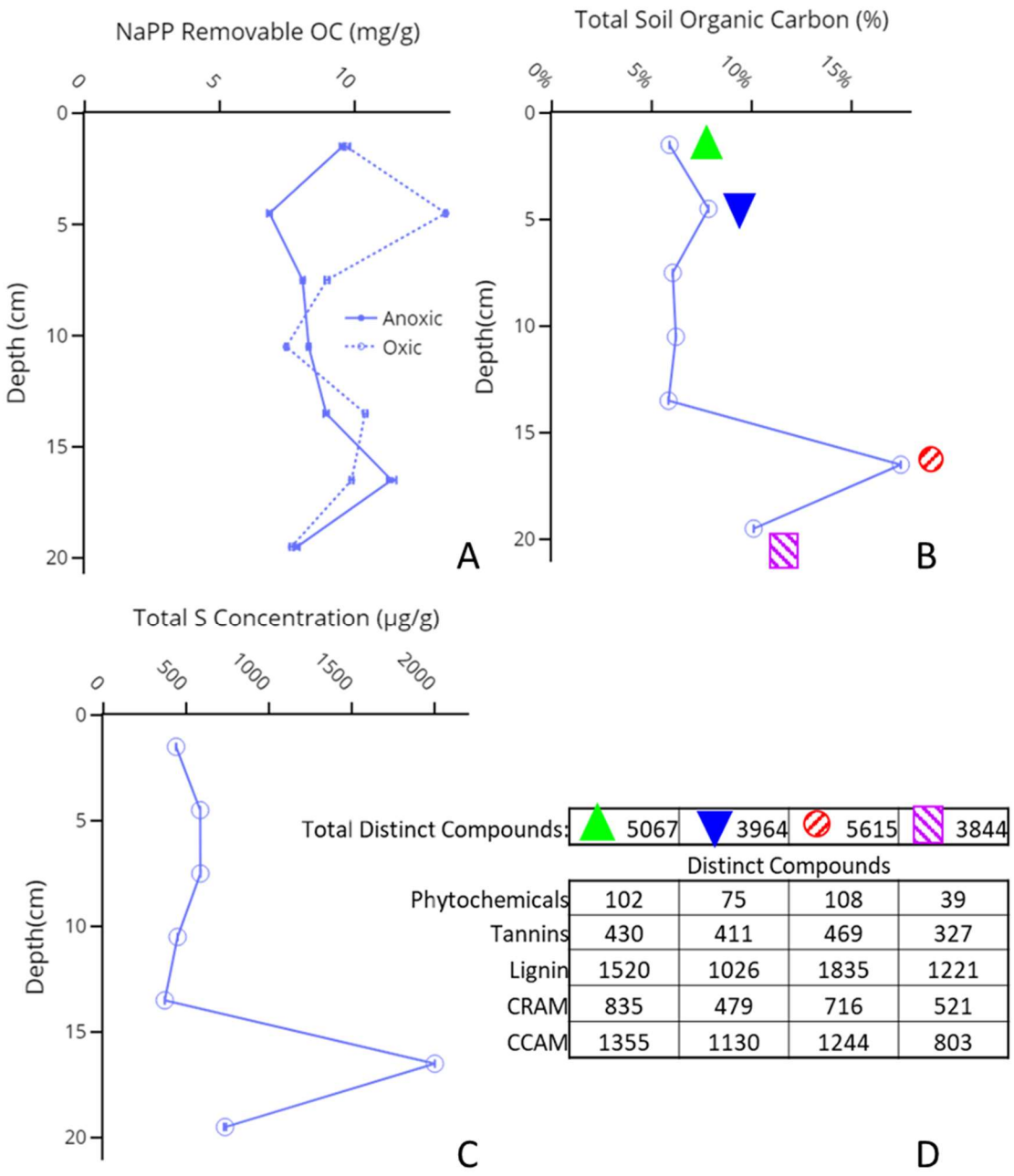

Distinct Compounds

Phytochemicals	102	75	108	39
Tannins	430	411	469	327
Lignin	1520	1026	1835	1221
CRAM	835	479	716	521
CCAM	1355	1130	1244	803

Figure 5-4: Steed Pond NaPP removable organic carbon in oxic and anoxic phases (A). Total soil organic carbon (TSOC) as determined by 0.5206 times the total OM via loss on ignition in SP core (B). Total sulfur from HF digestion of residual in SP (C). Organic matter diversity characterization for key SP sediments (D). Error bars originate from the analytical instrumental error.

Gaining stream conditions at Steed Pond move reducing water full of reduced Fe from the subsurface into the stream via hyporheic exchange. However, aqueous pools of U based on water extraction data (Figure 5-5C) are insignificant masses compared to mobilized U masses previously reported (Batson et al., 1996; Parker et al., 2022). Anoxic porewaters reasonably explain the difference between oxic and anoxic Fe released into water over the water extraction experiment (Figure 5-5A), as Fe(II) is more soluble than Fe(III) in circumneutral wetland pH values (Schwertmann, 1991; Stefánsson, 2007). If Fe were being released into waters by readily soluble organic ligands and Fe(II)/Fe(III)-OM complexes, a smaller difference between the oxic and anoxic regimes would be expected. Thus, the Fe solubility in the aqueous phase can be attributed to the solubility of Fe in local mineralogy in reducing water, but the U potentially available to upper porewaters remains inconsequential when compared to the greater U pool in the solid phase in Steed Pond sediments.

Contrasted with the Fe mineralogy and redox-based solubility, Ni and U profiles (Figure 5-5B and 5C) demonstrate more evidence of OM reactivity, accumulation within wetland OM,

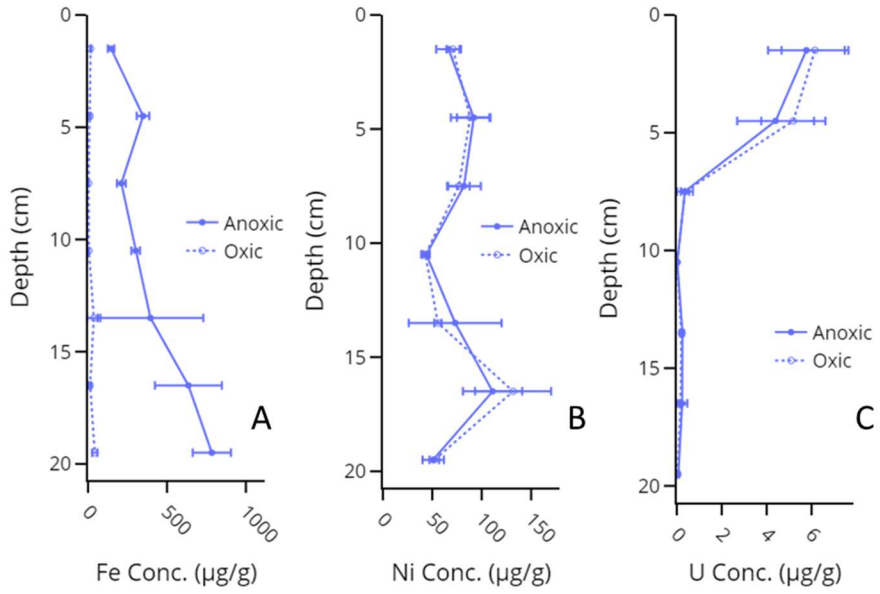

Figure 5-5: Water extractable concentrations of Fe (A), Ni (B), and U (C) in Steed Pond sediments in oxic and anoxic regimes. Error bars originate from the analytical instrumental error.

and release from deeper layers where OM has aged and weathered over time. The Ni profile (Figure 5-5B) has minimal variability with changes in oxygen regime, as Ni is not a redox-active element and would require changes in the redox state of local mineral surfaces or binding ligands to produce more labile Ni species. As the Ni and Fe (Figure 5-5A and 5B) profiles do not correspond in the water-extractable phase, it can be assumed that Ni is not bound directly to iron-bearing mineral phases but instead is complexed by OM and retained in the soil, being released by soluble Ni-OM complexes. Further, the U profile (Figure 5-5C) shows liberation of U where anthropogenic U has been deposited over the past 60 years (Batson et al., 1996; Parker et al., 2022; Sowder et al., 2003), but deeper layers release minimal U, as its natural abundance in wetland soils is lower than that of Ni (Dixon et al., 1996). Further, the U at the surface is relatively insoluble, given that three daily collections and recharges of reaction vessel water removed only 0.4% of the total U at depths 1.5 cm and 4.5 cm (Figure 5-5C, Figure B - 1). In light of the OM depth profile (Figure 5-4C) and characterization (Figure 5-4D), Ni appears to be accumulating where there is high OM with a high diversity of reactive but immobile lignin (16 cm), as well as depositing in the surface soils concurrently with U over the past 60 years (Batson et al., 1996; Keiluweit et al., 2016; Keiluweit et al., 2017; Liang et al., 1993; Parker et al., 2022; Sowder et al., 2003). Organic-bound Ni seems to be released where natural wetland cycling has sufficiently weathered the local soil and OM and gaining stream conditions cause a flux of subsurface water into the stream.

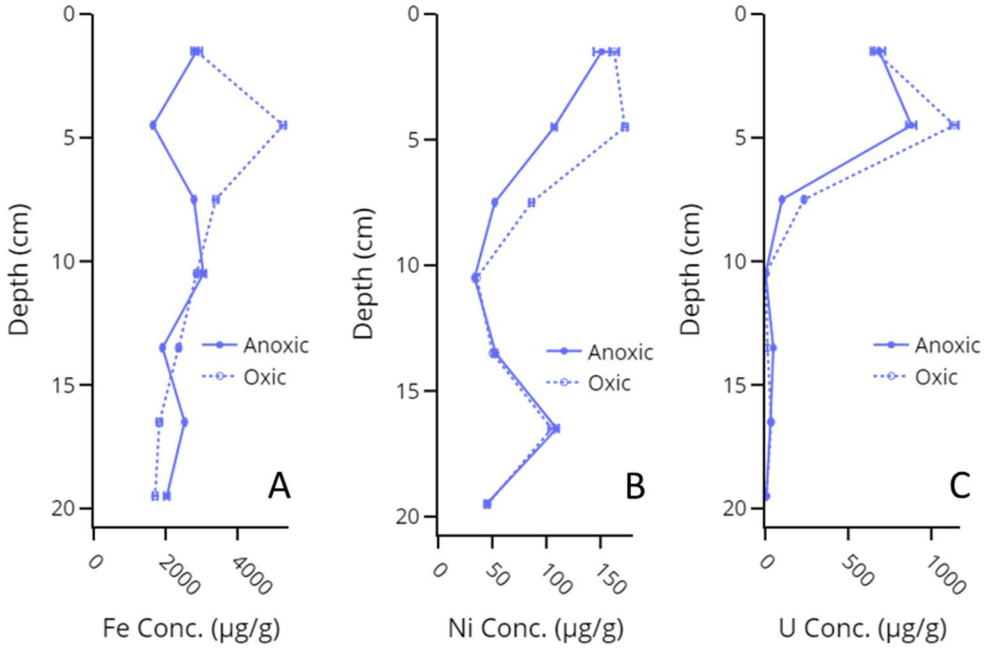

Figure 5-6: NaPP removable concentrations of Fe (A), Ni (B), and U (C) in Steed Pond sediments in oxic and anoxic regimes. Error bars originate from the analytical instrumental error.

Oxidation of OM appears to play a major role in the release of metals in SP surface soils. More C is removed in the oxic NaPP extraction (Figure 5-4A, most notably at a depth of 4.5 cm), and more Fe, U, and Ni are released at this layer in the oxic NaPP extraction (Figure 5-6). Iron released at 4.5 cm more than doubled between the anoxic and oxic conditions (Figure 5-6A), which is unexpected in light of ordinary redox-based solubility of Fe minerals (Schwertmann, 1991). However, Fe(II) and Fe(III) have been shown to mobilize in the presence of soluble oxidized OM (Keiluweit et al., 2016; Keiluweit et al., 2017; Liang et al., 1993). Nickel is not an environmentally redox-active metal, so this change between oxic and anoxic conditions can be attributed to the oxidation of the OM hypothesized to be sequestering Ni in the soil, whether that is the Fe-mineral surface, organic ligands, or a combination of both. Coupling the mobilization of Fe(II) and Fe(III) via oxidized OM to the additional release of Ni and U at 4.5 cm under oxic

conditions, it is evident that the OM is oxidizing at this depth, in addition to any oxidation of metals that may be occurring. Similar OM characterization of surface and deep soils from our local proxy site with similar hydrogeologic conditions indicates that organic moieties shift towards more mobility and reactivity when oxidized, compared to the same samples extracted in a completely anoxic atmosphere (Table B - 1).

In deeper soils of SP, the lack of change with redox conditions highlights metal retention in persistent and complex OM pools. No significant changes in Ni released in NaPP are observed at 16 cm (Figure 5-6B) where there is high OM content that has a high diversity of reactive but recalcitrant lignin. Compared to the CDB extraction at 16 cm (Figure B - 2), no additional Ni was removed in the NaPP extraction in either atmospheric regime. While these extractions were in parallel, not in sequence, I would nevertheless expect a larger change between the CDB and NaPP phases if the metals were being released due to redox-enhanced solubility (of Fe-oxide minerals being decomposed by the CDB) or if the metals were associated with more mobile OM fractions (being solubilized when oxidized). Therefore, lignin diversity within the OM-rich layer at 16 cm favors accumulation in deep SP soils based on structural incorporation into weathered mineralogy via complexation by immobile OM. Given that the CDB extraction (Figure B - 5) does not release appreciably different quantities of Fe at 16 cm compared to other extractions, the Fe present at this depth is likely immobile and structural, not coated in reactive Fe surface sites but instead potentially coated with aging, decomposing OM, as the soil is composed of 33% OM at 16 cm (Figure 5-4B).

While M-Area processes did not exclusively release depleted U (e.g., a uranium source with an anthropogenically enriched $^{238}U/^{235}U$ ratio due to selective extraction of ^{235}U during processing), one indicator that U present in shallow Tims Branch soils is undeniably

anthropogenic is the ratio of ^{238}U to ^{235}U. Ratios of $^{238}U/^{235}U$ in BP and SP soils (Figure 5-7) indicate exclusively anthropogenic U in BP and anthropogenic U in surface SP soils, while ratios closer to natural (natural $^{238}U/^{235}U = 137.8$) are prevalent in deeper soils. Beaver Pond soils, where 60% of all U released from M-Area still remains (Kaplan, et al., 2020), contain of $^{238}U/^{235}U$ ratios that vary with depth but remain wholly above the natural of $^{238}U/^{235}U$ ratio. Meanwhile, the U at Steed Pond has a maximum ratio equivalent to the maximum ratio at BP but decreases as a function of depth. Nickel, lead, chromium, and other metals (Evans et al., 1992; Reed and Swanson, 2006) were released periodically during M-Area processes but were wholly concurrent with the relatively continuous stream of U being released into Tims Branch. Uranium at the 16 cm depth is natural, based on the isotope ratio there, and has accumulated in a similar peak to the other metals. The isotope ratios in Figure 5-7 help contextualize natural U in these

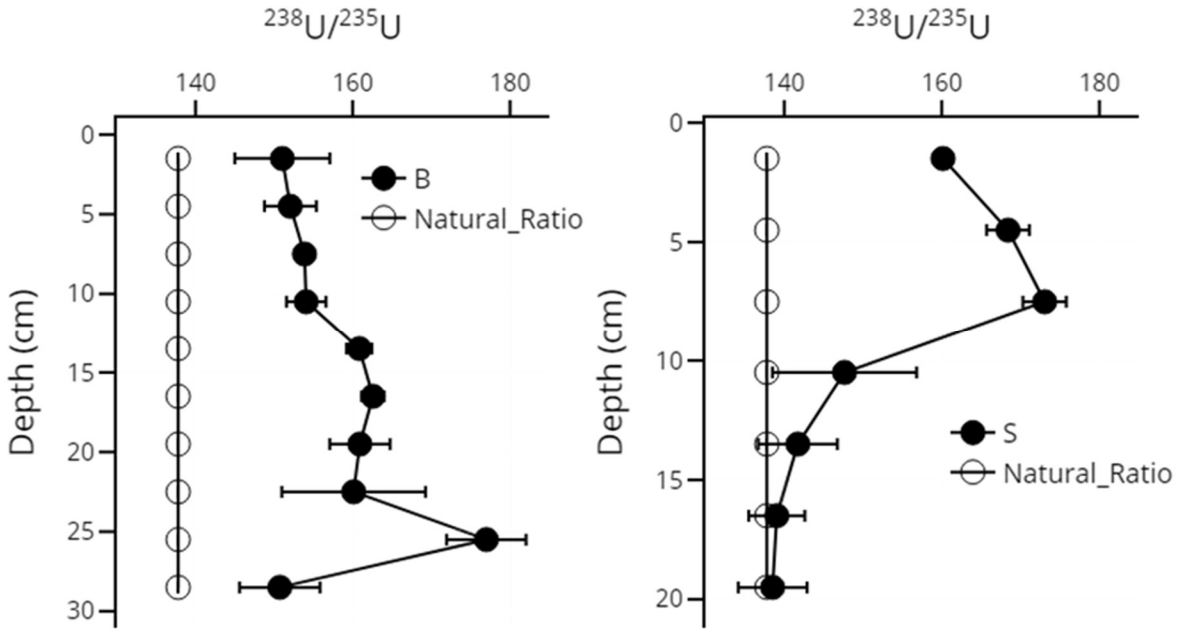

Figure 5-7: Isotopic ratios for uranium in Beaver Pond (left) and Steed Pond (right). Values greater than Natural are depleted ($^{235}U < 0.1\%$ by mass). Error bars originate from the analytical instrumental error propagated through replicate standard deviations.

wetland soils alongside metals like Ni and Pb that are often present at higher "trace" concentrations in wetlands than U is (Dixon et al., 1996).

While the magnitude of U deposition in SP soils overshadows its accumulation in deeper soils, the inset of Figure 5-8A shows a distribution of metals that indicate that U accumulates naturally with the other metals present in Tims Branch (Figure 5-8B-8E). At 16 cm, where lignin-diverse, OM-rich soil persists, a variety of heavy metals have accumulated (Figure 5-8). Soil characterization profiles shown in Figure 5-9 indicate that the soil at this 16 cm depth contains some silt and clay, in addition to the 17% TSOC (Figure 5-4). Upper soil samples show some variability, due to magnitude and frequency of releases to Tims Branch or due to natural wetland Fe and C cycling. Iron occurs at maxima of ~30,000 μg/g at 4.5 and 16 cm (Figure 5-8E), and Fe minerals are likely weathering over time in this gaining stream reach, decreasing in total concentration both over time and as a function of depth. However, the accumulation of natural U (Figure 5-7B) at 16 cm alongside other metals known to accumulate in wetlands from both natural and anthropogenic sources (Sobolewski, 1999) indicates that wetland OM—most notably the immobile but metal-reactive lignin that is diversely present in the 33% OM soil layer at 16 cm (Figure 5-4C and 4D)—is responsible for the accumulation observed in deeper SP soils. Harsh NaPP treatment targeting metals strongly bound to OM succeeded in removing no more than 10% of their maxima for metals other than U in SP (Figure 5-6), indicating that these metals are becoming so strongly incorporated into natural wetland Fe and C cycles that even a harsh, targeted treatment cannot strip these metals from structural, immobile OM.

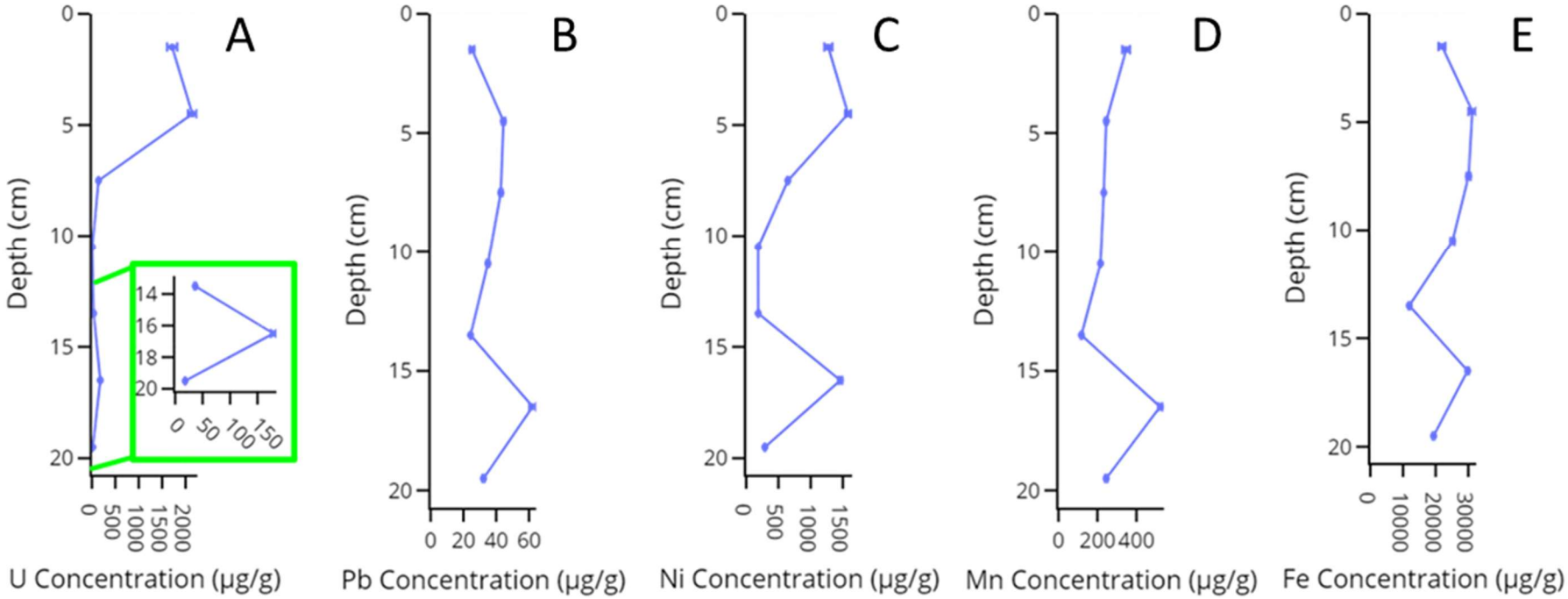

Figure 5-8: Total metal concentrations (U, Pb, Ni, Mn, and Fe, from left to right, respectively) at Steed Pond. The peaks at 16 cm correspond to the high OM layer in the Steed Pond core (Figure 5-4B). Error bars originate from the analytical instrumental error.

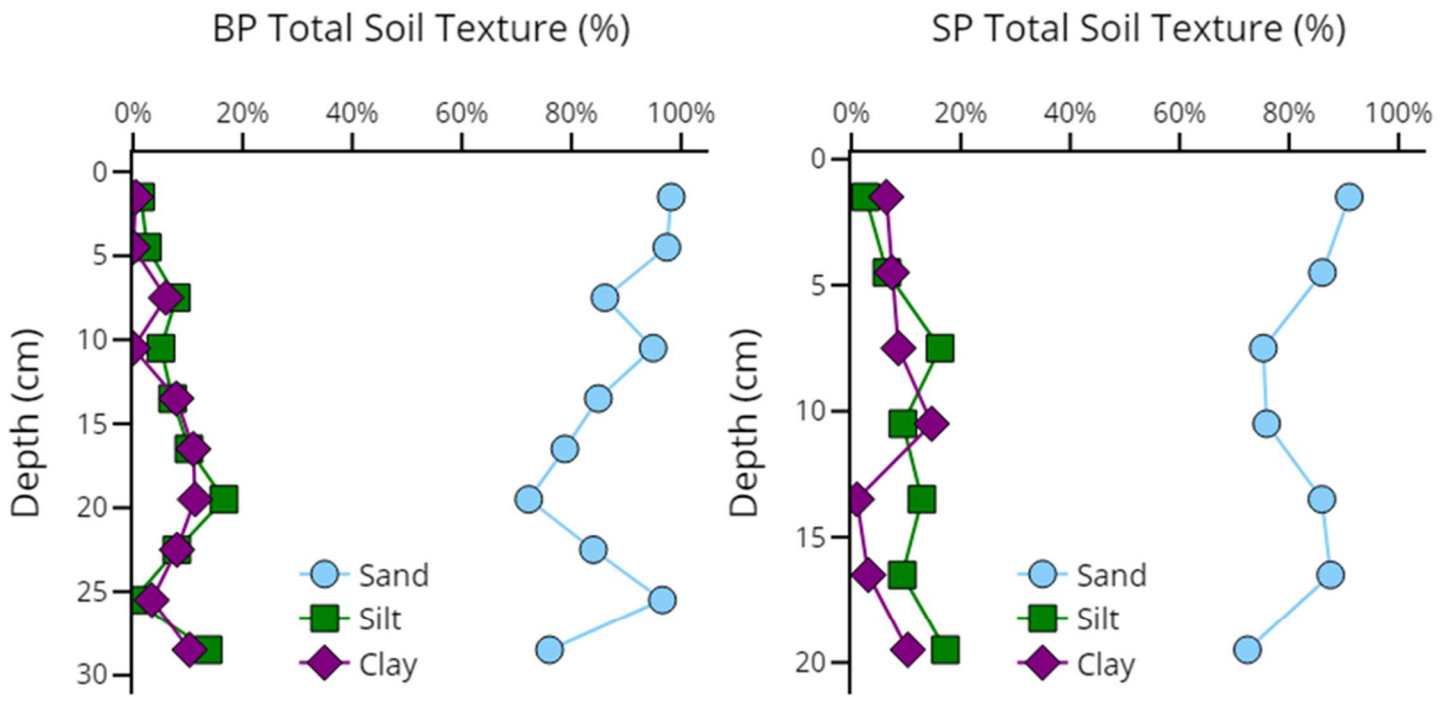

Figure 5-9: Beaver Pond soil texture characterization (left) and Steed Pond characterization (right) based on hydrometer measurements in Eq. 5-1, 5-2, and 5-3.

Conclusions

Based on the redox-preserved targeted extractions presented in this work, I conclude that OM pools— particularly the more immobile, structural, metal-reactive pools deeper in soil columns—are responsible for metal accumulation in Tims Branch. While this study only digested two soil cores, previous work (Batson et al., 1996; Evans et al., 1992; Kaplan et al., 2020; Parker et al., 2022; Sowder et al., 2003) supports the notion that the total concentrations presented here are relevant and indicative of the soils at BP and SP. The retention of 80% of U released between 1965 and 1984 (Kaplan, et al., 2020) has been jointly attributed in previous work (Parker et al., 2022) to surface-reactive Fe mineralogy present in the soil and the presence of OM deposited throughout the wetland at varying concentrations based on the complex hydrologic history of Tims Branch. However, this work demonstrates that OM governs metal availability and that Fe can be considered a "trace" metal that is coincidentally present at high concentrations. Through this lens, the profiles presented in Fig. 8 for the suite of metals relevant to Tims Branch can be better understood. Iron originating upgradient in the watershed has been consistently depositing at Steed Pond over time in natural wetland cycles (Schlesinger and Bernhardt, 2013), and inputs of other transition and heavy metals from M-Area have become incorporated into these cycles at magnitudes proportional to their original releases.

Four key conclusions emerge from this investigation of heavy metal distributions in anthropogenically contaminated wetland soils:

- Oxidation of metal-binding organic matter in surface soils causes the release of the metals from the soil, potentially into native porewaters
- Immobile pools of structural organic matter at deeper soil column depths are less susceptible to oxidative release of metals

- Metal-bearing soil OM required harsh NaPP treatment to remove from the sediment, indicating that, under natural conditions, it is immobile, along with the bound metals
- Wetland metal accumulation is occurring for natural abundances of heavy metals in Tims Branch. While accumulation of anthropogenic U in surface soils overshadows deeper U pools, U accumulation parallels the accumulation of Ni, Pb, Mn, and Fe in Steed Pond, as evidenced by the increase in natural U immobilized alongside these metals.
- Hydrologic contextualization of local geochemistry is required to understand how metal inventories may be mobilizing or accumulating in wetland soils; gaining and losing conditions present opportunities for metals, OM, or metal-OM complexes to be interacting with native porewaters, streamwaters, or metal-binding soils.

Future work will consist of identifying how these metal releases change seasonally, identifying to what degree the labile porewater metal fraction impacts overall metal fluxes within and from the wetland, and quantifying fluxes from the wetland in the aqueous- and solid-phases in light of porewater inventories and intensity of hydrologic events.

References

Batson, V.L., Bertsch, P.M. and Herbert, B.E. (1996) Transport of Anthropogenic Uranium from Sediments to Surface Waters During Episodic Storm Events. Journal of Environmental Quality 25, 1129-1137.

Chen, C., Hall, S.J., Coward, E. and Thompson, A. (2020) Iron-mediated organic matter decomposition in humid soils can counteract protection. Nature communications 11, 1-13.

Day, P.R. (1965) Particle fractionation and particle-size analysis, Methods of Soil Analysis: Part 1 Physical and Mineralogical Properties, Including Statistics of Measurement and Sampling. Wiley Online Library, pp. 545-567.

Dixon, K.L., Rogers, V.A., Conner, S.P., Cummings, C.L., Gladden, J.B. and Weber, J.M. (1996) Geochemical and physical properties of wetland soils at the Savannah River site. Savannah River Site (SRS), Aiken, SC.

EPA (1996) Method 3052: Microwave Assisted Digestion of Siliceous and Organically Based Matrices, Washington, DC, p. Revision 2.

Evans, A.G., Bauer, L.R., Haselow, J.S., Hayes, D.W., Martin, H.L., McDowell, W.L. and Pickett, J.B. (1992) Uranium in the Savannah River Site Environment, Aiken, SC, pp. WSRC-RP-92-315.

Guo, X., Zhang, S. and Shan, X.q. (2008) Adsorption of metal ions on lignin. Journal of Hazardous Materials 151, 134-142.

Hall, G.E.M., Vaive, J.E. and MacLaurin, A.I. (1996) Analytical aspects of the application of sodium pyrophosphate reagent in the specific extraction of the labile organic component of humus and soils. Journal of Geochemical Exploration 56, 23-36.

Jones, D.L. (1998) Organic acids in the rhizosphere-a critical review. Plant and Soil 205, 25-44.

Kaplan, D.I., Smith, R., Parker, C.J., Baker, M., Cabrera, T., Ferguson, B.O., Kemner, K.M., Laird, M., Logan, C., Lott, J., Manglass, L., Martinez, N.E., Montgomery, D., Seaman, J.C., Shapiro, M. and Powell, B.A. (2020) Uranium Attenuated by a Wetland 50 Years after Release into a Stream. ACS Earth Space Chem 2020, 1360-1366.

Kaplan, D.I., Xu, C., Huang, S., Lin, Y., Tolić, N., Roscioli-Johnson, K.M., Santschi, P.H. and Jaffé, P.R. (2016) Unique Organic Matter and Microbial Properties in the Rhizosphere of a Wetland Soil. Environmental Science and Technology 50, 4169-4177.

Keiluweit, M., Nico, P.S., Kleber, M. and Fendorf, S. (2016) Are oxygen limitations under recognized regulators of organic carbon turnover in upland soils? Biogeochemistry 127, 157-171.

Keiluweit, M., Wanzek, T., Kleber, M., Nico, P. and Fendorf, S. (2017) Anaerobic microsites have an unaccounted role in soil carbon stabilization. Nature Communications 8.

Kobashi, A., Choppin, G.R. and Morse, J.W. (1988) A study of techniques for separating plutonium in different oxidation states. Radiochimica Acta 43, 211-216.

LaRowe, D.E. and Van Cappellen, P. (2011) Degradation of natural organic matter: a thermodynamic analysis. Geochimica et Cosmochimica Acta 75, 2030-2042.

Lehmann, J., Hansel, C.M., Kaiser, C., Kleber, M., Maher, K., Manzoni, S., Nunan, N., Reichstein, M., Schimel, J.P., Torn, M.S., Wieder, W.R. and Kögel-Knabner, I. (2020) Persistence of soil organic carbon caused by functional complexity. Nature Geoscience 13, 529-534.

Lehmann, J. and Kleber, M. (2015) The contentious nature of soil organic matter. Nature 528, 60-68.

Liang, L., McCarthy, J.F., Jolley, L.W., McNabb, J.A. and Mehlhorn, T.L. (1993) Iron dynamics: Transformation of Fe (II)/Fe (III) during injection of natural organic matter in a sandy aquifer. Geochimica et Cosmochimica Acta 57, 1987-1999.

Masscheleyn, P.H., Pardue, J.H., DeLaune, R.D. and Patrick, J.W.H. (1992) Chromium redox chemistry in a lower Mississippi Valley bottomland hardwood wetland. Environmental Science & Technology 26, 1217-1226.

Mehra, O.P. and Jackson, M.L. (1958) Iron Oxide Removal from Soils and Clays by a Dithionite-Citrate System Buffered with Sodium Bicarbonate. Clays and Clay Minerals 7, 317-327.

Parker, C.J., Kaplan, D.I., Seaman, J.C. and Powell, B.A. (2022) Uranium partitioning from contaminated wetland soil to aqueous and suspended iron-floc phases: Implications of dynamic hydrologic conditions on contaminant release. Geochimica et Cosmochimica Acta 318, 292-304.

Powell, B.A., Fjeld, R.A., Kaplan, D.I., Coates, J.T. and Serkiz, S.M. (2004) Pu (V) O2+ adsorption and reduction by synthetic magnetite (Fe3O4). Environmental science & technology 38, 6016-6024.

Powell, B.A., Fjeld, R.A., Kaplan, D.I., Coates, J.T. and Serkiz, S.M. (2005) Pu (V) O2+ adsorption and reduction by synthetic hematite and goethite. Environmental science & technology 39, 2107-2114.

Powell, B.A., Kersting, A., Zavarin, M. and Zhao, P. (2008) Development of a Composite Non-Electrostatic Surface Complexation Model Describing Plutonium Sorption to Aluminosilicates. Lawrence Livermore National Lab.(LLNL), Livermore, CA (United States).

Reed, M.B. and Swanson, M.T. (2006) 300/M-Area-Fuel and Target Fabrication. New South Associates: Stone Mountain, GA, Stone Mountain, GA, p. Rep. No. 1189.

Schlesinger, W.H. and Bernhardt, E.S. (2013) Biogeochemistry: An Analysis of Global Change. Elsevier Science.

Schmidt, M.W., Torn, M.S., Abiven, S., Dittmar, T., Guggenberger, G., Janssens, I.A., Kleber, M., Kogel-Knabner, I., Lehmann, J., Manning, D.A., Nannipieri, P., Rasse, D.P., Weiner, S. and Trumbore, S.E. (2011a) Persistence of soil organic matter as an ecosystem property. Nature 478, 49-56.

Schmidt, M.W.I., Torn, M.S., Abiven, S., Dittmar, T., Guggenberger, G., Janssens, I.A., Kleber, M., Kögel-Knabner, I., Lehmann, J. and Manning, D.A.C. (2011b) Persistence of soil organic matter as an ecosystem property. Nature 478, 49-56.

Schultz, M.K., Burnett, W.C. and Inn, K.G.W. (1998) Evaluation of a sequential extraction method for determining actinide fractionation in soils and sediments. Journal of environmental radioactivity 40, 155-174.

Schwertmann, U. (1991) Solubility and dissolution of iron oxides. Plant and Soil 1991 130:1 130, 1-25.

Schwertmann, U., Wagner, F. and Knicker, H. (2005) Ferrihydrite-Humic Associations. Soil Science Society of America Journal 69, 1009-1015.

Sobolewski, A. (1999) A review of processes responsible for metal removal in wetlands treating contaminated mine drainage. International Journal of Phytoremediation 1, 19-51.

Sowder, A.G., Bertsch, P.M. and Morris, P.J. (2003) Partitioning and availability of uranium and nickel in contaminated riparian sediments. Journal of Environmental Quality 32, 885-898.

Stefánsson, A. (2007) Iron(III) hydrolysis and solubility at 25°C. Environmental Science and Technology 41, 6117-6123.

Sutton, R. and Sposito, G. (2005) Molecular structure in soil humic substances: The new view. Environmental Science and Technology 39, 9009-9015.

von Lützow, M., Kögel-Knabner, I., Ekschmitt, K., Flessa, H., Guggenberger, G., Matzner, E. and Marschner, B. (2007) SOM fractionation methods: relevance to functional pools and to stabilization mechanisms. Soil Biology and Biochemistry 39, 2183-2207.

Wen, J., Li, Z., Luo, N., Huang, M., Yang, R. and Zeng, G. (2018) Investigating organic matter properties affecting the binding behavior of heavy metals in the rhizosphere of wetlands. Ecotoxicology and Environmental Safety 162, 184-191.

VI. MOBILE URANIUM & NICKEL SOLIDS IN A CONTAMINATED WETLAND OVER THREE SEASONS: STREAMBANK EROSION MOVES MORE METAL THAN IRON-ORGANIC MATTER FLOCS

Introduction

Approximately 43,500 kg of uranium (U) was released into the Tims Branch wetland at the United States Department of Energy (DOE) Savannah River Site (SRS) in process waste effluents in the mid 1960's (Evans et al., 1992). Today, the wetland continues to sequester much of the U with 83% of the released U accounted for in a 1 km reach of the Tims Branch wetland. The most contaminated sections are former pond floors from an area with common beaver dams (Beaver Pond) and a former anthropogenically dammed pond for cattle watering (Steed Pond) (Kaplan et al., 2020; Parker et al., 2022). By 1984, process waste effluents had ceased, the Beaver Dam was removed, and the Steed Pond dam had failed, resulting in the exposure of these former pond floors to the atmosphere. Hydrologically, the presence of two dammed ponds where a creek opens up to a wide, flat wetland creates ideal settling basins for contaminated sediments to accumulate. Geochemically, the iron (Fe) content of local soils (Dixon et al., 1996) and high soil organic matter (OM) concentrations (Parker et al., 2022) provide ample mineral surfaces and complexing ligands to react with the U and concurrently released nickel (Ni). Coupled together, the hydrobiogeochemistry of Tims Branch has successfully retained 36,100 kg U for decades (Kaplan et al., 2020).

Organic matter is often responsible for the sequestration of metals in wetlands, as the high concentrations and diversity of OM are reactive with heavy metals (Sobolewski, 1999). Long-term studies of North American wetlands show that contaminated influents containing high concentrations of heavy metals react with wetland OM, and effluent waters are released with significantly decreased metal concentrations (Masscheleyn et al., 1992; Sobolewski, 1999).

Mixing of anoxic subsurface waters bearing Fe(II) and OM via hyporheic exchange with oxic surface waters leads to the formation and aggregation of Fe-OM flocs. The flocs are colloidal ferrihydrite and other amorphous Fe(III)-oxide minerals (Philippe and Schaumann, 2014) which are stabilized by OM and deposit in low energy stream reaches and pockets along the streambank (Lapworth et al., 2013; Liao et al., 2017; Liao et al., 2020). Such flocs have been hypothesized to play a significant role in U transport in Tims Branch, particularly in Steed Pond, where the gaining conditions favor their formation (Parker et al., 2022).

One variable inherently difficult to study with regard to wetland metal transport and retention is the frequency and impact of intense storm events. An important study of the late 1990's was conducted by Batson *et. al.,* (1996) to track U concentrations in dissolved and solid phases during storm events at Steed Pond. The study found that roughly 2.2 kg of U left the wetland in surface waters over the course of the two storm events studied but made no distinction between the composition of the solids and whether they were flocs, suspended contaminated solids, or a combination of the two (Batson et al., 1996). While flocs are considered suspended solids, they enter the stream channel in a different manner than suspended eroded streambank sediment; flocs form via the hyporheic influx of Fe(II)-rich porewaters and are scoured from streambanks by sharp increases in flow during storm events, while the omnipresence of streambed solids allows for those to erode and mobilize at a more constant rate. To differentiate the work presented here from the Batson et. al. (1996) study, I focus on floc-facilitated processes as well as the seasonal fluxes of streambed sediments. Our work seeks to fill this literature void by studying Steed Pond in addition to the previously undiscovered Beaver Pond with stream flow monitoring and rainfall measurements. I investigate differences before and after a storm event and study the changes in stream metal inventory.

Studies performed on entire watersheds have focused on tracking water quality as a function of storm onset and the return to baseflow. A series of studies richly characterized metal concentrations in dissolved, colloidal, and solid species as a function of time and space within watersheds and using bromine tracers to characterize watershed properties during the synoptic sampling schemes (Church et al., 1997; Kimball et al., 2007). Metals available in the stream increased in storm flow, and the collection and ultrafiltration of Fe-oxide colloids determined that these formed over dry periods and were the first stream constituent to be scoured and removed, undetected within subsequent fluxes of solids through the watershed (Kimball et al., 2007). Mine drainage runoff before, during, and after a storm in a Colorado watershed found similar results; Fe-oxide colloids bear some of the metals from the mine tailing headwaters, but the colloids require precise hydrogeochemical conditions to form and aggregate, and the colloidal species are the first to scour during high flow events (Church et al., 1997). These watershed studies have demonstrated that suspended eroded sediment loads bear higher metal inventories on kilometer scales compared to the short pulses of transient colloidal species (Church et al., 1997; Kimball et al., 2007). Our work intends to determine the specific impact of floc-facilitated U transport on the total U inventory within the wetland and estimate total seasonal fluxes of U.

This yearlong study aims to identify any seasonal effects in the processes both retaining metals within Tims Branch and potentially releasing them—from either the Beaver Pond area towards the downgradient Steed Pond stream reach, or from Steed Pond to the remainder of Tims Branch and ultimately Upper Three Runs Creek and the Savannah River. Four main components of the study were conducted over the past year. First, I investigate U and Ni inventories in flocs collected after 21 days of dryness preceding a 100-year storm event and collected again after 12

cm of rainfall had occurred over the 10-day storm system. Next, flocs collected biweekly from July 2021 through February 2022 were sequentially extracted to target metal inventories associated with organic matter and Fe-oxide minerals. During these biweekly campaigns, porewater and streamwater samples were collected at Beaver Pond and Steed Pond to inform the development of an annual profile of what is actively moving in the stream in the solid and aqueous phases. Finally, these stream inventories were correlated to stream stage, stream flow, rainfall, and piezometer data to create an initial estimate of potential U and Ni fluxes from the wetland. Previous studies characterized lateral deposition of U (Kaplan et al., 2020), U concentrations as a function of depth at each hotspot (Parker et al., 2022), U transport during storm events (Batson et al., 1996), and redox effects impacting U, Ni, and Fe partitioning in OM-rich soils at each hotspot (Chapter 5). This work builds upon these previous studies by using consistent methods to focus on temporal variability at Beaver Pond and Steed Pond.

Methods

Hydrologic Monitoring

The two study sites, the upgradient Beaver Pond contamination area and the downgradient former Steed Pond floor, were instrumented with stream gages, piezometers, and a streamflow velocity meter exclusively at Steed Pond. Stream gages were oriented with the screened face of an open PVC pipe parallel to stream flow 10 cm above the streambed in the center of the channel. Stream stage was measured by the transducer (Levellogger 5 Jr., Solinst) 1.5 m inland to minimize data artifacts caused by stream velocity pressure. The L-shaped stream gage design (Figure C - 1) and the inland piezometer were surveyed (Nikon Totalstation) to ensure all instrument depths were in reference to the stream gage inflow point. The piezometers were bored with a 2-inch diameter auger, and a 2-inch diameter screen was used, which totaled

12 cm in length at the end of the piezometer. Piezometers had matching transducers and the screened inflow point was installed so that the transducer would be at the same elevation as the stream gage screen, to ensure that the difference in pressure measurements would represent the head at the same absolute elevation in the stream and in the ground. For all surveying, the stream gage screen was the absolute reference, and the transducer was level with this point. Thus, the transducer in the piezometer was also at this absolute elevation. Transducers collected pressure measurements every 5 minutes and were corrected with barometric data collected at a nearby Solinst Barologger. The stream gage and piezometer were installed as a transect perpendicular to stream flow so that the data from the two instruments would yield a net head calculation along the transect.

Hydraulic conductivity surrounding the piezometer 1.545 m from the stream was determined by performing Hvorslev slug tests (Hvorslev, 1951) (n=3 at each location) by using Eq. 6.1 as follows:

$$K = \frac{r^2 \ln\left(\frac{L_e}{R}\right)}{2L_e t_{37}} \qquad \text{Eq. 6.1}$$

Where K is hydraulic conductivity (m/s), r is the radius of the piezometer, R is the radius of the bore, L_e is the length of the screen at the piezometer's end (m), and t_{37} is the time to 37% of the maximum head achieved at the slug test's onset. The average hydraulic conductivity was used as a representative of the radial hydraulic conductivity.

For the stream flow measurements, a Sontek IQ-Pipe stream flow meter was installed in the stream at Steed Pond and surveyed (Nikon N5 Totalstation) in reference to the stream channel cross-section, to program the instrument with the stream area and to integrate stream velocity with flowrate. This instrument was operational beginning September 13, 2021, and it made measurements every 30 minutes. The instrument runs on a 12V deep-cycle marine battery

and could make measurements for roughly 8 days before loss of power, and a new battery was exchanged roughly biweekly, resulting in the sparsity of data at times. This data sparsity lead to cycles of roughly 8 days of data followed by 6 or 7 without (until I was on site to replace the marine battery). The instrument returned stream cross-sectional area (based on user-provided stream channel surveys to establish the streambanks as a reference), stream velocity, and stream flowrate (m^3/s, after multiplying the area and velocity together). Sontek IQ units perform most effectively when water levels are dynamic; thus, during flow periods at or below baseflow, measurements were occasionally erratic but resembled baseflow conditions.

At the Steed Pond sampling location, the 5-minute stream gage data was used to find a relationship to stream flowrate. An exponential relationship:

$$y = ae^{bx} \qquad \text{Eq. 6.2}$$

Correlated the stream flowrate (m^3/s) and stream stage (m) to one another, where stream flowrate is y, stream stage is x, and a and b are fit parameters. Data was split in half, and one half was used to train the model while the other half was used to test the model; thus, the R^2 correlation coefficient reported was calculated using the stream stage (x) values of the *test* dataset in the stream flow model and comparing to the known y (stream flowrate) values. While the data extrapolate beyond the bounds of measurement temporally, the most severe rainfall and flow event during the sampling season was recorded with the instrument. As such, the data do not extrapolate beyond the flowrates measured by the IQ instrument. One final assumption is that the stream channel has not changed in area or in roughness (i.e., the absence/presence of streambank vegetation, flow deviations from fallen trees, significant erosion), which renders this stream flowrate model useful only adjacent to these sampling campaigns and while researchers are frequently visiting the site to ensure that no major changes have occurred.

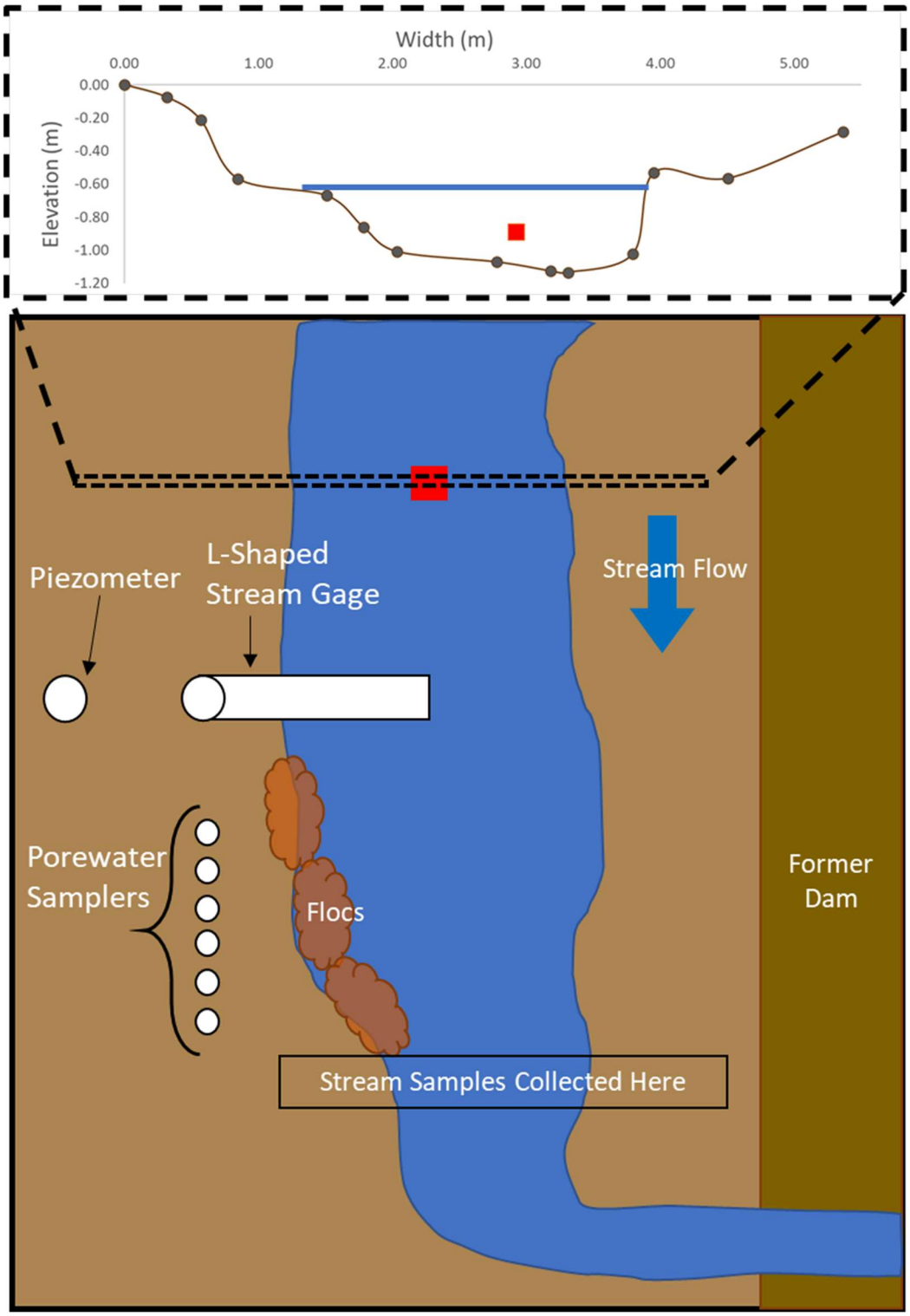

Figure 6-1: Map of Steed Pond sampling site and instrumentation. The inset represents the surveyed streambed and streambank points input into the Sontek unit and is an upstream view. The red box corresponds to the Sontek unit and its surveyed coordinates. Flocs were collected along the left bank, where they were frequently observed to be accumulated on stream banks and stream beds. The blue line in the inset represents the frequent stream stage relative to the Sontek.

Pre- and Post-Storm Floc Sampling

Flocs were collected after 21 days without rainfall in Tims Branch and again after the storm the following week in early June 2021 (n= 12, each site, each event). Flocs were present only at Steed Pond and only before the storm event. After the rainfall at Steed Pond and for both sampling events at Beaver Pond, flocs were not visible. Suspended solids roughly 2 cm from the streambed were collected so that ordinary stream sediments were not accounted as flocs. A 50 mL hand syringe was used to deliberately collect samples from the condensed floc mats covering streambeds and streambanks. These mats resemble the ochre, "fluffy" section of the water column in Figure 4-1, the portion labeled "Settled Floc Mat." Ordinary streamwater grab-sampling would likely incur enough turbulence to dislodge the floc mats and prevent n=12 samples from being collected before flocs advanced downgradient.

In the laboratory, the samples were vacuum filtered through tared 0.45 μm filters (Thermo Scientific, cellulose nitrate, 47 mm) and the filtrate collected. Filters were dried at 50°C for 24 hours to eliminate residual water and then weighed on a microbalance (Mettler Toledo MX-5 Ultra Microbalance, Mettler Toledo). Filters were placed into a 50 mL centrifuge tube with 10 mL of DDI H_2O (>18 mΩ) and sonicated for 30 min. Filters were removed from the slurry, dried at 50°C for 24 hours, and weighed on the microbalance to determine both the total solids collected and the total solids digested, by difference. The slurry was amended with 20 mL concentrated HNO_3 to achieve a 2:1 HNO_3:H_2O digestion matrix and were allowed to degas for 24 hours while OM volatilized. After another addition of 10 mL concentrated HNO_3, samples were shaken at 50°C for 24 hours. Reactions for all Beaver Pond and the post-storm Steed Pond samples were complete at this step. Pre-storm Steed Pond samples rich in floc required further treatment. Suspensions were centrifuged at 4400 rpm for 20 minutes and the supernatant

decanted and collected. Another 30 mL addition of 2:1 HNO_3:H_2O was added, and suspensions were shaken and sonicated to redistribute the floc pellet. The 24-hour degas followed by 24-hour heat and shake cycle was repeated, and the supernatant of the centrifuged suspension was added to the initial digestate. Aliquots of all digestate and filtrate samples were diluted for analysis by inductively coupled plasma mass spectrometry (ICPMS, Thermo RQ) in a 2% HNO_3 analysis matrix.

Bi-monthly Stream and Porewater Sampling

Stream water and porewater was collected every other week from July until February. Unlike the initial pre-storm and post-storm sampling event, sampling was done periodically. Thus, field observations of the extent of floc persistence in the main water channel versus floc mats which were settled on the streambed were critical to evaluation of these data. All sampling events had some degree of floc formation and accumulation on streambanks. However, the flocs varied from dark brown mats less than 1 cm thick to vivid orange-ochre mats roughly 7 cm thick on the banks (July 20, 2021). This July 20th sampling event was the only event in which the flocs were visibly present in the stream and thereby collected during our streamwater grab samples, described below. Otherwise, stream channels were relatively clear, or lightly turbid and brown with high OM and increased sediment loads.

For streamwater samples, four 125 mL grab samples were collected in the stream in a T-shape, three at the top of the water column (in the middle and each side, 10 cm deep from the surface) and one at the bottom of the stream channel (10 cm or less, when water levels were lower than 20 cm total). Samples were taken at a sandy clayey bed where water level varied between ~20 and 40 cm when I was collecting samples. Stage rose higher than this when we were not present. Additionally, corresponding 40 mL samples were collected in glass vials for

TOC analysis (Shimadzu TOC-V TOC Analyzer) after filtration through a 0.45 µm syringe filter. All 125 mL grab samples were vacuum filtered and processed as the floc samples were managed in Section 2.2, with the only difference being that PTFE filters were used from July onward, as their durability allowed for higher recoveries of solids for digestion. When samples contained dense floc material, the second digestion was performed, and the supernatant was combined with the primary digestate when samples had clearly not fully digested.

The total concentration of analytes in both the stream aqueous filtrates and the digested solids in each top and bottom stream water column sample was determined using Equation 6.3.

$$[Me]_{Total} = \frac{\sum_{i=1,2,3,4}([Me]_{SS,i} * SS_i * V_i + [Me]_{aq,i} * V_i)}{\sum_{i=1,2} V_i} \quad \text{Eq. 6.3}$$

Where [*Me*] can be either U, Ni, or Fe, indices 1 through 4 represent the four water column samples, $[Me]_{SS}$ is the concentration in the stream solids (µg/g, dry), $[Me]_{aq}$ is the <0.45 µm aqueous fraction concentration (µg/L), *V* is the volume of water collected for that sample (L), *SS* is the suspended solids loading in the stream (g/L) for all stream solids collected by a 0.45 µm filter. The $[Fe]_{Total}$, $[U]_{Total}$, and $[Ni]_{Total}$ concentrations calculated at each location represent the entire mass concentration in the sample, including the aqueous and floc contributions of Fe, U, and Ni (Eq. 6.3). This can be considered an integrated mass for reactive transport modeling efforts. This integrated mass includes dissolved species (<0.45 µm, $[Me]_{aq}$ in Eq. 6.3), and colloids and suspended sediment (>0.45 µm, $[Me]_{SS}$ in Eq. 6.3). No size differentiation was made between colloidal floc species and eroded sediments, as sample processing limitations resulted in only one filtration step.

Beginning with the July 20th sampling event, additional floc samples were collected in Steed Pond. One sample was digested with the 2:1 HNO_3:H_2O method, while the other three were digested following a simplified version of the sequential extraction of environmental solids

(Schultz et al., 1998). Three phases were targeted in the flocs: water extractable (assumed to be the filtrate), the organic-bound metals (extracted with sodium pyrophosphate and referred to as NaPP), and the metals bound in Fe-oxide minerals (extracted with Citrate-Dithionite-Bicarbonate, referred to as CDB).

After filtration, massing of the dried filters, and collection of the solid floc material, reaction vessels were amended with 30 mL of 0.1 M $Na_2P_2O_7$ and rotated end over end for 24 hours (Hall et al., 1996). Upon centrifugation, the supernatant was decanted, collected, and an aliquot was diluted to 2% HNO_3 for ICPMS analysis. The alkaline extraction results in a supernatant pH of roughly 10. As such, the tar black, viscous solution was confirmed to consist of soluble material when filtered through an 0.45 μm filter and passed through. The solids that remained in the reaction vessel after supernatant collection were amended with CDB. Adapted from Mehra and Jackson (1958), the CDB extraction targeted Fe-oxides in the soil. Reaction vessels were prepared by amending the remaining floc with 30 mL of 0.3 M $NaHCO_3$/0.2 M Na-Citrate, and the extraction was initiated by adding 1 g of $Na_2S_2O_{4(s)}$, producing rapid, vigorous effervescence (Mehra and Jackson, 1958). These were heated at 50°C for 30 minutes then centrifuged, and the supernatant was decanted and collected. An aliquot of the supernatant was diluted in 2% HNO_3 for ICPMS analysis.

Porewater samples were collected with porous cup samplers (Soil Moisture Company, Simpler Micro Samplers) inserted to various depths (n=6 at each site). At Steed Pond, samplers were inserted to collect at depths of 10, 15, 20, 25, 30, and 35 cm, while at Beaver Pond, samplers sampled from depths of 15, 25, 35, 45, 55, and 67 cm. All depths were relative to the soil surface. Samplers at Beaver Pond were deeper due to the lower water table and dominantly losing stream conditions for most of the year. Roughly 50 mL of porewater was collected from

each porous cup sampler for each sampling event, and a 5 mL aliquot of this was dispensed into a glass vial for TOC analysis (Shimadzu TOC-V TOC Analyzer) after filtration through a 0.45 μm syringe filter. All samples were similarly prepared for analysis via ICPMS in a 2% HNO_3 analysis matrix. Measurements of pH (PCTSTestr 50, Oakton Instruments), oxidation-reduction potential (ORP, ORPTestr 50, Oakton Instruments), and dissolved oxygen (DO, Hanna Instruments HI 4192) were recorded for each stream water and porewater sample.

There were four primary objectives of this work. The first is to determine the impact of a 3-week dry period and subsequent 100-year storm on floc scouring within Steed Pond. I hypothesize that the scouring will move greater masses of U and Ni from the Steed Pond area than the masses due to ordinary baseflow concentrations in suspended solids. The second objective is to study floc composition biweekly over multiple seasons, and I hypothesize that U will be predominantly associated with either the NaPP- or CDB-extractable phase rather than equally distributed across both phases. The third objective is to track porewater and streamwater concentrations of U, Fe, Ni, and organic carbon biweekly throughout the year. I hypothesize that metal transport in the stream will be consistent across seasons and that porewater chemistry will not heavily impact stream-mobilized inventories of the metals, due to limiting hydrologic factors in the hyporheic zone. Finally, the last objective was to track local hydrology and the stream flowrate to construct a flowrate model with which to integrate U concentrations over time to estimate U masses moved throughout the year. I hypothesize that erosion of U-contaminated solids will drive stream U transport but will not account for the remaining U in the mass balance of the 43,500 kg U released from M-Area.

Results

The flocs observed in Steed Pond are more abundant after prolonged periods without rainfall, and Figure 6-2 shows Steed Pond in conditions where flocs coat the streambed, stream vegetation, and much of the streambank. Flocs in steed pond coat the entirety of the left photo in Figure 6-1, and the right photo shows the flocs caught in the vegetation that has grown in the stream channel. The floc samples (top) shown in Figure 6-3 were collected June 2, 2021, and the corresponding post-storm samples were as clear as the pre-storm Beaver Pond samples (bottom). Data from the piezometers and stream gages at Beaver Pond and Steed Pond are presented as Net Head (m) in Figure 6-4 and Figure 6-5, respectively. The net head calculation assumes that a positive value indicates gaining stream conditions (with the subsurface head being higher than the stream). Beaver Pond is gaining during 0.98% of the study duration, and Steed Pond is gaining for more than 60% of the study.

Figure 6-2: Photos from Steed Pond on June 2, 2021. Upstream, against the flow, parallel to the former dam (left) and downstream, with flocs collecting on low energy pockets created by dense vegetation (right).

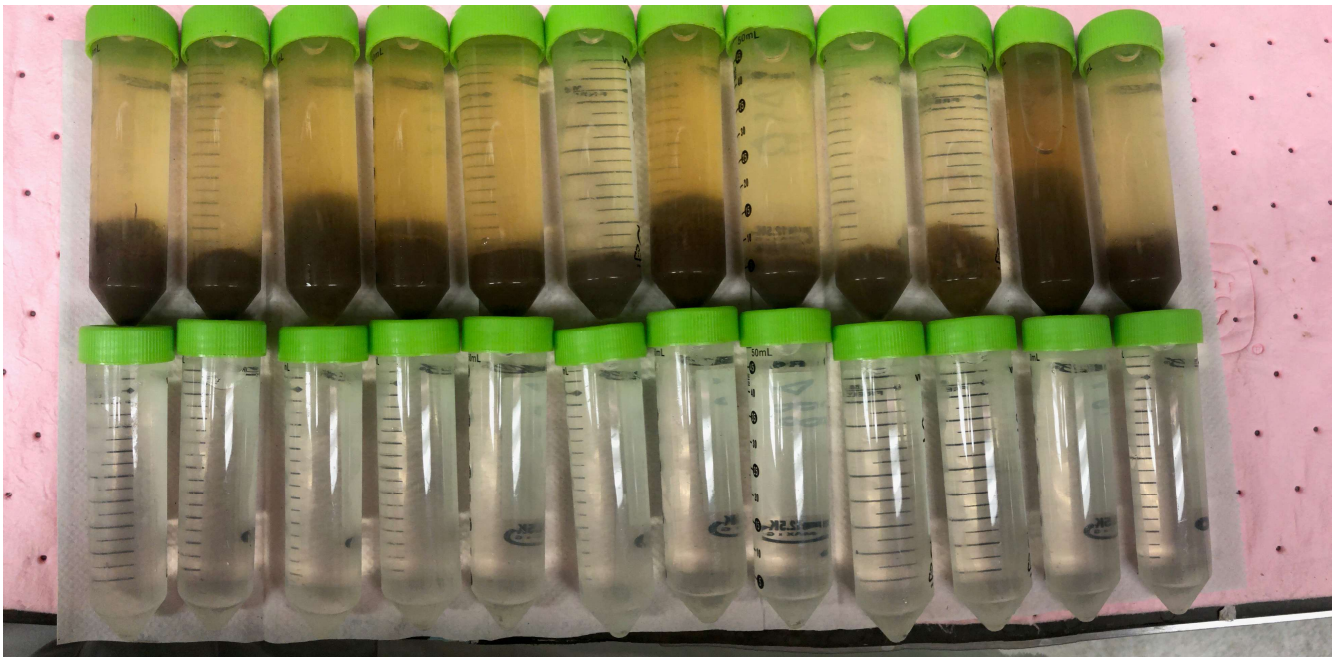

Figure 6-3: Flocs collected from Steed Pond (top) and Beaver Pond (bottom) on June 2, 2021, after 21 days of dryness and two days before a 10-day storm system bearing 12 cm of rainfall.

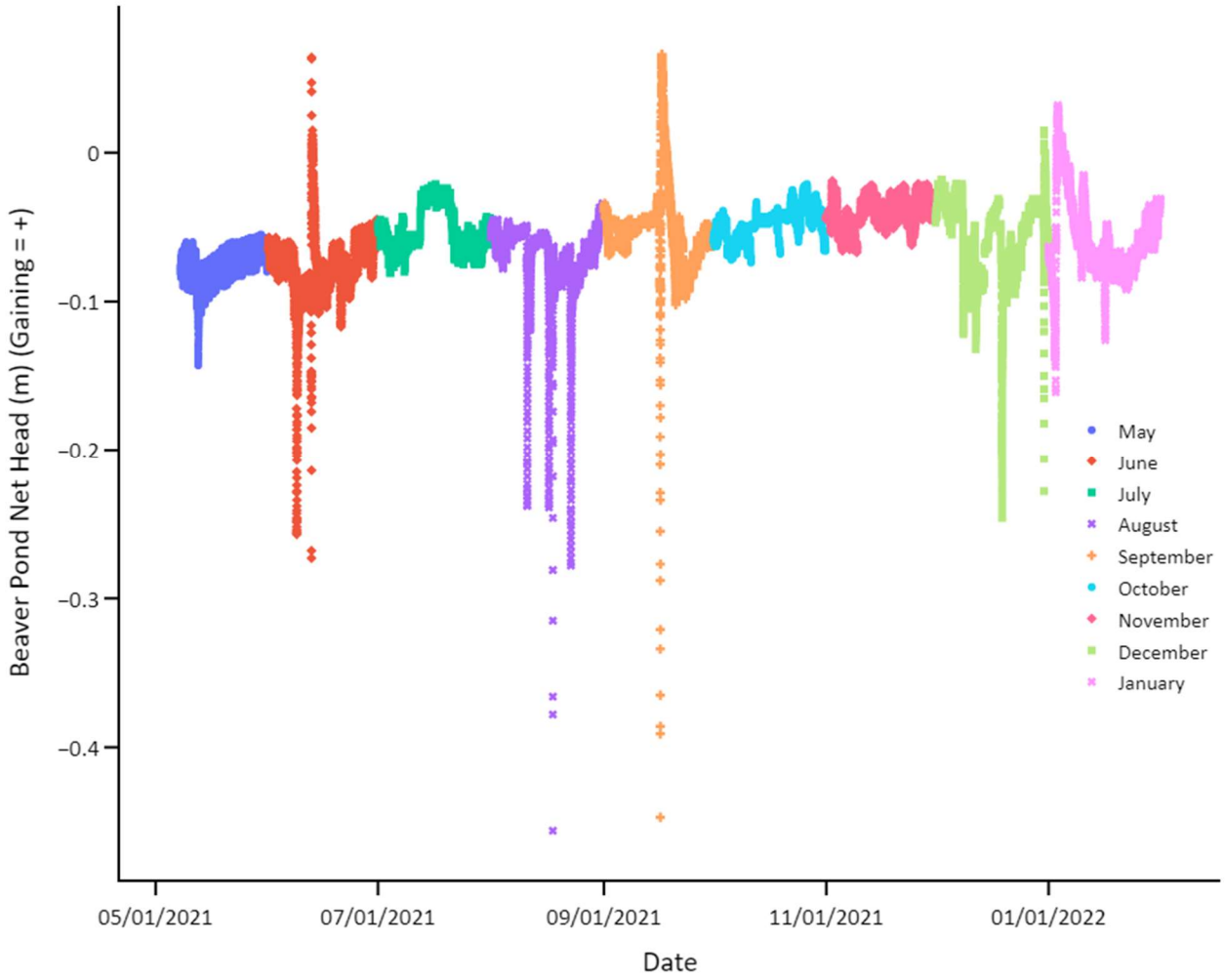

Figure 6-4: Net head at Beaver Pond, where a positive value is gaining (from subsurface into stream).

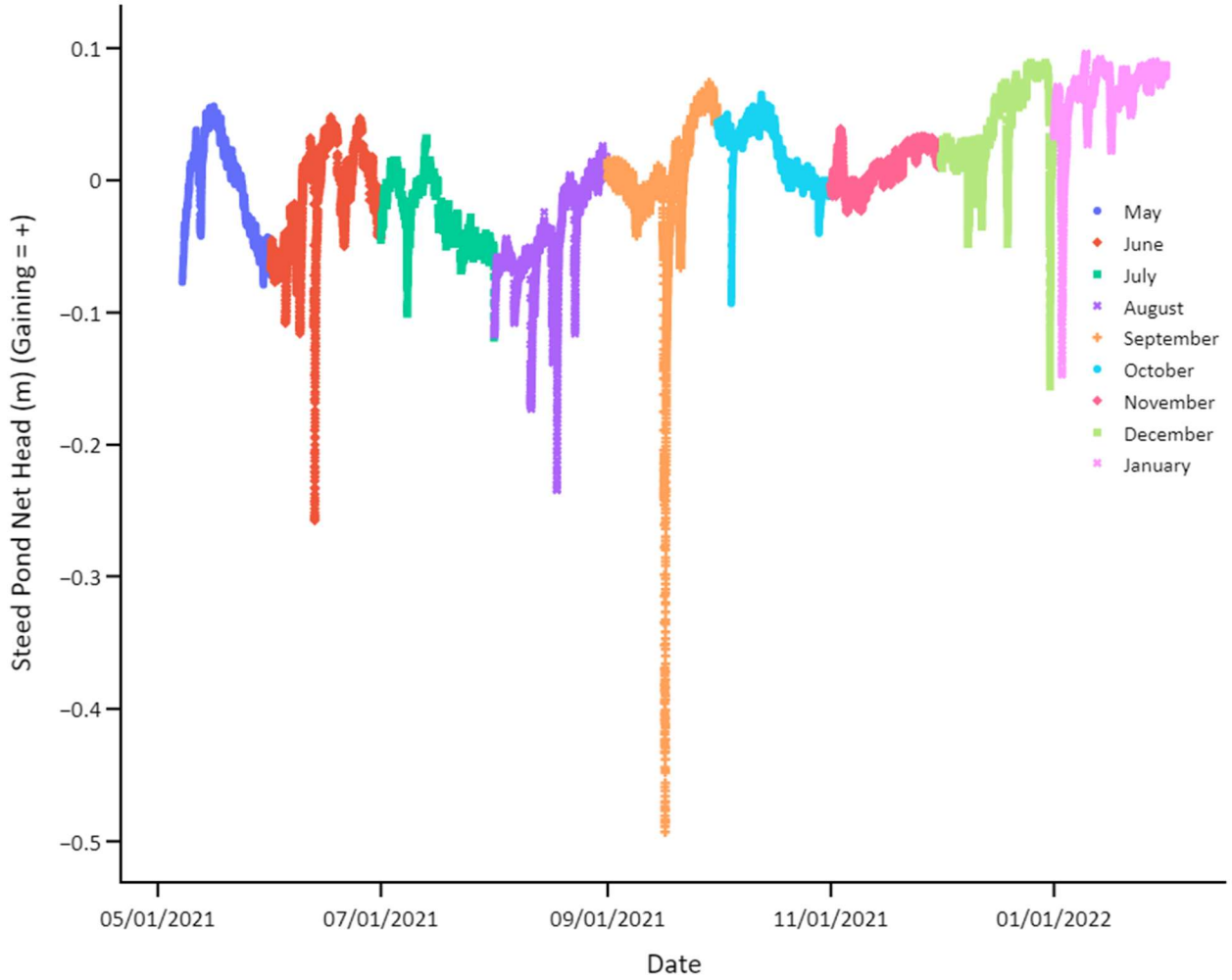

Figure 6-5: Net head at Steed Pond, where a positive value is gaining (from subsurface into stream).

Floc concentrations differed between the pre- and post-storm samples at Steed Pond but did not differ at Beaver Pond, where water was consistently clear and free from flocs. Table 6-1 displays the U and Ni concentrations for each site at each time. Further, Table 6-1 synthesizes the concentrations with the suspended solids loading (g/L) to show the impact of suspended solid mass on total metal inventories in the stream.

Table 6-1: Floc concentrations and total mobile inventories on streambank floc mats before and after the June 2021 100-year storm event for Steed Pond (gaining stream section) and Beaver Pond (losing stream section). Totals were calculated by multiplying solid concentrations (µg/g) by suspended solids loadings (g/L) to yield (µg/L) (Eq 6.3).

Steed Pond	Solid [U] (µg/g)	Solid [Ni] (µg/g)	Suspended Solids (g/L)	Total [U] (µg/L)	Total [Ni] (µg/L)
Pre-Rainfall	382.6 ± 83.3	220.9 ± 46.5	4.453	1703.9 ± 371.1	983.7 ± 207.1
Post-Rainfall	22.3 ± 14.2	49.3 ± 45.7	0.014	0.3 ± 0.2	0.7 ± 0.6

Beaver Pond	Solid [U] (µg/g)	Solid [Ni] (µg/g)	Suspended Solids (g/L)	Total [U] (µg/L)	Total [Ni] (µg/L)
Pre-Rainfall	33.0 ± 18.4	18.3 ± 8.7	0.036	1.2 ± 0.7	0.7 ± 0.3
Post-Rainfall	28.0 ± 17.0	59.2 ± 98.2	0.016	0.4 ± 0.3	0.9 ± 1.6

Figure 6-6 displays time series sequential extraction concentrations of Fe, U, and Ni in the flocs alongside the metal fraction (of the summed sequential total) in each phase. Note the consistency of U association to the NaPP phase at roughly 80-85% and the fluctuations over time for Fe and Ni. Figure 6-7 displays floc concentration data plotted with respect to Fe instead of as a time series, to present the data from a different perspective.

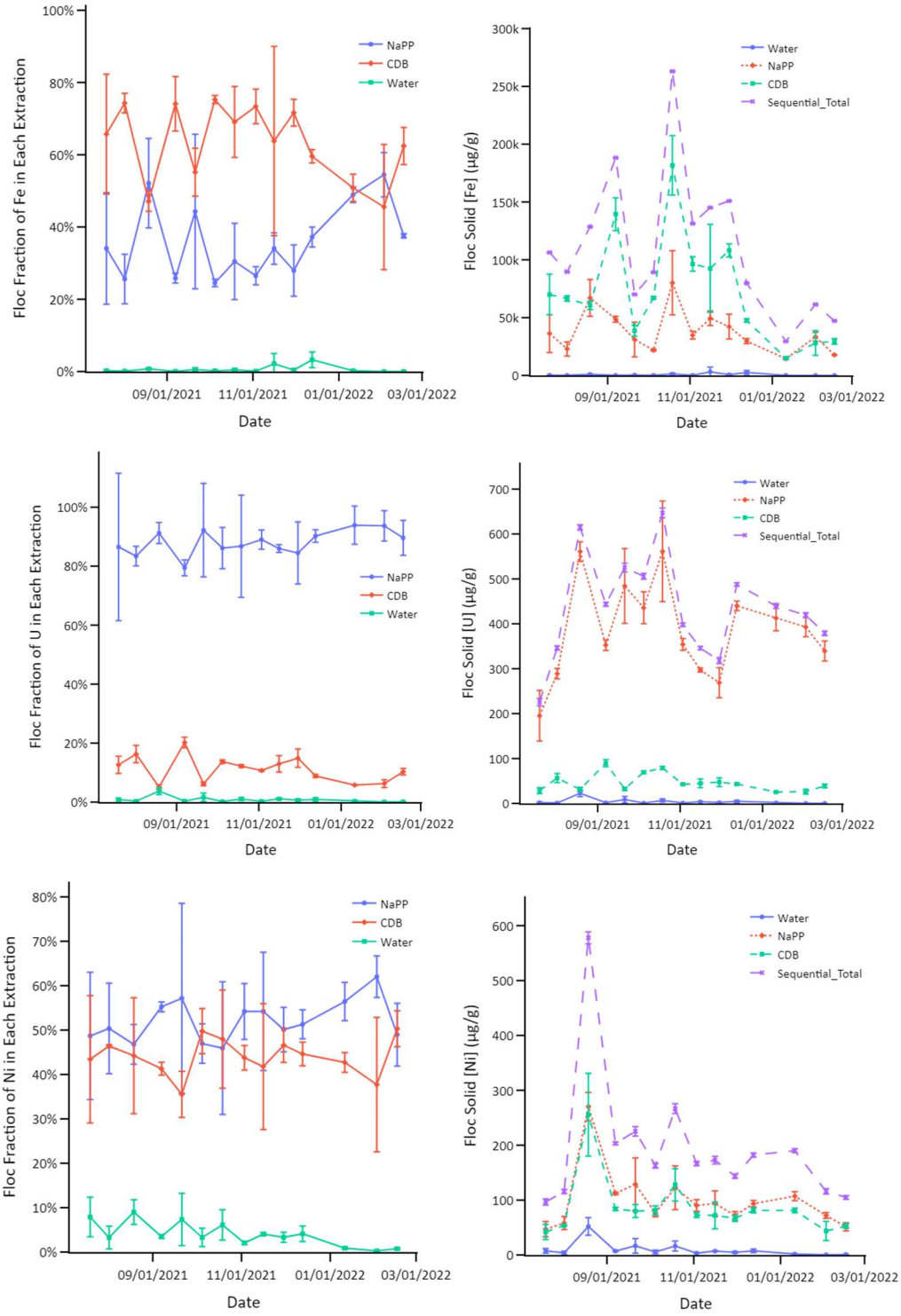

Figure 6-6: Floc concentrations of Fe (top row), U (middle row), and Ni (bottom row) on a µg/g basis. Right plots are the absolute concentrations of each metal in each extractant phase, in µg/g. The Sequential Total represents the summed value of all phases for that date. Left plots are the percentage of metals in each phase, where the Sequential Total = 100%.

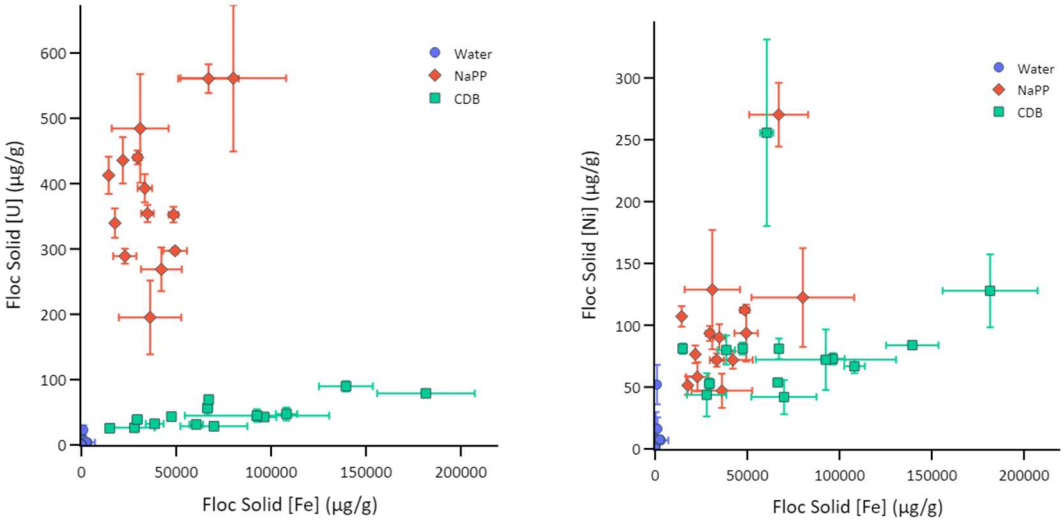

Figure 6-7: Floc concentrations of U plotted against Fe (left) and Ni against Fe (right).

Maximum porewater Fe concentrations were two orders of magnitude higher at SP than at BP. However, concentrations at both sites decreased between the October 20th and November 3rd sampling events and remained low for subsequent sampling events. Figure 6-8 displays two sets of porewater data. The first (top row) is the time series data of porewater Fe concentrations at BP (left) and SP (right). The second (bottom row) is the porewater Fe (left) and Ni (right) plotted as a function of corresponding porewater U concentrations.

Along with the porewater samples collected during each sampling campaign, stream water samples resulted in total stream concentrations based on from dissolved (filtered through 0.45 µm filters) and particulate stream contributions. The time series concentrations for Fe, U, Ni, and DOC at both BP and SP are shown in Figure 6-9. The July 20th sampling event collected visible flocs in the stream channel at Steed Pond. Otherwise, samples were consistently free from flocs, and any solids collected were suspended sands, silts, and clays rather than orange floc aggregates.

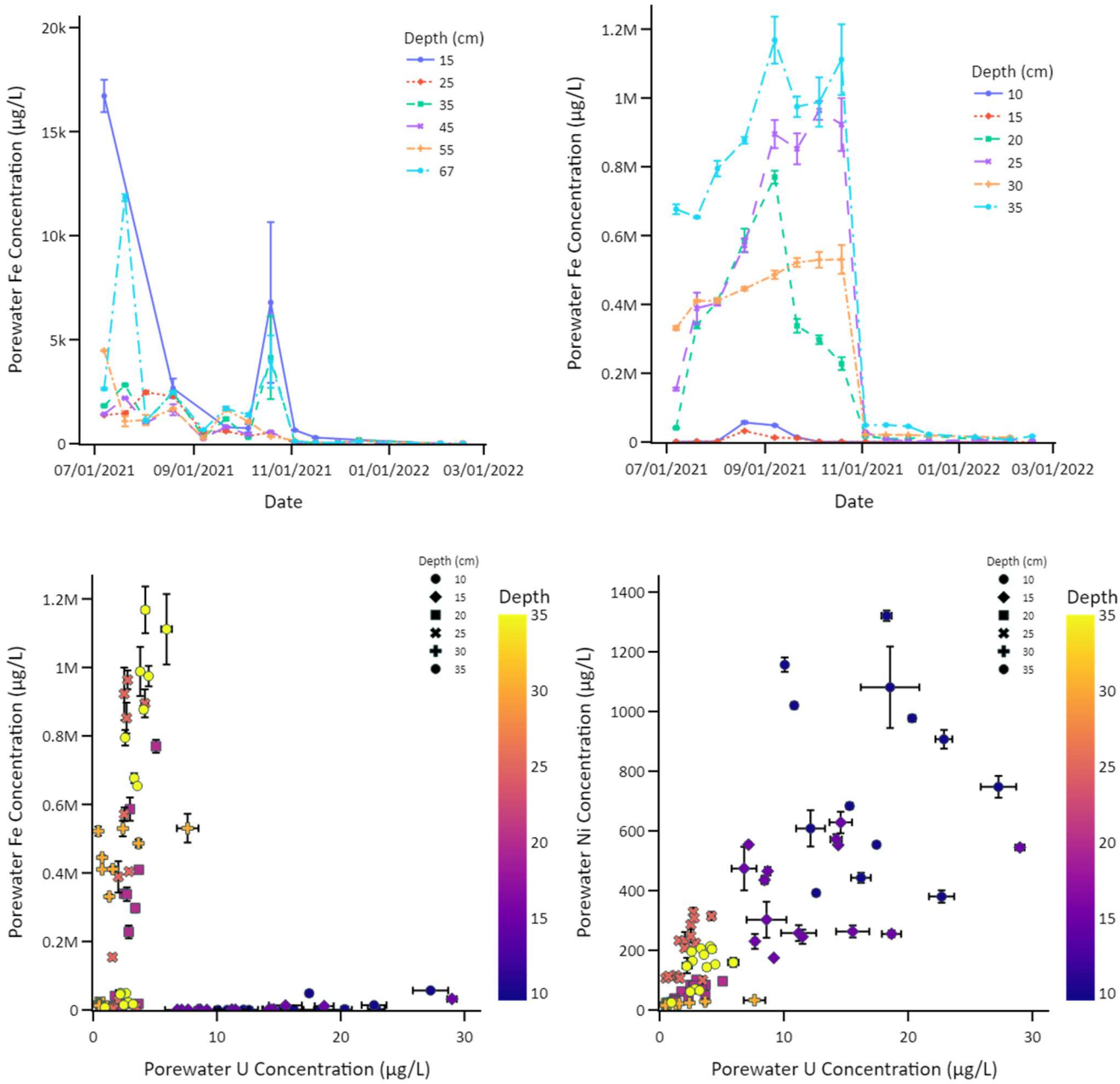

Figure 6-8: Porewater Fe concentrations over time as a function of depth in Beaver Pond (top left) and Steed Pond (top right). Porewater Fe versus U (bottom left) and Ni versus U (bottom right). Error bars are based on one standard deviation of the analytical error (ICPMS).

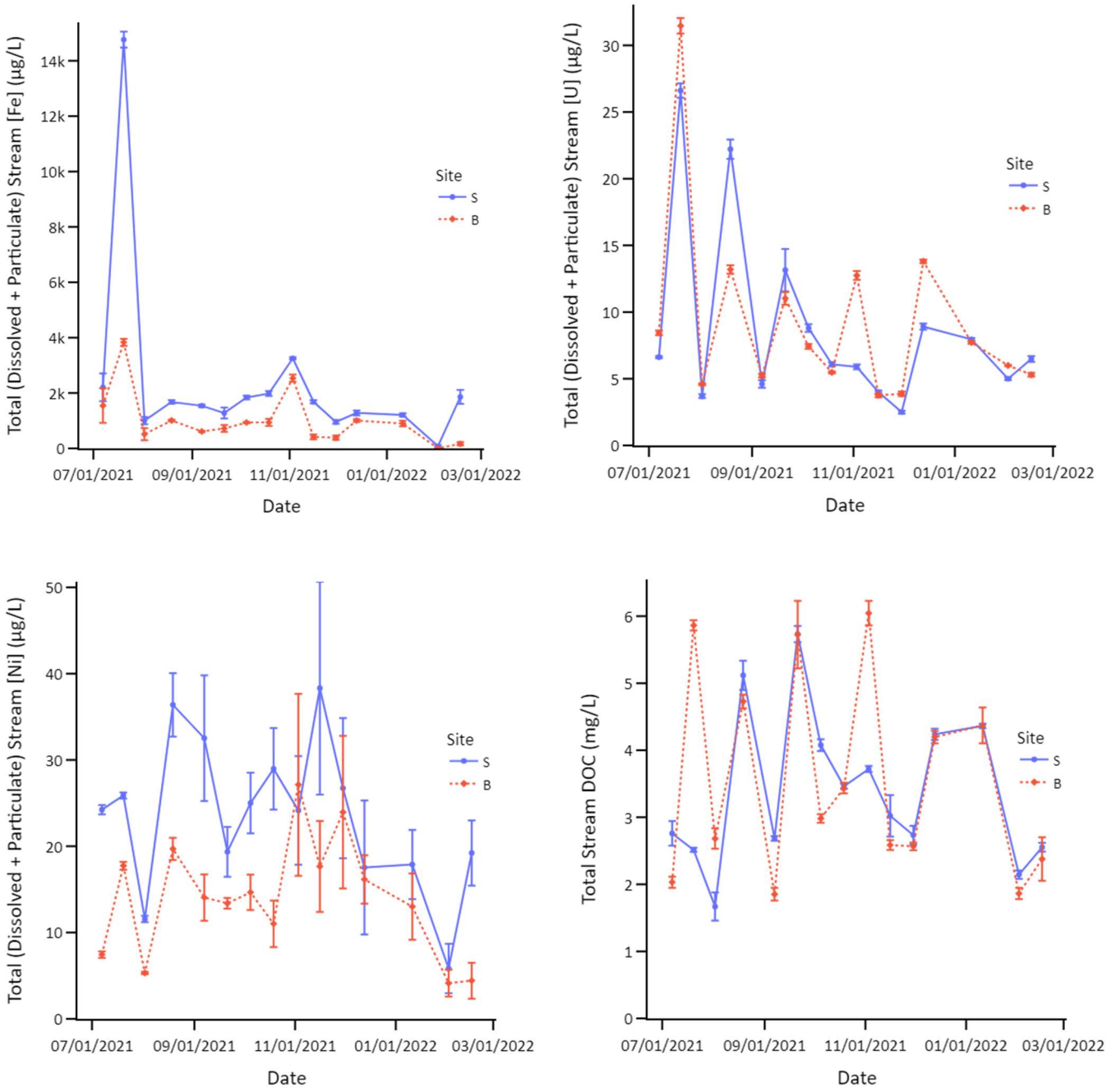

Figure 6-9: Total stream inventories of Fe (top left), U (top right), Ni (bottom left), and Total stream dissolved organic carbon (DOC, bottom right). Error bars represent one standard deviation from the average of stream samples on each date (n=4), and lines are not data, they are present for the reader's clarity.

The precipitation data, stream stage data, stream flowrate data, and stream flowrate model (based on stream stage data, Eq. 6-2) are presented in Figure 6-10. There are apparent correlations between precipitation, flowrate, and stream stage during and after storm events. Further, the intensity of a rainfall event increases the time required for the stream to return to baseflow conditions. The flowrates over time at Steed Pond are plotted again in Figure 6-11 alongside the U concentrations in the stream. An integration of these concentrations and flowrate data over time result in the final element of Figure 6-11, the cumulative U curve, which shows how much U has moved through Steed Pond during the sampling period of early July 2021 to mid-February 2022. According to calculations using this model, roughly 12 kg of U moved during the study, which yields an estimate of 24 kg U per year from Steed Pond if no significant changes to the streambed occur and the storms experienced during the study are representative of precipitation the rest of the year.

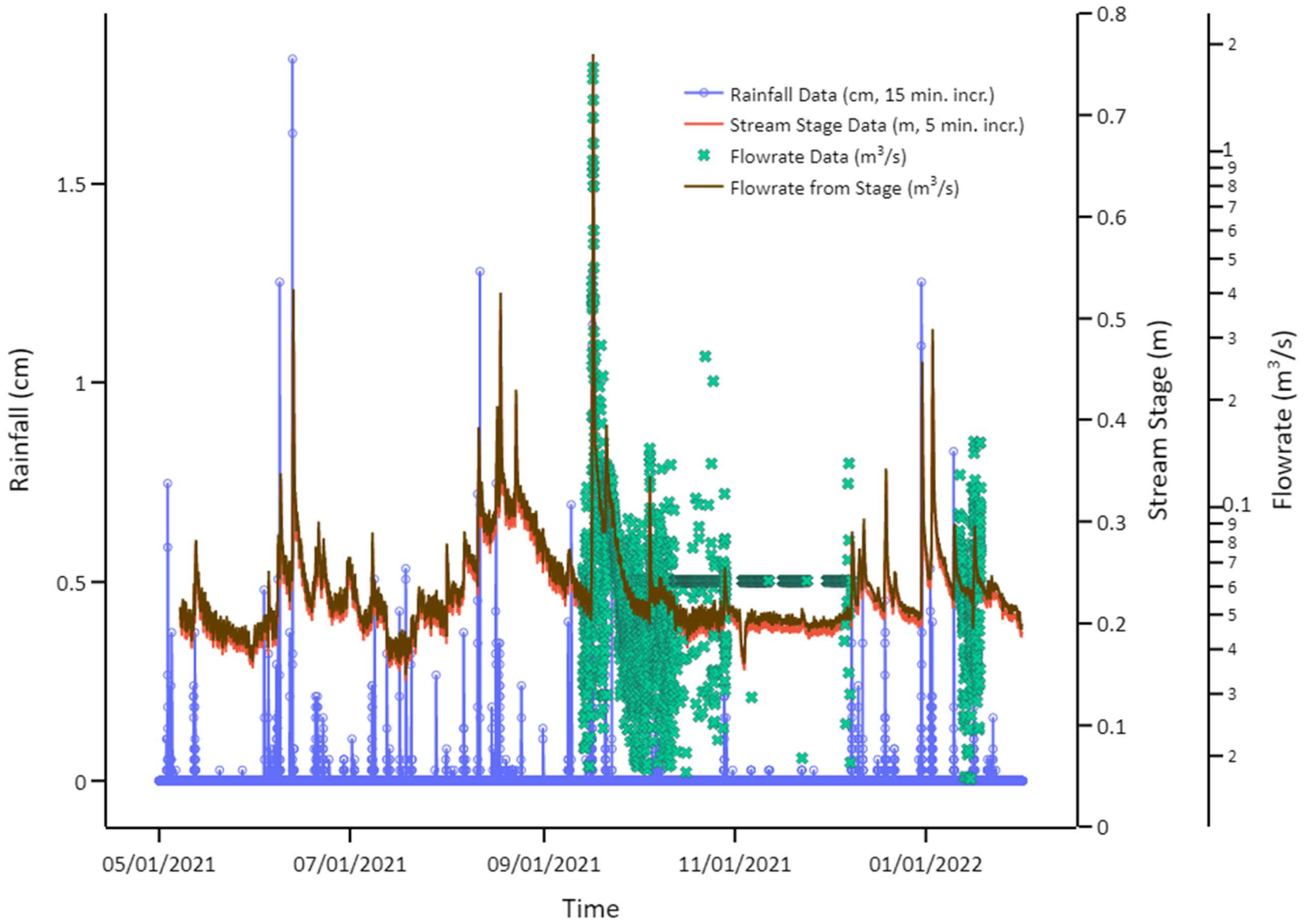

Figure 6-10: Precipitation data, stream stage data, and stream flow model developed from stream stage data and sparse stream flow data. Rainfall data are in 15-minute increments, stream stage data are in 5-minute increments, and stream flow measurements were made every 30 minutes when the instrument was operational and collecting data.

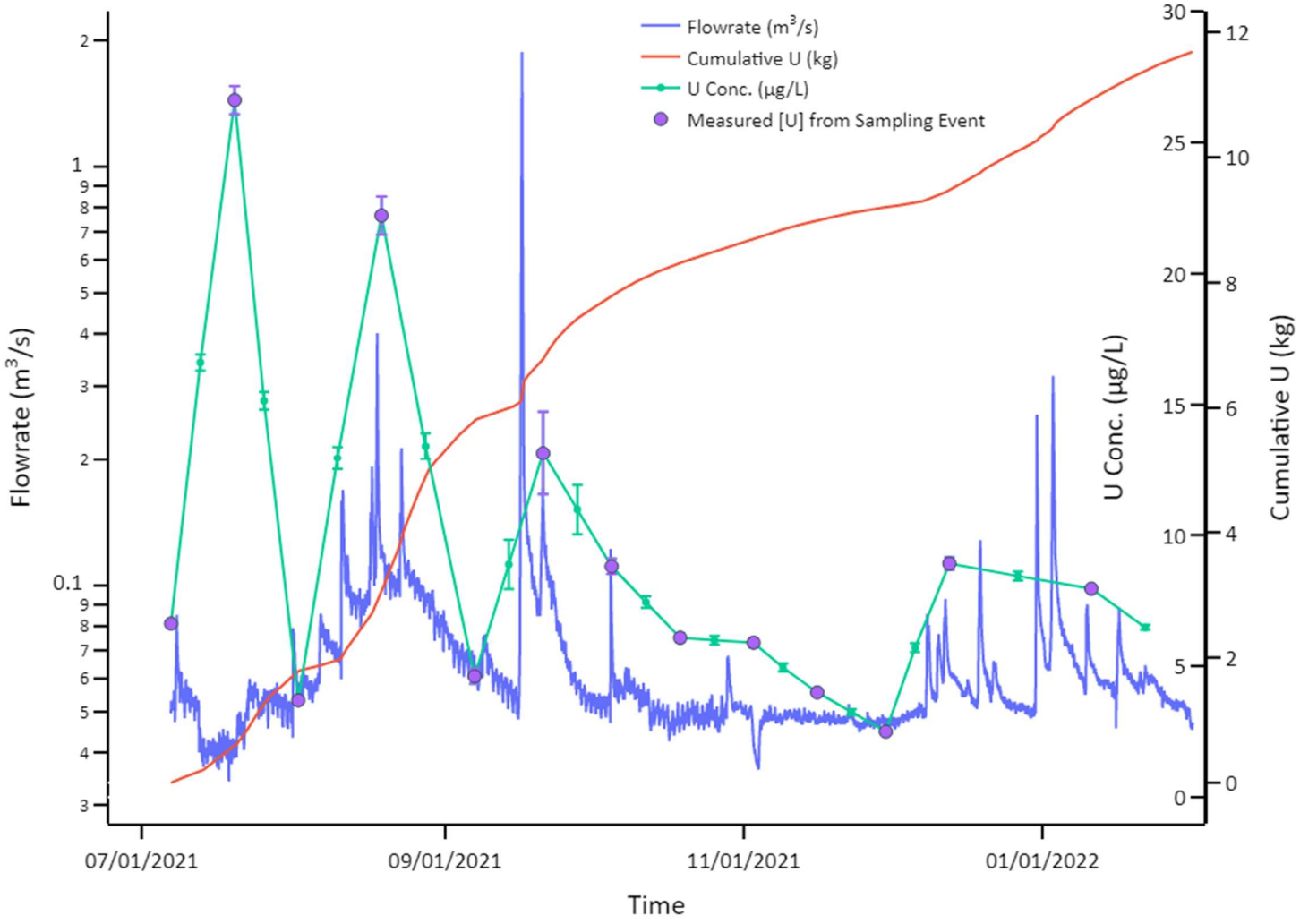

Figure 6-11: Cumulative U moving in stream (dissolved and particulate) at the former Steed Pond dam. Concentrations of U in stream are interpolated (green small circles) with an average between sampling events and measured concentrations of U (larger purple markers) are actual data. The line between these data is added for reader clarity and is not data or a model. However, Cumulative U and Model Flowrate have 1-minute resolution and appear as lines.

Discussion

Three key relationships emerged as primary factors to consider when estimating annual fluxes of U from Tims Branch after observing wetland concentrations for a year.

- storm-driven floc discharge
- seasonal floc composition variations and,
- porewater behaviors

First, fluctuations between sustained dry periods (roughly 3 weeks with less than 1 cm of precipitation) and intense storm events impacted the presence of flocs on Steed Pond streambanks, their U concentration, and the scouring of these flocs during the storm event. Second, the partitioning of metals between the water extractable, NaPP extractable, and CDB extractable phases remained constant for U year-round but fluctuated for Ni and Fe. Finally, the porewater concentration profiles in Tims Branch support the two transport mechanisms of U within and from the wetland. The first mechanism is the erosion of contaminated sediment at Beaver Pond, and the second is floc formation via hyporheic exchange of porewaters into the stream. At Beaver Pond, porewater behaviors indicate that the primary driver for U transport is not U porewater incorporation in aqueous stream complexes or colloidal species; therefore, erosion of contaminated solids (Parker et al., 2022) drive transport from Beaver Pond. Meanwhile, porewaters at Steed Pond support the hypothesis that deeper, reduced porewaters bear soluble Fe(II) and flow into the stream via hyporheic exchange, resulting in floc formation. However, these flocs only amount to a small fraction of the unaccounted for 2610 kg of U when conservative estimates are calculated, with the 2610 kg being the difference between the recorded 43,500 kg U released from M-Area and the 40,890 kg accounted for along Tims

Branch. These three relationships will be the lenses through which these data are presented, discussed, and compiled into a rudimentary U flux estimate from Tims Branch per year.

Storm Intensity Impact on Floc Discharge

Collecting flocs on June 2, 2021, after 21 days of dryness, resulted in the densest floc mat observed by our research team in four years of studying Tims Branch. Observations during roughly 40 sampling campaigns over four years support the hypothesis that flocs are more richly present in Steed Pond streambeds and along streambanks on days when there has been sufficient dryness beforehand—often referred to as "antecedent dryness" in this work—to allow time for flocs to develop and collect on streambanks without scouring by high velocity streamflow induced by precipitation events. When prodded and perturbed, flocs dislodge from the streambanks and a portion of these remain suspended in the flowing stream channel while the remainder settle into mats once more in the low energy segments of the stream bank (common field observations by researchers). This pre- and post-storm study was designed to test this hypothesis during the most extreme conditions: 21 days of zero precipitation, followed by 12 cm rainfall distributed over 10 days.

The photos the Steed Pond site in Figure 6-2 and of samples in Figure 6-3 show the presence of flocs in Steed Pond and the lack of any solids other than a few sand grains in Beaver Pond, highlighting the impact of the dry period on floc formation and accumulation at Steed Pond and the unequivocal lack of floc formation at Beaver Pond. After the storm, all samples were as transparent as the pre-storm Beaver Pond samples. Pre-storm flocs in Steed Pond had high solid-phase U and Ni concentrations, and the difference between the prominent flocs at Steed Pond and the lack of flocs at Beaver Pond becomes more apparent upon integration with the Suspended Solids (SS) (Table 1), where total concentrations in the floc mat were 1-2 mg/L U

and Ni (after multiplication of μg/g and g/L). Uncertainties for all values here are based on one standard deviation of n=12 samples at Steed Pond and n=12 at Beaver Pond. The targeted and deliberate method of collecting these flocs in Steed Pond with the hand syringe rather than ordinary grab samples skews the total U and Ni calculations high based on the higher SS loading near the stream back relatively to the average stream channel SS loading. However, this value is useful as a maximum limit on how much floc could accumulate on stream banks, given the antecedent dry period before the storm.

Following the 12 cm of rainfall over 10 days, solid-phase concentrations in Steed Pond decreased an order of magnitude and changed minimally in Beaver Pond. Post-storm concentrations in the solid phase (μg/g) and integrated with SS (g/L) to yield streambank totals (μg/L) are found in Table 1. Due to the low concentrations of flocs at both sites after the storm, these inventories were less than 1 μg/L for U and Ni at both Beaver Pond and Steed Pond after the precipitation. Focusing on these differences at Steed Pond, the results of this study are evidence for the scouring effect of storms that occur after a distinct dry period for floc formation. The flocs were present on the banks before the storm (Figure 6-2B) and were gone after the storm, as the water was clear, and no flocs were collected. As such, it can be assumed that the storm event stripped the banks of these flocs. Without estimating the duration of floc removal or how much flow was required to dislodge the flocs, it remains abundantly evident that a mat of dense flocs loaded with 382.6 ± 83.3 μg/g U and 220.9 ± 46.5 μg/g Ni was transported from the Steed Pond streambanks during those 10 days.

Focusing on Beaver Pond, the pre- and post- storm samplings continue to support the hypothesis that U transport from Beaver Pond is controlled by erosional processes. These processes lead to the removal of contaminated solids, such as sand grains and soil particles, from

the sediments that once comprised the Beaver Pond floor (Parker et al., 2022). Previous studies of Tims Branch indicate that there is a mobile fraction of U independent of Fe-rich solids (Parker et al., 2022), differentiating the mobility of BP solids from that of the Fe-rich flocs present at Steed Pond. Further, the concentration of U in these solids at BP is independent of antecedent dryness, indicating that these solids are not actively forming via hydrogeochemical processes such as hyporheic exchange, but rather they are being drawn from a pool of contaminated solids. Characterization of this pool of contaminated solids has identified relationships between U and solid-phase OM accumulated in BP, which supports the immobility of this pool except for the erosion of exposed solid particles (Kaplan et al., 2020; Parker et al., 2022, Chapter 5). Beaver Pond U has remained wholly immobilized, as 60% of the 43.5 Mg of U released from M-Area remains in Beaver Pond after nearly 60 years (Kaplan et al., 2020). Thus, local geochemistry is not mobilizing the U plume bound to soil and it is expected the U will remain sequestered so long as decadal changes in hydrology do not change the course of Tims Branch.

Seasonal Floc Composition

Bearing in mind that the presence of flocs and the concentration of U in flocs depends on antecedent wetting and dryness within the wetland, one facet of our seasonal study aimed to identify what phase the U and Ni were most closely associated with. Metal concentrations in environmental samples digested via sequential extraction (Schultz et al., 1998) can be compared as fractions of the phase targeted by each extracting reagent. In the Steed Pond floc system, the relevant phases are the aqueous solution surrounding the flocs, the organic matter matrix stabilizing the flocs, and the Fe-oxide minerals within the flocs, predominantly ferrihydrite (Lapworth et al., 2013). Regarding the Fe-oxides, there are two potential options for U incorporation mechanisms: whether the U and other trace metals are binding to the mineral

surface or co-precipitating as the redox gradient in the hyporheic zone induces Fe(II) oxidation and precipitation of the amorphous Fe-oxides. Digesting separate floc samples from each sampling campaign in sequence provided insights into these phase associations, which correspond to the filtrate of floc solution (water extractable/equilibrium phase), the NaPP extraction of the OM phase, followed by the CDB extraction targeting Fe-oxide minerals.

In the floc composition, Fe fluctuates broadly between the OM and Fe-oxide phases (Figure 6-6). The percentage of Fe extracted by CDB (50-75% of all Fe) is explained by the fact that this extraction targets Fe-oxide minerals, and the amorphous mineral colloids that aggregate to form the flocs will dissolve in this stage, not the NaPP extraction, which selectively cleaves the bonds between OM and metal cations, removing the OM from mineral surfaces and metal cations from large polymeric OM ligand complexes (Hall, et al., 1995). As such, the Fe partitioned into the OM, as opposed to the Fe comprising the solid iron oxides, were presumably released during this extraction step. Further, the NaPP extraction occurs at roughly a pH of 10, where Fe-oxides are even more insoluble than in circumneutral natural pH ranges (Schwertmann, 1991; Stefánsson, 2007). Thus, the Fe removed in the NaPP step preceding the CDB extraction is likely bound in the OM matrix, rather than being discrete mineral surfaces available for sorption of other cations.

Uranium is consistently 80-95% associated with the OM in flocs. In the absence of x-ray absorption spectra or other spectroscopy, I cannot claim that U is definitively bound to OM. However, it is clear that the majority of U in flocs is removed in the middle NaPP step and only 5-20% ever remains for extraction via CDB (Figure 6-6). Given the sequential nature of the extraction procedure, this study concludes that the U remains associated with OM at a relatively constant proportion throughout all seasons. On plots of U-Fe and Ni-Fe in all three phases of floc

extraction (Figure 6-7), the $[U\text{-}Fe]_{NaPP}$ relationship shows no significant trend ($R^2 = 0.1788$, significant at $\alpha = 0.95$), but the $[U\text{-}Fe]_{CDB}$ relationship appears linear ($R^2 = 0.6093$, significant at $\alpha = 0.95$), indicating that once the U-rich OM is stripped away by the NaPP extraction, any U that co-precipitated with the Fe-oxides is exposed and can be dissolved when the Fe minerals decompose during CDB treatment. If linear relationships were observed between U and Fe in both extractions, one could assume that the U being removed in the NaPP extraction is associated with smaller Fe colloidal species that had only recently aggregated and were most easily targeted within the overall OM matrix, resulting in the direct association of U and Fe, not U and OM. However, the lack of this linear trend in both phases suggests that there are two separate U uptake mechanisms. First, U may be accumulating by binding to organic ligands within the greater OM matrix that surrounds and may coat Fe colloids. Second, U may be co-precipitating with Fe in these Fe-oxide minerals. Further *in situ* spectroscopic characterization is required to determine the precise bonding environment of U in the flocs, but the data presented here indicate that of the two possible and coexisting mechanisms of U uptake, U is heavily associated with material extractable during the NaPP stage of a sequential extraction procedure.

Nickel uptake in flocs (Figure 6-6) more closely resembled the variability of Fe, except that Ni was more prevalent in NaPP rather than CDB, and there was an appreciable contribution in the aqueous phase. In previous sequential extraction work performed on Steed Pond sediments, 60% of Ni in sediments was associated with Fe-oxides (Sowder et al., 2003). Given the comparable ionic radii, Ni may co-precipitate within iron oxide flocs and thus be more resistant to NaPP leaching. However, the work of Sowder et al. (2003) was performed on the contaminated sediments at the former Steed Pond floor, not newly formed flocs along streambanks. Thus, the 35-50% association with Fe-oxides is comparable to past studies (Sowder

et al., 2003), but the increased association with OM could be induced by ligand complexation that increases solubility in local porewaters, resulting in uptake into the organic matrix (Sholkovitz and Copland, 1981). As the Ni was released concurrently with M-Area U (Reed and Swanson, 2006), studying the behaviors of redox-inactive Ni over time in parallel with redox-active U helps researchers elucidate the role of redox in the sequestration and mobilization of each contaminant.

Porewater Source Term Aqueous Monitoring

Beaver Pond porewaters have less variability and lower concentrations than those in Steed Pond. The U and other heavy metals sequestered in Beaver Pond have remained immobile for decades and heavily favor the solid phase in the OM-rich soils (Kaplan et al., 2020; Parker et al., 2022). Flocs are not observed in Beaver Pond, indicating that there is not an impactful hydrogeochemical flux from the porewaters into the streams. Likewise, the Beaver Pond reaches of Tims Branch exhibit gaining stream conditions only 0.98% of the year (Figure 6-4). Dissolved organic carbon is the only analyte in Beaver Pond that exceeds Steed Pond concentrations, while concentrations of U, Fe, and Ni reach two orders of magnitude higher in Steed Pond. Concentrations of Fe in both Beaver Pond and Steed Pond display a relationship with the temperature during winter, as the temperatures began decreasing before the November 3rd sampling and have remained low during the winter months (Figure C - 2).

Steed Pond porewaters appeared to have a strong spatial dependence on porewater U, Fe, and Ni concentrations. Porewater samples in Steed Pond that were shallower and more oxidized (ORP) contained less Fe, more U, and more Ni. This fits well the conceptual model of the system, as U and Ni persist together in upper sediments at Steed Pond (Chapter 5), and the deeper, more reduced sediments contain soluble Fe(II). Analyte plots in Figure 6-8 show the

disparity between Fe and U in Steed Pond (bottom left) and the linear trend between U and Ni (bottom right). The sharp decrease in Steed Pond porewater Fe in November 2021 (Figure 6-8, top right) does not appear to impact the incorporation of U and Ni into the flocs (Figure 6-6). Further, the lack of a correlation between porewater Fe and U in Steed Pond indicates that if a geochemical relationship develops that couple U and Fe, it is developing in the hyporheic zone or in the oxic streamwaters, as there is clearly not a relationship when these constituents are in the porewaters. Plots comparing each analyte to one another and plotted as a function of ORP at both Beaver Pond and Steed Pond are available in Figure C - 3, Figure C - 4, Figure C - 5, and Figure C - 6.

The hydraulic conductivity (calculated using Eq. 6.1) at Beaver Pond was ($1.28 \times 10^{-4} \pm 3.44 \times 10^{-5}$) m/s (n = 4) while at Steed Pond it was 5.79×10^{-7} m/s (n = 1). At Steed Pond, the slug test took roughly 18 hours, so only one replicate could be performed in the sampling scheme.

Total Stream Transport of U, Fe, and Ni

There is less total (solids plus aqueous) U, Ni, and Fe present in the central stream channel than hypothesized based on previous research performed by our team (Parker et al., 2022). It was hypothesized that flocs would appreciably contribute to metal transport from the Steed Pond stream reaches. However, as shown in Figure 6-9, total concentrations of U and Ni in the water column (in μg/L, as contributed by both the dissolved and particulate phases calculated using Eq. 6.3) vary between sampling events but are similar at both Steed Pond and Beaver Pond.

The sharp increase in stream-available Fe in July 2021 at Steed Pond is due to higher floc content in the stream channel (Figure 6-6). Flocs were visible in the stream channel (Figure 6-3),

and the increase in Fe content compared to Beaver Pond indicates that this was a floc-facilitated increase in stream Fe transport. However, under the flow conditions of most sampling events, the flocs had aggregated and settled on the stream bed or banks. These settled, stable floc mats are not readily suspended in the water column and are therefore do not contribute greatly to the stream uranium concentrations. An equivalent increase at both sampling locations would imply that the stream contained higher masses of eroded streambank sediment rather than newly formed flocs. Additionally, Tims Branch received 2.01 cm of rainfall the morning of the sampling, leading to an increase in stream solids at both locations as the high stream stage began returning to baseflow. However, the flocs on the streambank during the July 20th sampling event had relatively low U and Ni concentrations (Figure 6-6), resulting in an increase in Fe in the stream but no sharp rise in U or Ni. The week preceding the sampling event experienced five days with rainfall, of which three were over 2 cm in magnitude (Figure 6-10). This disparity highlights the need for future research to focus on finer temporal resolution in sampling to elucidate the direct relationship between U concentrations in flocs and the antecedent rainfall events.

Porewaters impact stream water U concentrations during gaining stream periods to a lesser degree than was hypothesized. If porewaters were proportionally impacting stream quality on gaining days, I would expect to see flocs form during the November 3rd event (sampling was preceded by 24 hours of gaining conditions) and no more Fe in streams during the winter season, since porewaters have significantly decreased concentrations of Fe (Figure 6-8). Instead, I observe an increase in SS, $[Fe]_{solids}$, and $[Fe]_{aq}$ on Nov. 3rd, but no sustained decrease of Fe concentrations in the stream (Figure 6-9). The average groundwater discharge flux at Steed Pond is 1.69 x 10-9 m/s, which explains why the decreased Fe concentration in porewaters lead to a

subsequent decrease in floc presence for the remainder of the winter season. With such a low flux, only concentrations in the 1 x 10^6 μg/L range would induce floc formation. With a low flux and low concentration, floc formation was low. The corresponding rise in SS (Figure 6-9 and SS in Figure C - 7) at Beaver Pond on Nov. 3rd and lack of substantial Fe increase in flocs (Figure 6-6) indicates that Fe mobility in the stream is not a floc-formation effect, but rather a stream turbidity effect throughout the entire wetland.

Over seasonal timescales, the sharp decrease in porewater Fe and gradual decrease in porewater DOC both appear to have minimal impacts on stream-available Fe as suspended sediments (Figure 6-9) or as flocs (Figure 6-6). This implies that the concentrations of Fe and DOC required to form flocs are still being achieved during winter when soil microbes are less active due to decreased temperatures (Zelles et al., 1991). While Fe concentrations in flocs are lower during winter (Figure 6-6), they are not orders of magnitude lower, as observed in the porewater Fe concentrations (Figure 6-8). Thus, floc formation seems to be driven more by the hyporheic flux during gaining conditions rather than being proportionally driven by Fe concentrations in the porewaters alone. There is likely still some Fe flowing from porewaters into the stream to produce flocs, but it is lower than what was present in the summer (22 mg/L Fe in November porewaters versus 1.2 g/L Fe in September porewaters). There was also a decrease in the flocs in the stream during the winter, but not by the orders of magnitude I would expect based on the decrease in porewater Fe. Thus, it is hypothesized that colloid transport of Fe particles produced under more oxic pore water conditions in the winter could produce the observed flocs. Further research investigating floc morphologies is needed to characterize the impacts of Fe concentrations on floc formation and the ratios of Fe minerals and OM present in the flocs.

Stream flowrate was calculated at the Steed Pond stream gage using the exponential relationship in Eq. 6.2, where the high frequency stream stage data (x in Eq. 6.2) was used to populate the sparser streamflow dataset (y, in Eq. 6.2). The resulting R^2 correlation coefficient on a linear y-axis was 0.998 when the *test* half of the dataset was used in the mathematical model. The complete model of stream flowrate is presented in Figure 6-10, along with the rainfall data for Tims Branch and the stream stage data at Steed Pond. The rainfall data was provided in 15-minute increments, and the rise of stream stage following precipitation events (Figure 6-10) provides a visualization for the inherent hydrologic lag between rainfall and increased stage. Further, the sustained return to baseflow conditions when intense storm events impact the wetland can be observed prominently in late August and Early September 2021.

This streamflow model and the U concentrations in the stream (calculated with Eq. 6.3 and shown in Figure 6-9) were synthesized into a rough estimation of the U flux from Steed Pond between July 2021 and February 2022. By integrating the U_{Total} concentrations in the stream (μg/L, Figure 6-9) with the volumetric flowrate (m^3/s, Figure 6-10) over time, totals of 12 kg of U (Figure 6-11) and 29 kg of Ni (Figure C - 8) are estimated to have moved through Steed Pond during the study. Given the need to extrapolate the flowrate data back in time and interpolate U and Ni concentrations between sampling events, an estimate of the uncertainty is not provided. Based on the channel-stability assumptions made when developing the flowrate model, this flux should not be used retroactively to calculate previous fluxes of U over time beyond the last year, during which Steed Pond has been observed by our team frequently.

If U transport in Tims Branch passing the former Steed Pond dam continues at this rate, 1500 years would be required to mobilize all remaining U (Kaplan et al., 2020). While using 2021 as a model year for the next 1500 years is a poor assumption, it provides an initial guided

estimate of how long the U plume will persist if conditions remain constant and indicates that the sequestered U presents minimal risk to off-site exposure. Concentrations in the stream when I sampled in Tims Branch did not exceed 30 µg/L, which is the EPA drinking water limit for U concentrations. Further, Tims Branch makes confluence with Upper Three Runs Creek and ultimately the Savannah River. These two bodies of water allow for sufficient dilution of U leaving Tims Branch. While storms (for which U stream concentrations were not measured) may change the amounts of U leaving Tims Branch, concentrations of U in the stream in flowrates that I observed do not appear to presently pose significant off-site risk.

The U estimated to be moving from Steed Pond (Figure 6-11) represents dissolved, particulate, and colloidal phases, as the total was calculated using Eq. 6.3. No distinction can be quantitatively made regarding the geochemical relationship of U and Ni to the total stream solids filtered by 0.45µm filters since no sequential filtration was performed or any separation between floc and suspended sediments or sand grains. However, as mentioned earlier in this chapter, it is visually apparent when flocs impact stream solid loads. Between July 2021 and February 2022, only during the July 20th sampling event was heavy floc observed actively mobilizing in the central water column at Steed Pond during sampling (Figure 6-9). As such, the stream inventories mobilized during the study (Figure 6-11) can be interpreted predominantly as contributions from the aqueous phase and the erosion of contaminated solids.

Based on the current lateral extent of Tims Branch U contamination (Kaplan et al., 2020), the records of U masses released from M-Area (Reed and Swanson, 2006), and conservative risk-assessing calculations of floc-facilitated metal transport from Steed Pond, flocs are not the primary risk driver for downgradient stream quality. Roughly 83% of U from M-Area releases remains in Tims Branch (Kaplan et al., 2020), and soil characterization (Arey et al., 1999;

Kaplan et al., 2020; Seaman et al., 2001; Sowder et al., 2003, Chapter 5) indicates that extensive anthropogenic Ni contamination persists in the wetland, though in the absence of detailed M-Area release records for Ni a mass balance determination is not possible. Using Eq. 6.4 and the following assumptions helps create an estimate of M_{Me}, the mass of a metal (U or Ni) that has moved due exclusively to floc-facilitated transport since M-Area releases beginning in 1965:

$$M_{Me} = DA[Me]f_{storm}t \quad \text{Eq. 6.4}$$

The first conservative assumption is that metal concentrations in the flocs, [Me] (μg/L, loaded onto banks per storm event), are at a maximum in samples shown in Figure 6-2 and that floc mats are roughly 10 cm deep (D) (double the extent of the floc mat captured in Figure 6-2). Next, a stream reach length of 23.77 meters (from the former Steed Pond dam to where the stream bends northward) and width of 5.365 m are based on survey data from piezometer and stream gage installation. The width used here is the cross-sectional length of the streambed if the stream was 1 m high (boundaries for Sontek IQ inputs and expected maximum flowrates). These length and width values comprise the area of floc formation and accumulation (A). Finally, I assume that 100 intense storms occur per year (f_{storm}) that have each experienced the three-week dry period observed before the June 2021 sampling event. If a storm scours all flocs that have accumulated on streambanks, as occurred in June 2021 with our deliberate sampling before and immediately after the rainfall period, then only 132 kg of U and 76.5 kg of Ni would have moved over the last 60 years (t). This clearly does not account for a significant portion of the 43,500 kg of U that was released from M-Area (Reed and Swanson, 2006). Thus, flocs are not the dominant transport mechanism for U and Ni contamination from the Tims Branch wetland.

While flocs do not appear to drive U and Ni release from Steed Pond on decadal scales, pulses of flocs released when storm events scour the streambanks pose a potential risk to

downgradient water quality. Based on the pre- and post-storm floc collections in June 2021, concentrations of up to 1700 µg/L U and nearly 1000 µg/L of Ni could be available in the stream when flocs are perturbed and become suspended in the water column. Thus, if the change in streamflow is rapid enough to scour all flocs rapidly, downgradient water monitoring efforts could experience concentrations of U and Ni orders of magnitude higher than usual.

Conclusions and Broader Impacts

The incorporation of U and Ni into the natural wetland Fe and C cycle has resulted in the sequestration of the majority of M-Area U released and a significant portion of process effluent Ni. Over the past 30 years, studies of the Tims Branch wetland have sought to elucidate the roles of hydrology, geochemistry, the complexities of wetland organic matter in retaining metals, and the degree of transport within and from the wetland (Arey et al., 1999; Batson et al., 1996; Evans et al., 1992; Kaplan et al., 2017; Kaplan et al., 2020; Li et al., 2014; Parker et al., 2022; Seaman et al., 2001). While no individual study has fully characterized the U and Ni accumulation patterns in the wetland, this work synthesizes past knowledge to begin isolating the effects of highly coupled processes in wetland contaminant transport, specifically in Tims Branch. Four key conclusions emerge from this study:

- Flocs form in greater mass and are loaded with greater U and Ni concentrations when there are prolonged periods of dryness preceding storm events.
- Flocs pose a risk to downstream water quality only during pulses of streambank scouring of flocs and sediments induced by storm events and increased streamflow.
- Eroded sediments are likely the primary source of U and Ni within and from the Tims Branch wetland year-round.

- Porewater Fe concentrations sharply decrease when temperatures decrease for the winter season, but this decrease does not induce congruent order-of-magnitude decreases in floc formation. Porewater U and Ni concentrations do not exhibit similar seasonal variation.

This study does not aim to make retroactive estimates of year-round fluxes of U and Ni throughout the wetland's history; instead, this work concludes that Fe-OM flocs are unlikely to be the primary transport mechanism for the fraction of the 43.5 Mg of U that has left the Beaver Pond and Steed Pond reaches of Tims Branch. Further, the U flux observed in the stream channel—independent of floc-facilitated storm scouring events—amounts to roughly 12 kg U over the 9-month study period. Future work should be focused on differentiating contaminated soil grains eroding upgradient at Beaver Pond and in surface soils at Steed Pond from these flocs.

Flocs demonstrate a fundamental hydrogeochemical short-circuit effect, whereby reservoirs of contaminants in anoxic porewaters in gaining stream reaches can rapidly mobilize in streamwaters as these flocs move downgradient after hyporheic exchange and floc aggregation. However, the impact of flocs on overall water quality in a given watershed or stream reach is highly dependent on specific hydrologic conditions, the form of the contaminant in the sediment, and its affinity for Fe-oxide surfaces or OM ligands. In Steed Pond, storm events do scour flocs and mobilize U- and Ni-rich solids downgradient, but the antecedent dryness required for flocs to aggregate and accumulate in low energy pockets of streambanks prevents flocs from negatively impacting water quality and advancing the U plume beyond Steed Pond on decadal scales. If conditions in Tims Branch differed and gaining conditions regularly moved reduced porewaters through the OM-rich Beaver Pond hotspot, flocs could become an impactful transport mechanism. It is important to understand that a precise coupling of hydrology and geochemistry in a contamination system is necessary to render flocs a viable transport

mechanism over decades. Identifying the key hydrologic fluxes and potential geochemical reservoirs will allow researchers to effectively isolate the fluxes that have the highest potential to impact downgradient stream quality.

References

Arey, J.S., Seaman, J.C. and Bertsch, P.M. (1999) Immobilization of uranium in contaminated sediments by hydroxyapatite addition. Environmental Science and Technology 33, 337-342.

Batson, V.L., Bertsch, P.M. and Herbert, B.E. (1996) Transport of Anthropogenic Uranium from Sediments to Surface Waters During Episodic Storm Events. Journal of Environmental Quality 25, 1129-1137.

Church, S.E., Kimball, B.A., Fey, D.L., Ferderer, D.A., Yager, T.J. and Vaughn, R.B. (1997) Source, transport, and partitioning of metals between water, colloids, and bed sediments of the Animas River, Colorado. US Geological Survey Open-File Report 97, 151.

Dixon, K.L., Rogers, V.A., Conner, S.P., Cummings, C.L., Gladden, J.B. and Weber, J.M. (1996) Geochemical and physical properties of wetland soils at the Savannah River site. Savannah River Site (SRS), Aiken, SC.

Evans, A.G., Bauer, L.R., Haselow, J.S., Hayes, D.W., Martin, H.L., McDowell, W.L. and Pickett, J.B. (1992) Uranium in the Savannah River Site Environment, Aiken, SC, pp. WSRC-RP-92-315.

Hall, G.E.M., Vaive, J.E. and MacLaurin, A.I. (1996) Analytical aspects of the application of sodium pyrophosphate reagent in the specific extraction of the labile organic component of humus and soils. Journal of Geochemical Exploration 56, 23-36.

Hvorslev, M.J. (1951) Time lag and soil permeability in ground-water observations. Waterways Experiment Station, Corps of Engineers, US Army.

Kaplan, D.I., Buettner, S.W., Li, D., Huang, S., Koster van Groos, P.G., Jaffé, P.R. and Seaman, J.C. (2017) In situ porewater uranium concentrations in a contaminated wetland: Effect of seasons and sediment depth. Applied Geochemistry 85, 128-136.

Kaplan, D.I., Smith, R., Parker, C.J., Baker, M., Cabrera, T., Ferguson, B.O., Kemner, K.M., Laird, M., Logan, C., Lott, J., Manglass, L., Martinez, N.E., Montgomery, D., Seaman, J.C., Shapiro, M. and Powell, B.A. (2020) Uranium Attenuated by a Wetland 50 Years after Release into a Stream. ACS Earth Space Chem 2020, 1360-1366.

Kimball, B.A., Bianchi, F., Walton-Day, K., Runkel, R.L., Nannucci, M. and Salvadori, A. (2007) Quantification of changes in metal loading from storm runoff, Merse River (Tuscany, Italy). Mine Water and the Environment 26, 209-216.

Lapworth, D.J., Stolpe, B., Williams, P.J., Gooddy, D.C. and Lead, J.R. (2013) Characterization of suboxic groundwater colloids using a multi-method approach. Environmental Science and Technology 47, 2554-2561.

Li, D., Seaman, J.C., Chang, H.S., Jaffe, P.R., Koster van Groos, P.G., Jiang, D.T., Chen, N., Lin, J., Arthur, Z., Pan, Y., Scheckel, K.G., Newville, M., Lanzirotti, A. and Kaplan, D.I. (2014) Retention and chemical speciation of uranium in an oxidized wetland sediment from the Savannah River Site. Journal of Environmental Radioactivity 131, 40-46.

Liao, P., Li, W., Jiang, Y., Wu, J., Yuan, S., Fortner, J.D. and Giammar, D.E. (2017) Formation, aggregation, and deposition dynamics of nom-iron colloids at anoxic-oxic interfaces. Environmental Science and Technology 51, 12235-12245.

Liao, P., Pan, C., Ding, W., Li, W., Yuan, S., Fortner, J.D. and Giammar, D.E. (2020) Formation and Transport of Cr(III)-NOM-Fe Colloids upon Reaction of Cr(VI) with NOM-Fe(II)

Colloids at Anoxic-Oxic Interfaces. Environmental Science and Technology 54, 4256-4266.

Masscheleyn, P.H., Pardue, J.H., DeLaune, R.D. and Patrick, J.W.H. (1992) Chromium redox chemistry in a lower Mississippi Valley bottomland hardwood wetland. Environmental Science & Technology 26, 1217-1226.

Mehra, O.P. and Jackson, M.L. (1958) Iron Oxide Removal from Soils and Clays by a Dithionite-Citrate System Buffered with Sodium Bicarbonate. Clays and Clay Minerals 7, 317-327.

Parker, C.J., Kaplan, D.I., Seaman, J.C. and Powell, B.A. (2022) Uranium partitioning from contaminated wetland soil to aqueous and suspended iron-floc phases: Implications of dynamic hydrologic conditions on contaminant release. Geochimica et Cosmochimica Acta 318, 292-304.

Philippe, A. and Schaumann, G.E. (2014) Interactions of Dissolved Organic Matter with Natural and Engineered Inorganic Colloids: A Review. Environmental Science and Technology 48, 8946-8962.

Reed, M.B. and Swanson, M.T. (2006) 300/M-Area-Fuel and Target Fabrication. New South Associates: Stone Mountain, GA, Stone Mountain, GA, p. Rep. No. 1189.

Schultz, M.K., Burnett, W.C. and Inn, K.G.W. (1998) Evaluation of a sequential extraction method for determining actinide fractionation in soils and sediments. Journal of environmental radioactivity 40, 155-174.

Schwertmann, U. (1991) Solubility and dissolution of iron oxides. Plant and Soil 1991 130:1 130, 1-25.

Seaman, J.C., Arey, J.S. and Bertsch, P.M. (2001) Immobilization of nickel and other metals in contaminated sediments by hydroxyapatite addition. Journal of Environmental Quality 30, 460-469.

Sholkovitz, E.R. and Copland, D. (1981) The coagulation, solubility and adsorption properties of Fe, Mn, Cu, Ni, Cd, Co and humic acids in a river water. Geochimica et Cosmochimica Acta 45, 181-189.

Sobolewski, A. (1999) A review of processes responsible for metal removal in wetlands treating contaminated mine drainage. International Journal of Phytoremediation 1, 19-51.

Sowder, A.G., Bertsch, P.M. and Morris, P.J. (2003) Partitioning and availability of uranium and nickel in contaminated riparian sediments. Journal of Environmental Quality 32, 885-898.

Stefánsson, A. (2007) Iron(III) hydrolysis and solubility at 25°C. Environmental Science and Technology 41, 6117-6123.

Zelles, L., Adrian, P., Bai, Q.Y., Stepper, K., Adrian, M.V., Fischer, K., Maier, A. and Ziegler, A. (1991) Microbial activity measured in soils stored under different temperature and humidity conditions. Soil Biology and Biochemistry 23, 955-962.

VII. CONCLUSIONS & FUTURE WORK

Conclusions

The work presented here is intended to sequentially investigate the persistence of U in the Tims Branch wetland across multiple scales. Preliminary work done with collaborators at SRNL helped identify the hotspots of U in the wetland and identify the bounds of its lateral extent (Kaplan et al., 2020). The first block of this study focused on characterizing the depth profiles of U in the Beaver Pond and Steed Pond hotspots while identifying the relationships with Fe and OM in the wetland. Along with these depth profiles, water samples taken throughout the wetland identified the potentially mobile fractions of U and Fe associated with stream solids—both Fe-OM flocs at Steed Pond and eroded streambank sediments at Beaver Pond. The next phase of work focused on the general speciation of metals and OM in the study sites. Parallel extraction of redox-preserved cores allowed for us to investigate how oxidation impacts the reservoirs of U, Ni, and Fe in various targeted extractant phases. From this, the importance of soil OM became abundantly clear, as detailed OM characterization at key metal accumulation depths indicated that high diversity of metal-reactive OM compounds in deeper OM-rich soil layers were accumulating trace heavy metals, in addition to natural isotopic ratios of U (while U introduced from M-Area processes was predominantly depleted of ^{235}U).

The final section of this work tracked metal inventories in streams, flocs, and porewaters over 9 months and supported the previous findings of a coupling between U, Fe, and OM. The seasonal sampling determined that flocs along streambanks at Steed Pond contain a consistent 80%/20% ratio of U associated with the OM matrix versus the Fe-oxide minerals, and flocs could have only moved 132 kg of U over 60 years with conservative risk assessing estimations of

storm frequency, intensity, and rate of floc accumulation. Three key findings emerged from this body of work:

- Uranium has begun to incorporate into natural wetland Fe and C cycling, as evidenced by accumulations in Beaver Pond and Steed Pond, where correlations in depth profiles indicate incorporation as U moves downgradient in the wetland sediment.
- Organic matter in Tims Branch drives U and other heavy metal accumulation in OM-rich soil layers, and the pools of U and Ni at both hotspots are strongly bound to soil OM, likely rendering these metals immobile in the absence of harsh extraction treatments.
- The majority of U and Ni transport from Tims Branch is not due to floc formation and scouring. While it is an important fundamental hydrogeochemical flux in riparian systems with sharp redox gradients at the hyporheic interface, floc formation does not move U in high enough masses from Steed Pond to account for missing U in the current mass balance. Erosion of contaminated sediments, especially from Beaver Pond, is likely more responsible for this deficit.

These key findings, one from each section of the work, highlight the scaling of this study from the entire wetland to the geochemical composition of colloidal Fe-OM flocs. If the DOE was to utilize this body of work in assessing remediation methods for the heavy metals present in Tims Branch, the current recommendation would be to make no amendments to the wetland and allow the wetland to naturally sequester the U and Ni as it has been for 60 years. Currently, erosion of streambanks at Beaver Pond appears to be the most impactful contribution of U flux within and from the wetland, and the stream channel shows no signs of changing here, as the braided stream channels emerge roughly 0.5 km farther downgradient in the wetland. As such, no further erosion of the flat basin appears to be occurring, and porewaters are not leaching

appreciable U from the strongly complexing OM present in the soil column. More research is required to adequately characterize the role of sediment transport in Tims Branch—independent of floc formation and scouring at Steed Pond.

Future Work

The work presented here explores the extent of U contamination in Tims Branch and what geochemical components are retaining U in the wetland, while simultaneously eliminating the possibility of Fe-OM flocs as a significant flux of U on decadal scales. Future work should focus on sediment transport of U within and from Tims Branch. Four focus areas would enhance the scientific community's understanding of the U remaining in Tims Branch: sediment characterization, determination of hydrologic constants for the wetland, dating of U daughters at Steed Pond, and direct collection of stream samples during storm events.

Sediment characterization at Beaver Pond is an important step towards differentiating types of solid-phase U transport within Tims Branch. Flocs form exclusively at Tims Branch and do not appear to currently play a role in decadal U transport. Meanwhile, studies have observed the mobilization of U in stream solids associated with a solid phase at Beaver Pond that contains distinctly less Fe than the Steed Pond flocs (Parker et al., 2022) (Parker, Paper 3). A detailed microscopy characterization of these sediments, both from filtration and isolation and direct collection from a streambank cross-section, would begin to determine what phase this U is associated with when eroded from the streambanks. Current work leads us to hypothesize that U is associated with OM-coated particles, being retained by the OM on soil grains that are less Fe-rich than downgradient subsurface deposits. Thus, using microscopy and energy dispersive x-ray spectroscopy (EDX) to determine if U is collecting on Si-rich sand grains or another mineral

phase would inform future spectroscopy work to ultimately determine the atomic U bonding environment.

To compliment the characterization of mobilized U-contaminated particles at Beaver Pond, a rudimentary determination of the wetland residence time and dispersivity would begin to couple local geochemical processes to ongoing surface water modeling efforts. Using a synoptic sampling scheme to sample at roughly 10 locations (7 along the main stream channel, and 3 in the wider braided-stream section of the wetland between Beaver Pond and Steed Pond) within the Tims Branch wetland simultaneously would allow for the release of a tracer at the opening of the bottleneck upgradient from Beaver Pond and stream samples at 15 minute intervals to determine when the tracer has reached the Steed Pond dam and to what degree the tracer diffuses from the main stream channel. This coordinated effort would allow for an approximation of wetland residence time during baseflow and an initial quantification of how U leaving Beaver Pond may be dispersing laterally in the wetland. A potential tracer would be NaBr, to measure increased conductivity in the stream samples without interfering with local geochemistry. Another tracer that would further characterize the wetland would be a tagged solid or suite of particle sizes into the stream. While a radiotracer would be difficult to permit on the DOE SRS, radiolabeled solids (potentially ^{13}C-enriched styrene nanoparticle conglomerations) of various sizes in equilibrium with an aqueous solution would allow for characterization of the aqueous-phase transport within Tims Branch and estimated residence times for various particle size classes during baseflow. This detailed hydrologic analysis of Tims Branch would compliment the aforementioned sediment characterization to begin to estimate fluxes of U due to erosion.

Age dating of U daughter products would allow for an improved understanding of the relative age of when U present in the wetland was deposited. Using the ingrowth of U daughters

and their accumulation in sealed samples would allow researchers to determine not just the isotopic ratio of U (whether it was depleted from M-Area processes or naturally accumulated during the wetland's lifetime), but also how long ago the U was sedimented compared to surrounding heavy elements. Employing this method in Steed Pond would determine whether U moving in flocs currently was deposited by sediment transport from Beaver Pond or whether this U is being eroded from original deposits from M-Area into the original Steed Pond. Likewise, this method could determine when U in Tims Branch South, another hydrogeochemically similar wetland 8 km downgradient, was deposited, and if it was deposited recently, was it associated with flocs or ordinary suspended sediments. The relative age of U in Tims Branch would augment the rudimentary U transport model presented in this work by providing estimates of mobility before present day, as measuring hydrologic transport is simpler moving forward rather than estimating past fluxes. Our current understanding of the wetland's geochemistry is sufficient to begin informing a reactive transport model, and dating past sedimentation of U in the wetland will help us understand the decadal hydrologic fluxes most relevant to the system.

Finally, recreating the Batson (1996) study by collecting stream samples during and after significant storm events would help differentiate between floc and sediment transport mechanisms in Tims Branch. The Batson study was performed only a few years after the collapse of the Steed Pond dam, thus only a few years of exposure to the atmosphere and initial erosional processes (Batson et al., 1996). Recreating this study now would help us understand how vegetation and a single stream channel has impacted transport during storm events. With the recent knowledge of flocs forming after significant dry periods and then being swiftly scoured, repeating the storm intensity study would allow for simple, but more detailed, characterization of stream solid loads. Other studies of storm impacts on solid transport in watersheds (Church et al.,

1997; Kimball et al., 2007) indicate that flocs and other colloidal Fe species aggregate in dry baseflow (i.e., baseflow with little to no precipitation) but are the first solid phase to be scoured from streambanks, detectable shortly after storm onset and increased stream flow. As such, collecting stream samples at fine temporal resolution at storm onset and deliberately filtering in sequence to isolate size fractions, OM content, and Fe content in digested material would allow researchers to distinguish between the initial pulse of scoured flocs in the stream, prolonged sediment loading in the stream, and the composition of these two solid-phase components. Flocs do not appreciably impact total U mobility from the wetland, but as stated in Chapter 6, the pulse of flocs being scoured could pose measurable, albeit brief, risks to downgradient water quality.

These four methods of investigating U transport in Tims Branch would leverage the work of Chapters 4, 5, and 6 and advance the literature even further while providing detailed characterization of this specific study site alongside important fundamental principles of geochemical transport. The impact of a quality scientific endeavor should exceed the specific study site. Whether that improvement arises from remediation of water to reduce risk for stakeholders downgradient or from an improved characterization of fundamental principles that can be applied to other study sites, the improvement should be tangible. With the work in Chapters 4, 5, and 6, flocs were determined to be inconsequential with regards to the total U inventory in Tims Branch, but also began to investigate specific hydrologic and geochemical principles involved in the hydrogeochemical short-circuit of porewater metals and OM into the stream via hyporheic exchange. Likewise, the future work posed here would richly characterize the suspended solid transport of U occurring in Tims Branch and would begin to elucidate the relationship between general storm intensity and the geochemical composition of solids being mobilized in storm events.

References

Batson, V.L., Bertsch, P.M. and Herbert, B.E. (1996) Transport of Anthropogenic Uranium from Sediments to Surface Waters During Episodic Storm Events. Journal of Environmental Quality 25, 1129-1137.

Church, S.E., Kimball, B.A., Fey, D.L., Ferderer, D.A., Yager, T.J. and Vaughn, R.B. (1997) Source, transport, and partitioning of metals between water, colloids, and bed sediments of the Animas River, Colorado. US Geological Survey Open-File Report 97, 151.

Kaplan, D.I., Smith, R., Parker, C.J., Baker, M., Cabrera, T., Ferguson, B.O., Kemner, K.M., Laird, M., Logan, C., Lott, J., Manglass, L., Martinez, N.E., Montgomery, D., Seaman, J.C., Shapiro, M. and Powell, B.A. (2020) Uranium Attenuated by a Wetland 50 Years after Release into a Stream. ACS Earth Space Chem 2020, 1360-1366.

Kimball, B.A., Bianchi, F., Walton-Day, K., Runkel, R.L., Nannucci, M. and Salvadori, A. (2007) Quantification of changes in metal loading from storm runoff, Merse River (Tuscany, Italy). Mine Water and the Environment 26, 209-216.

Parker, C.J., Kaplan, D.I., Seaman, J.C. and Powell, B.A. (2022) Uranium partitioning from contaminated wetland soil to aqueous and suspended iron-floc phases: Implications of dynamic hydrologic conditions on contaminant release. Geochimica et Cosmochimica Acta 318, 292-304.

VIII. APPENDICES

A. URANIUM PARTITIONING FROM CONTAMINATED WETLAND SOIL TO AQUEOUS AND SUSPENDED IRON-FLOC PHASES: IMPLICATIONS OF DYNAMIC HYDROLOGIC CONDITIONS ON CONTAMINANT RELEASE

Figure A - 1: Photos at the Steed Pond sampling area (top) and Beaver Pond sampling area (bottom). Note the orange floc coating stream plants and the streambed at Steed Pond. This contrasts the clear water and sandy bed of Beaver Pond, where flocs do not form.

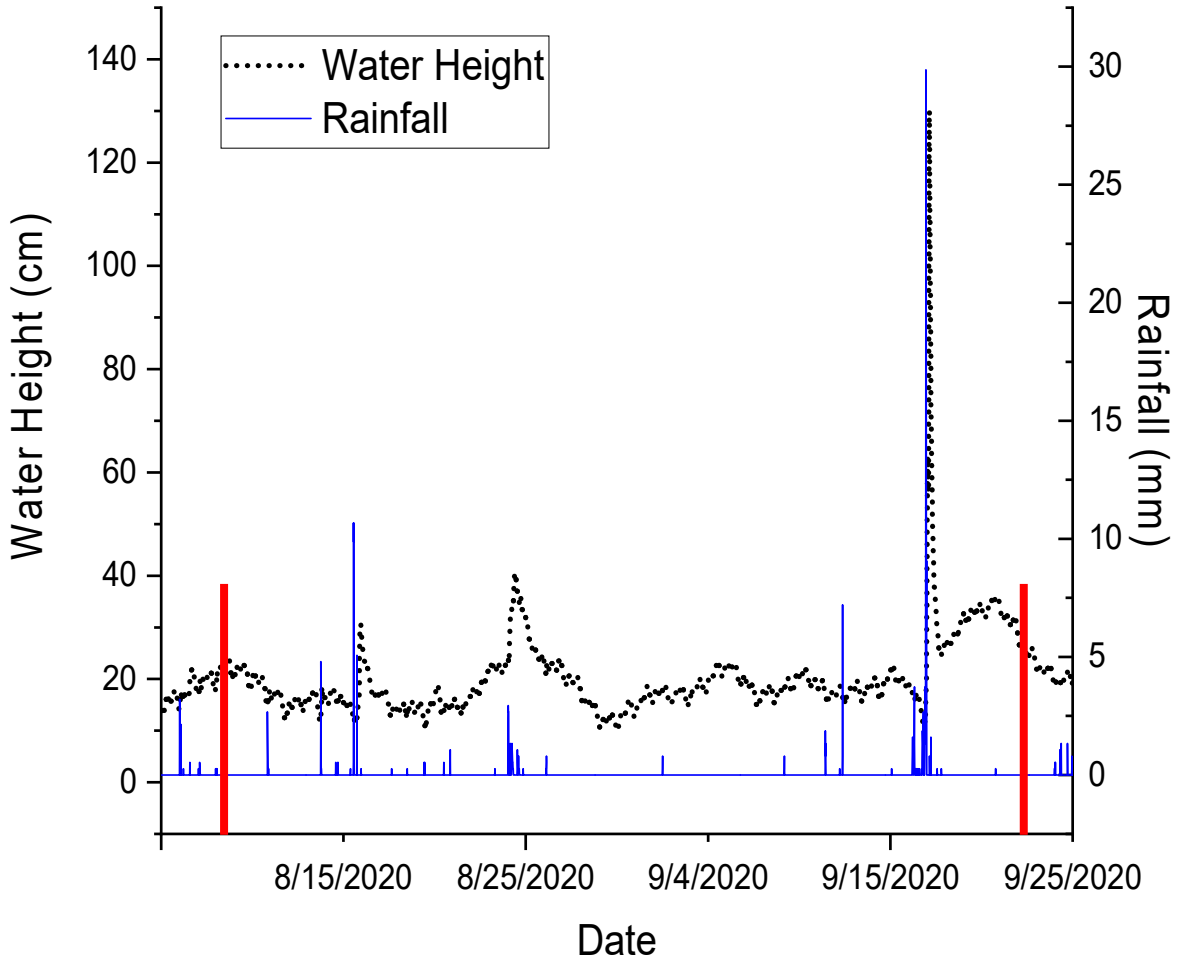

Figure A - 2: Complete rainfall and stream height data for August and September 2020.

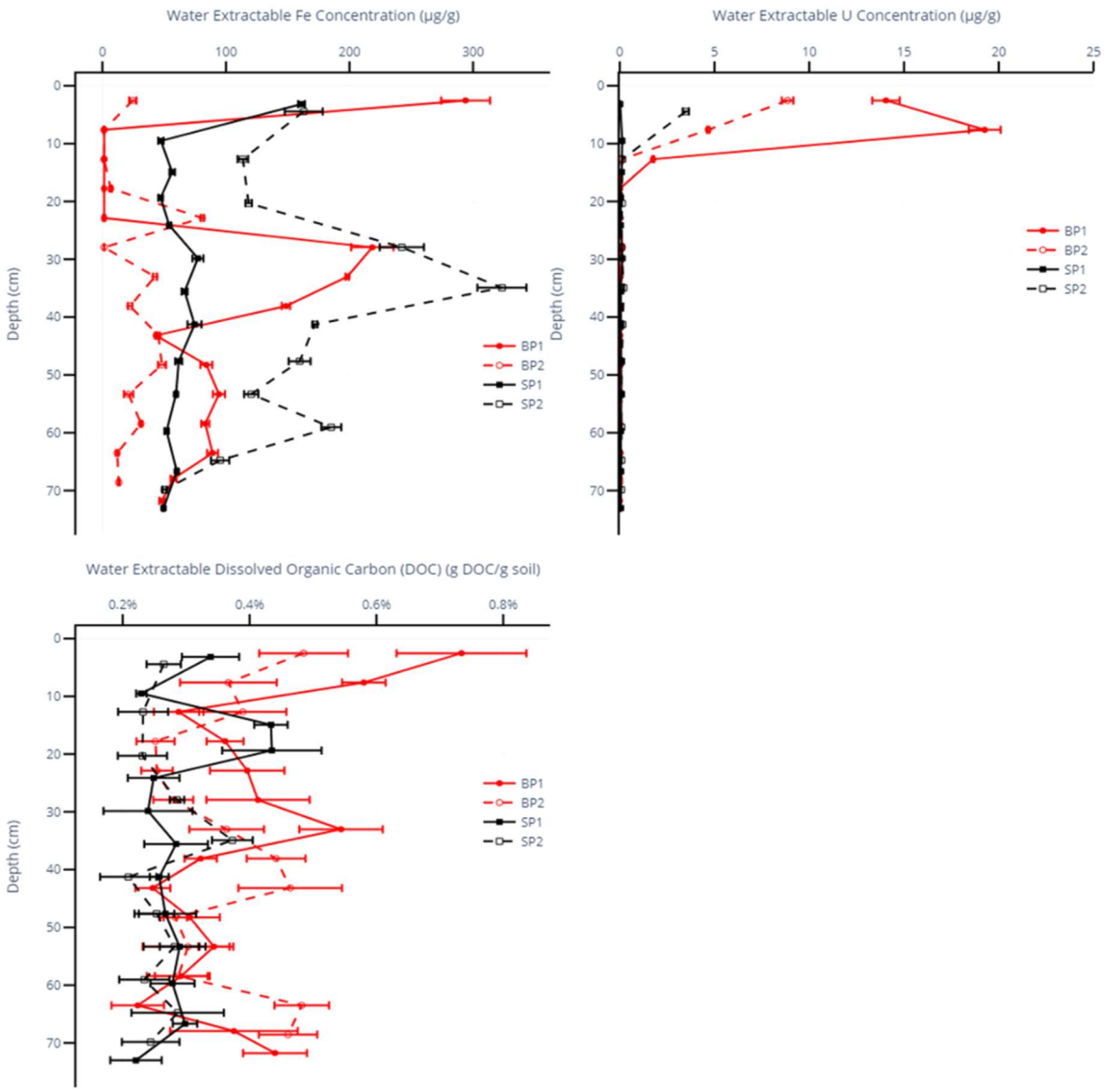

Figure A - 3: Water Extractable Fe, U, and Dissolved Organic Carbon (DOC) in soil cores recovered from Beaver Pond (BP-1 and BP-2) and Steed Pond (SP-1 and SP-2). Lines are not data, they are present to guide the reader. Error bars represent analytical error and may be hidden by symbol.

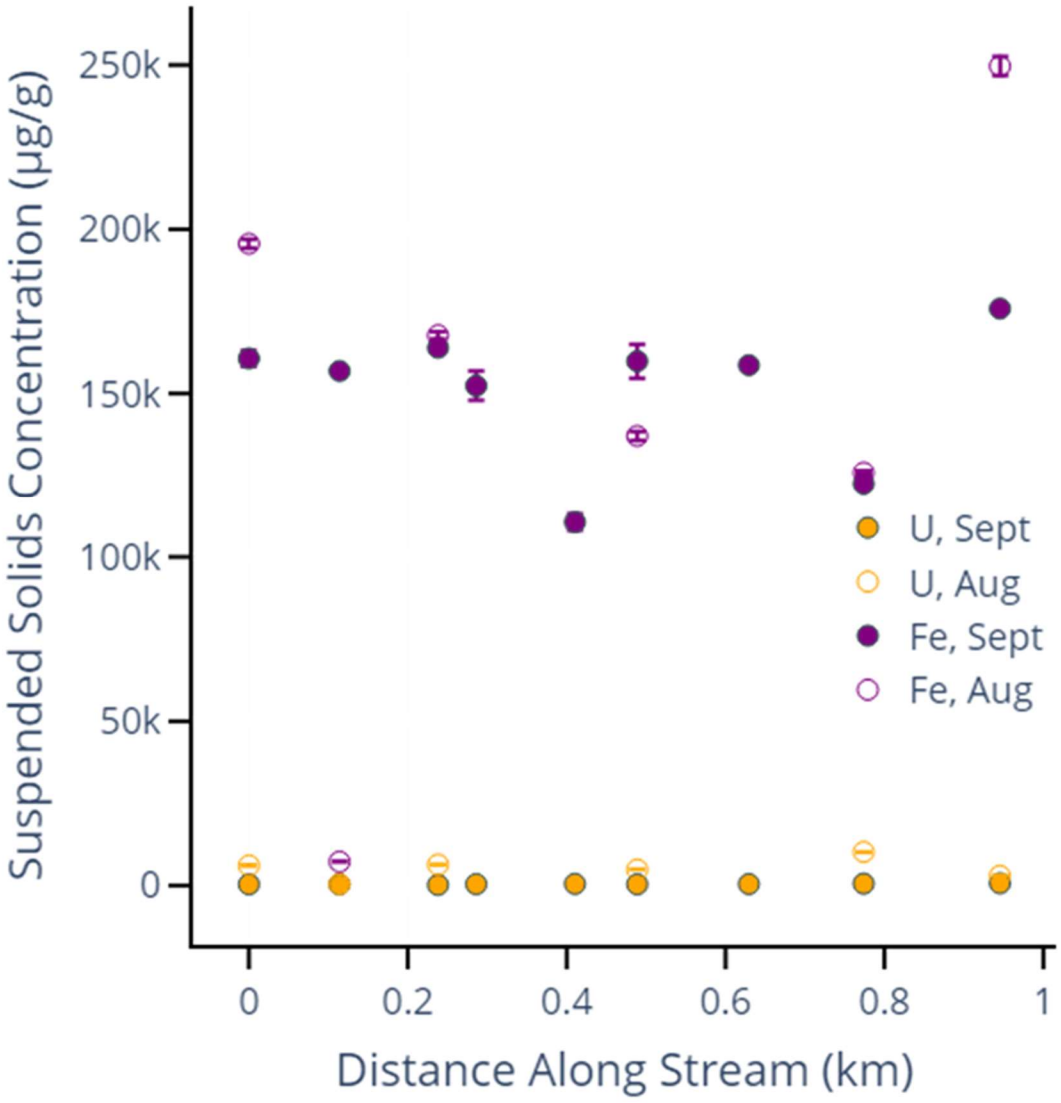

Figure A - 4: Linear Scale of U and Fe concentrations in the suspended solids. Error bars are present for all samples but may be hidden behind marker for September samples. Error bars represent analytical error.

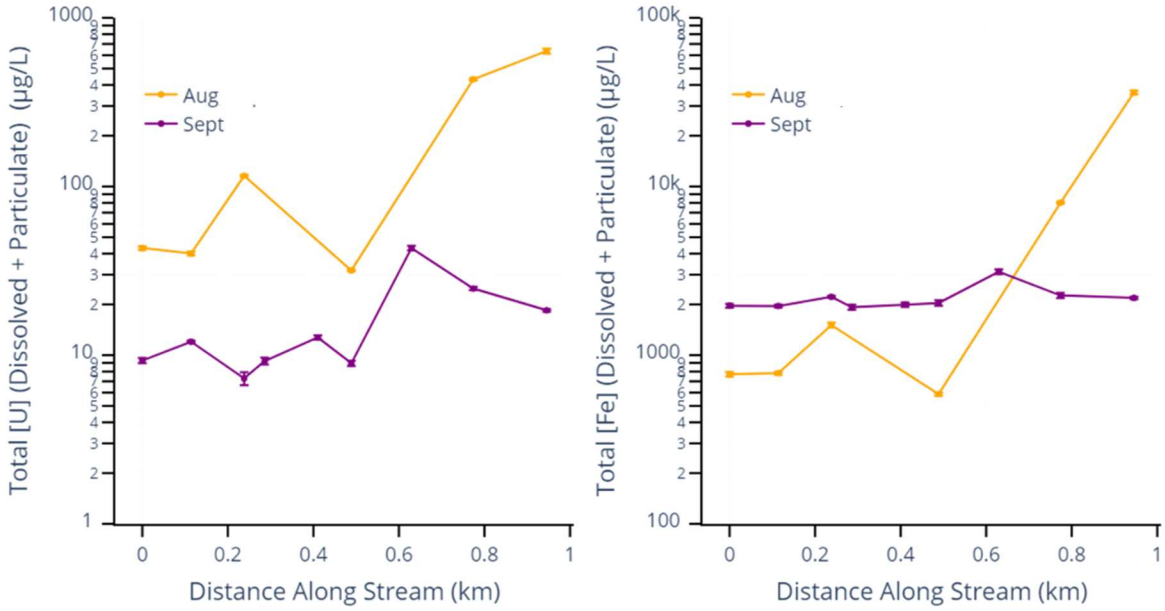

Figure A - 5: Log scale of Total U and Total Fe in stream, corresponding with Fig. 7. Lines are not data, they are present to guide the reader. Error bars represent analytical error and may be hidden by symbol.

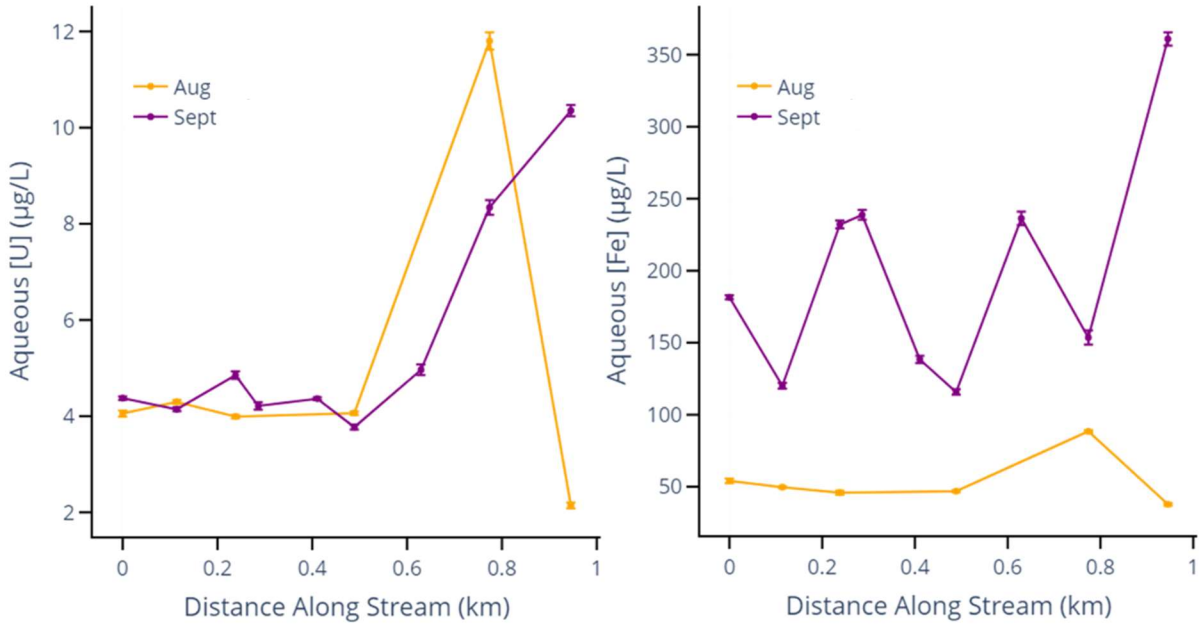

Figure A - 6: Aqueous contributions of U and Fe to the Total inventories in Fig. 7. Note the difference in y-axis scales, as the aqueous contributions were roughly 1-3% of the Total inventory at all sampling times and locations. Lines are not data, they are present to guide the reader. Error bars represent analytical error and may be hidden by symbol.

B. LEACHING OF URANIUM & NICKEL FROM ANTHROPOGENICALLY CONTAMINATED WETLAND SEDIMENTS UNDER OXIC & ANOXIC CONDITIONS: INFLUENCE O F IRON AND ORGANIC MATTER SPECIATION

Table B - 1: Metal concentrations from NaPP soil extraction in anoxic and oxic conditions from Hunnicutt Creek, Clemson, SC, and the corresponding OM characterizations for carbon-bearing mobile cyclic (CRAM) and chain (CCAM) compounds.

	[Ni] (µg/g)	[U] (µg/g)	[Fe] (µg/g)	CRAM Abundance (%)	CCAM Abundance (%)
Anoxic_Top	1.4 ± 0.27	0.18 ± 0.04	905.1 ± 79.16	17.2	44.5
Anoxic_Bottom	2.01 ± 1.77	0.53 ± 0.4	832.88 ± 43.13	29.2	39.9
Oxic_Top	0.25 ± 0.04	0.09 ± 0.01	604.24 ± 7.01	10.1	27.6
Oxic_Bottom	0.24 ± 0.03	0.13 ± 0.003	632.94 ± 28.27	16.1	22.4

C.

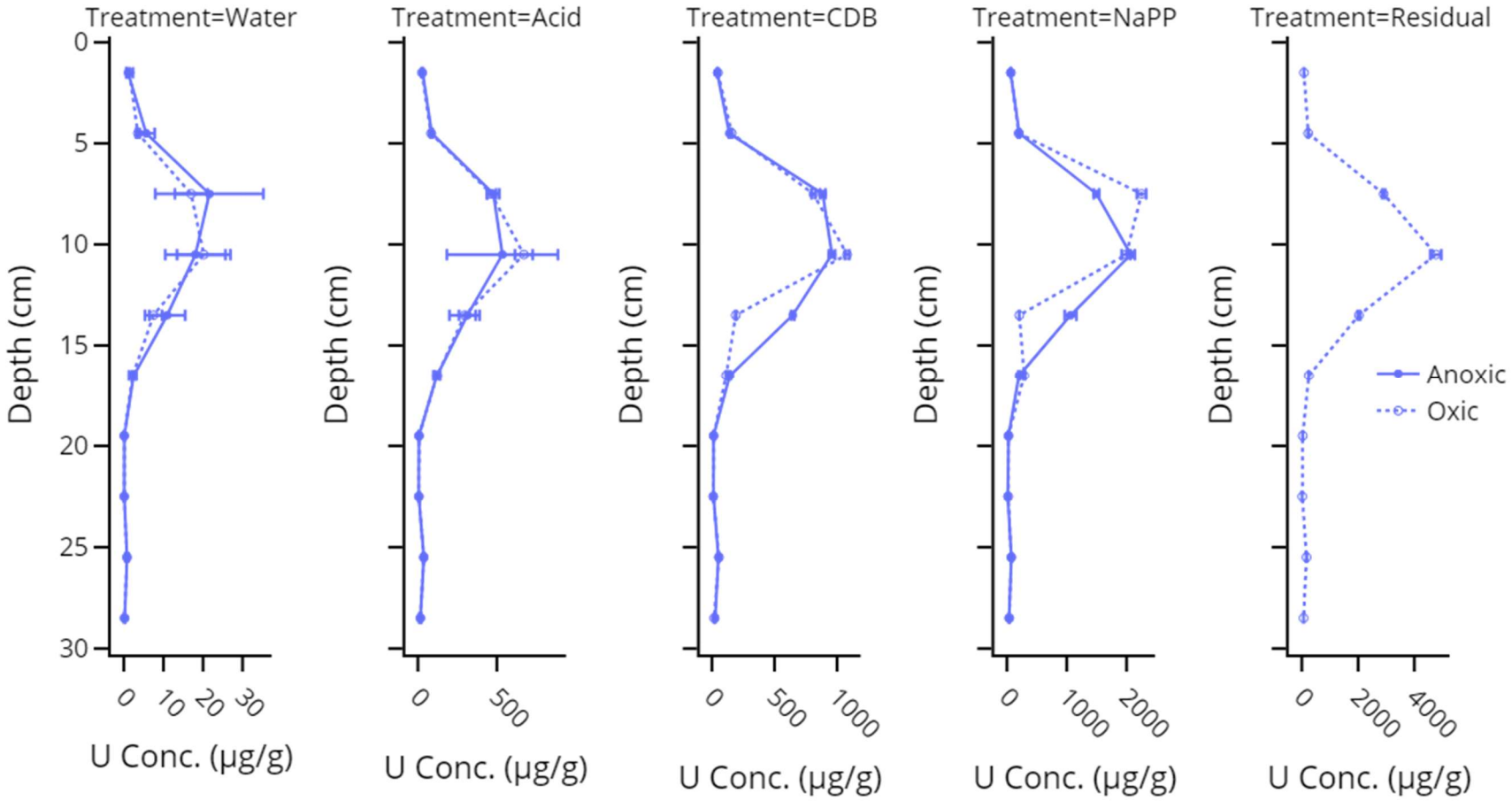

Figure B - 1: Concentrations of U in each extractant phase and under oxic and anoxic conditions at Beaver Pond.

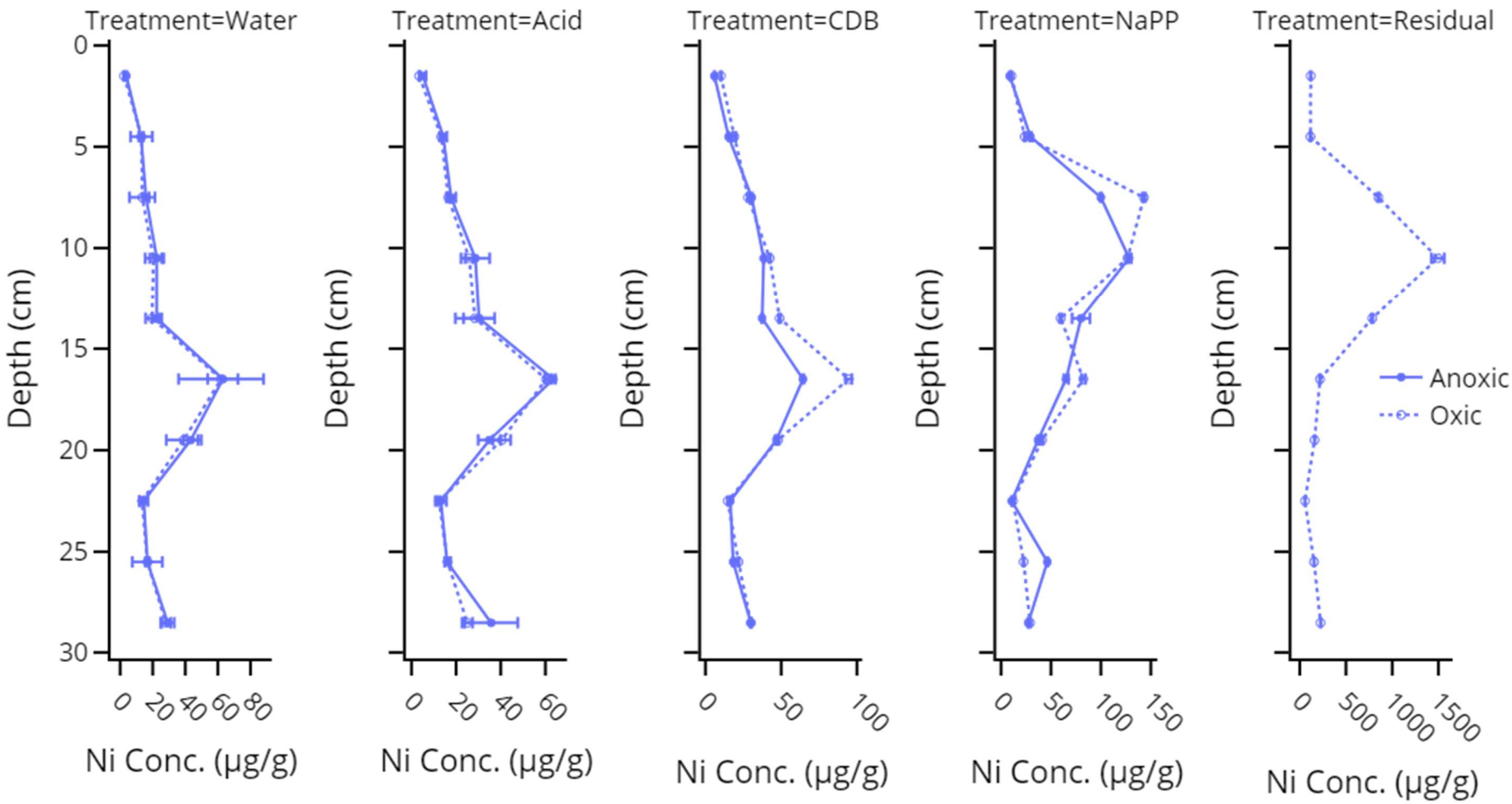

Figure B - 2: Concentrations of Ni in each extractant phase and under oxic and anoxic conditions at Beaver Pond.

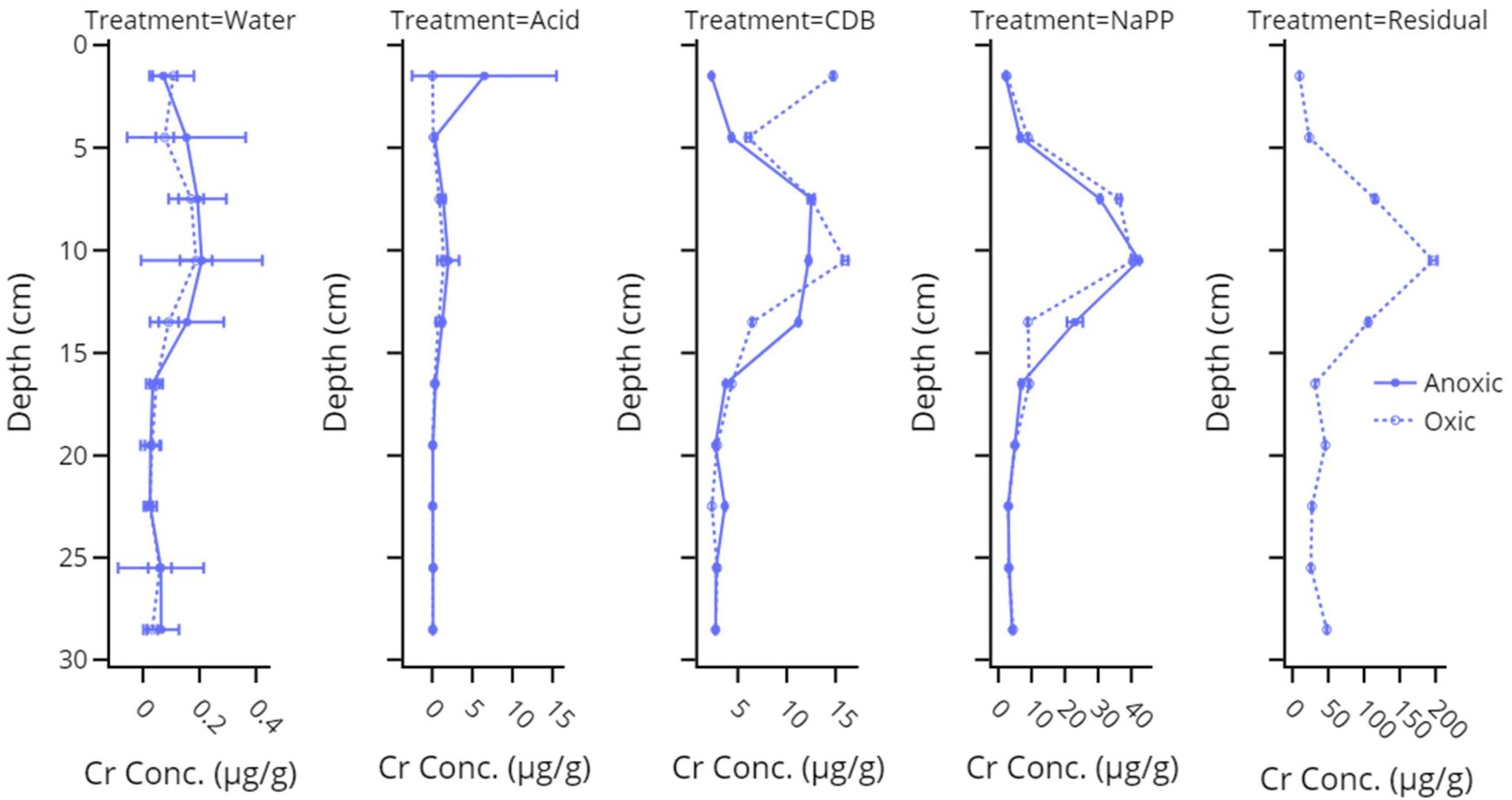

Figure B - 3: Concentrations of Cr in each extractant phase and under oxic and anoxic conditions at Beaver Pond.

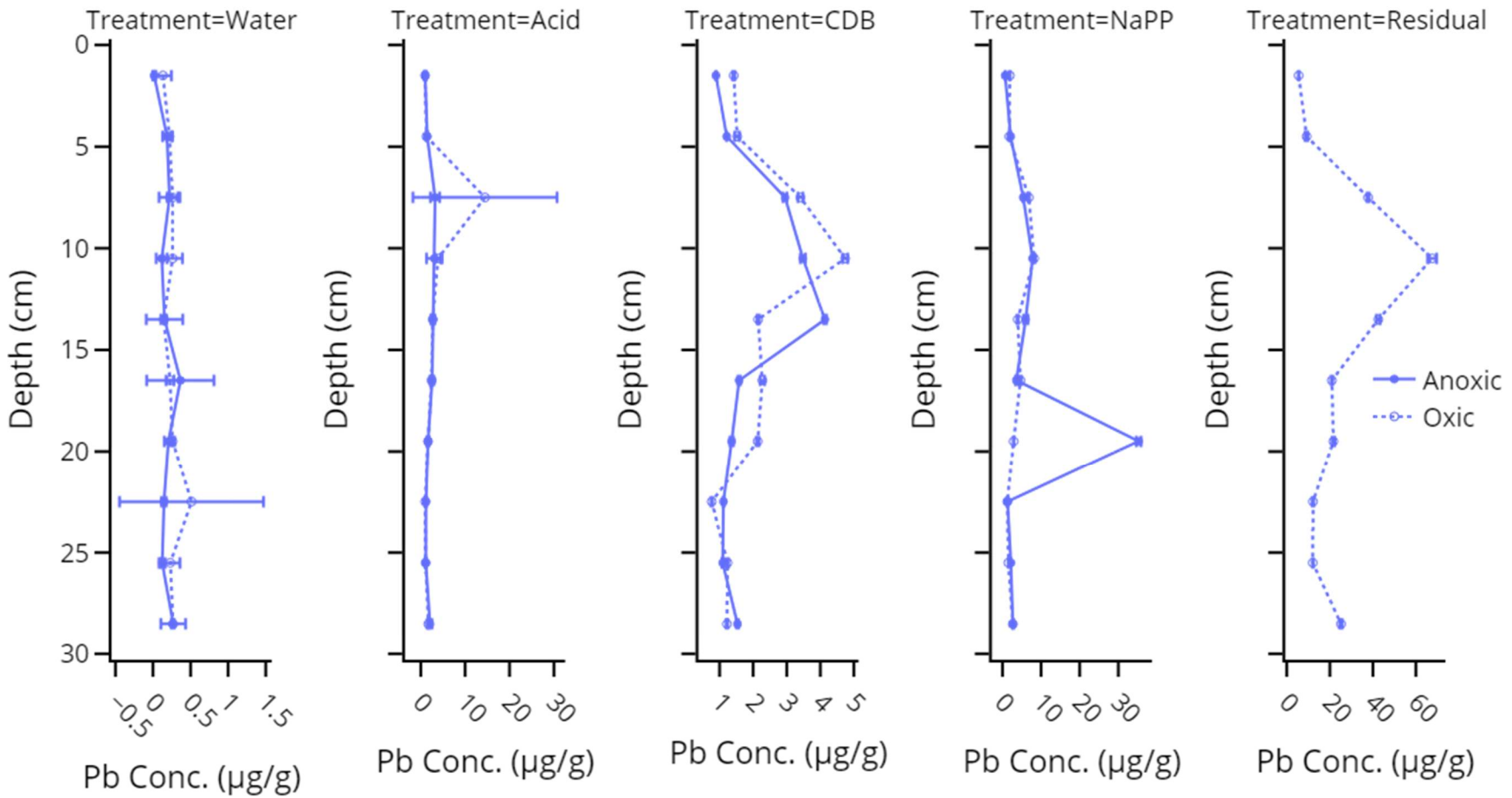

Figure B - 4: Concentrations of Pb in each extractant phase and under oxic and anoxic conditions at Beaver Pond.

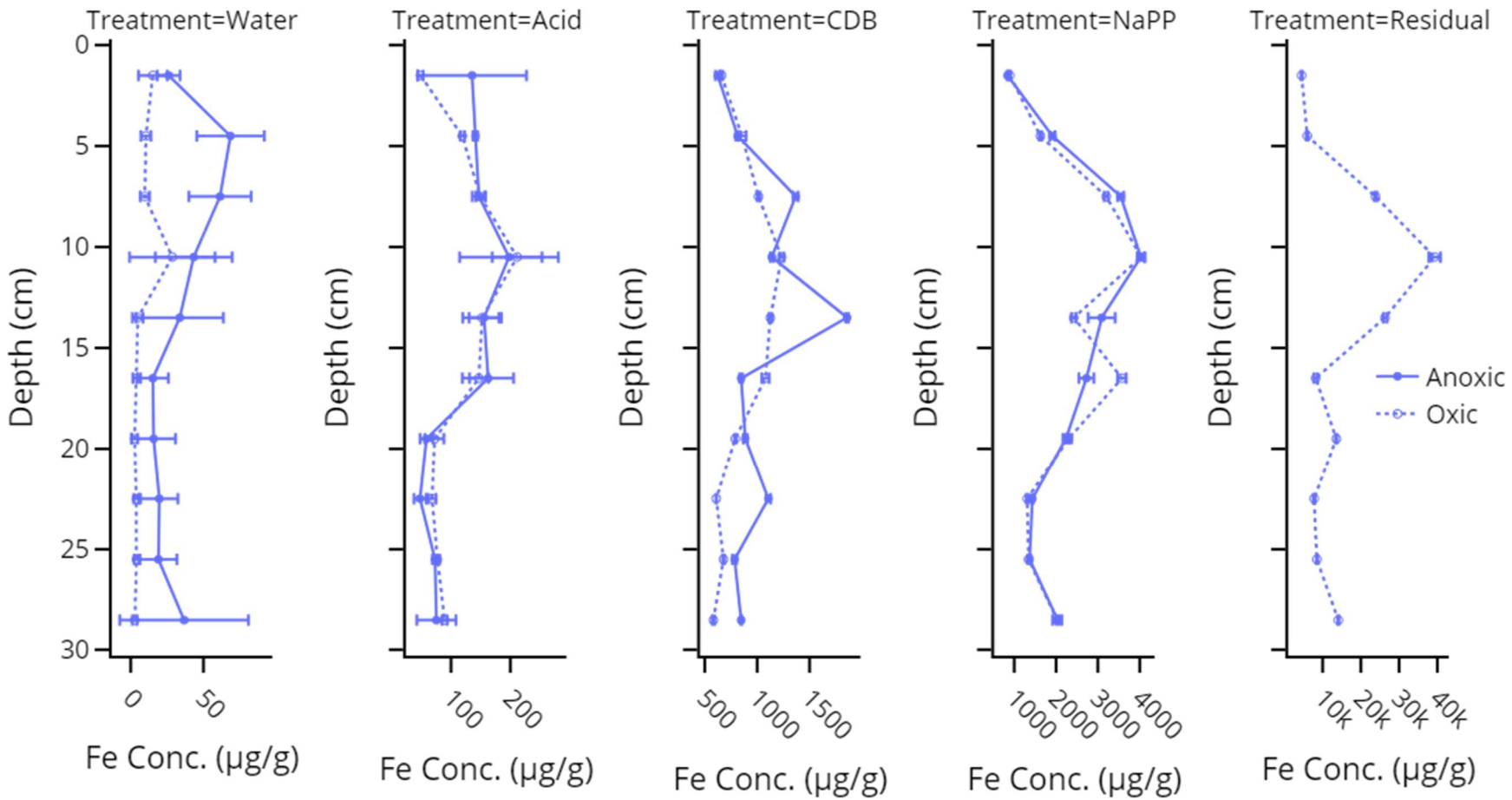

Figure B - 5: Concentrations of Fe in each extractant phase and under oxic and anoxic conditions at Beaver Pond.

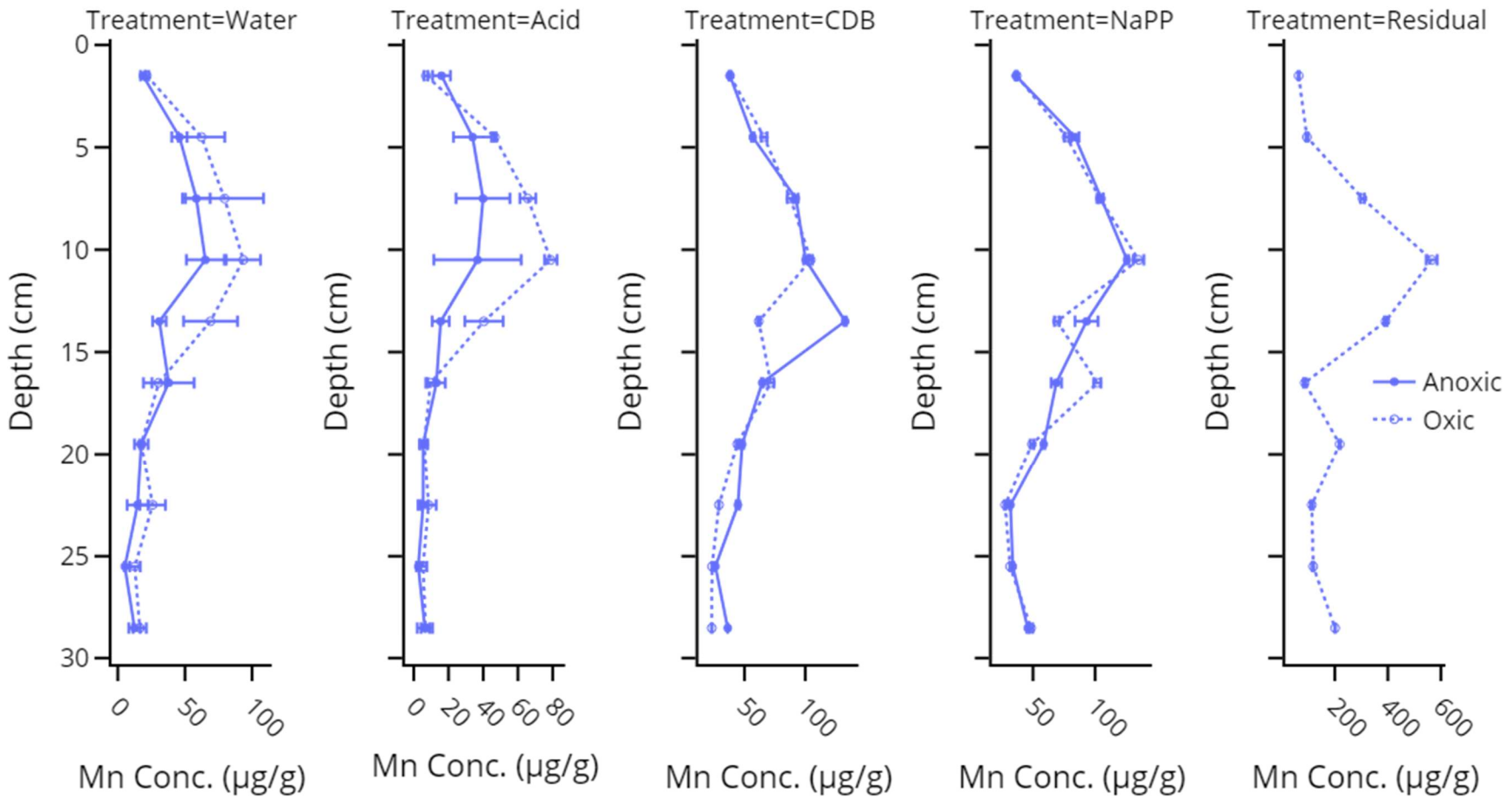

Figure B - 6: Concentrations of Mn in each extractant phase and under oxic and anoxic conditions at Beaver Pond.

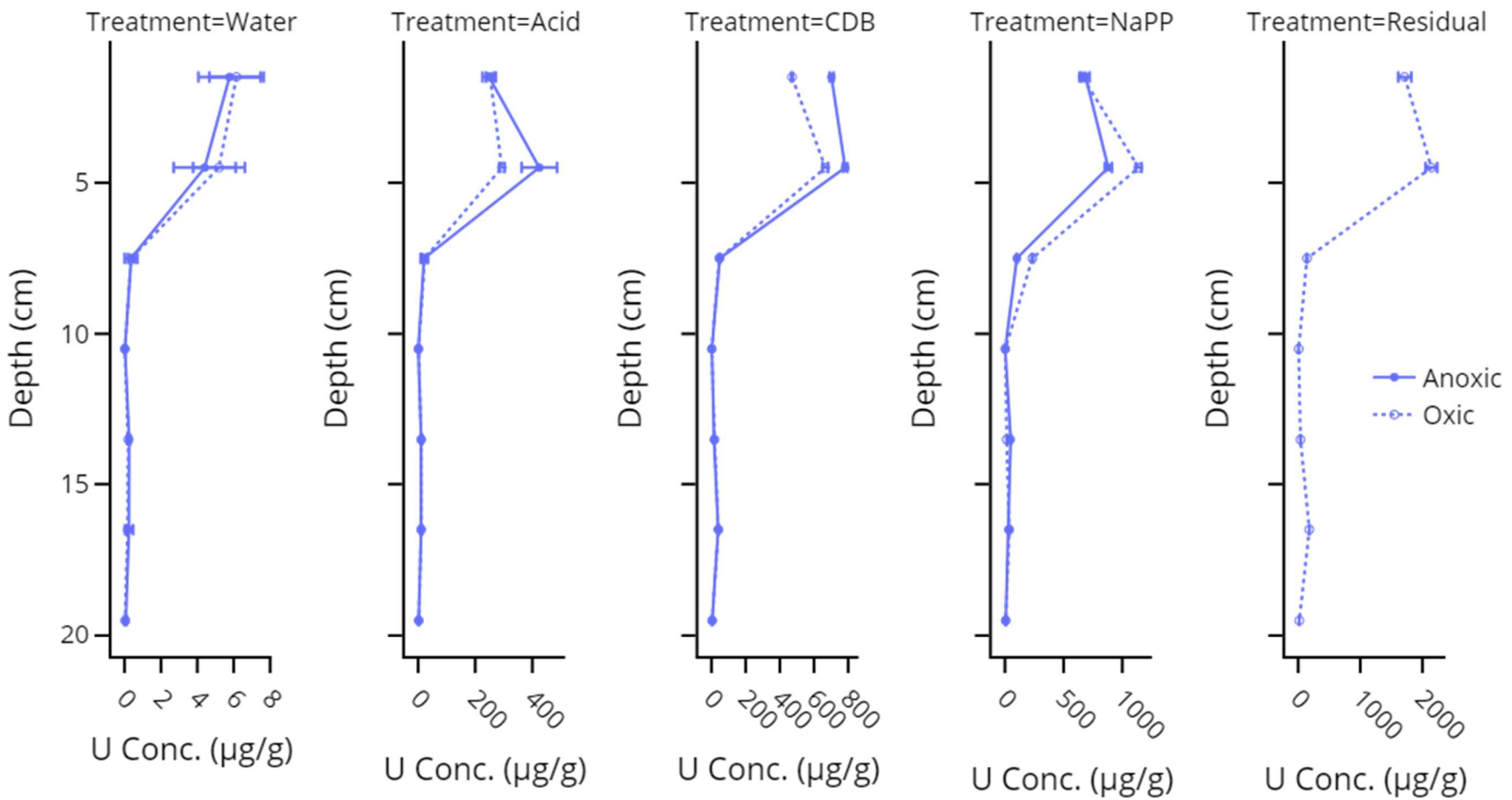

Figure B - 7: Concentrations of U in each extractant phase and under oxic and anoxic conditions at Steed Pond.

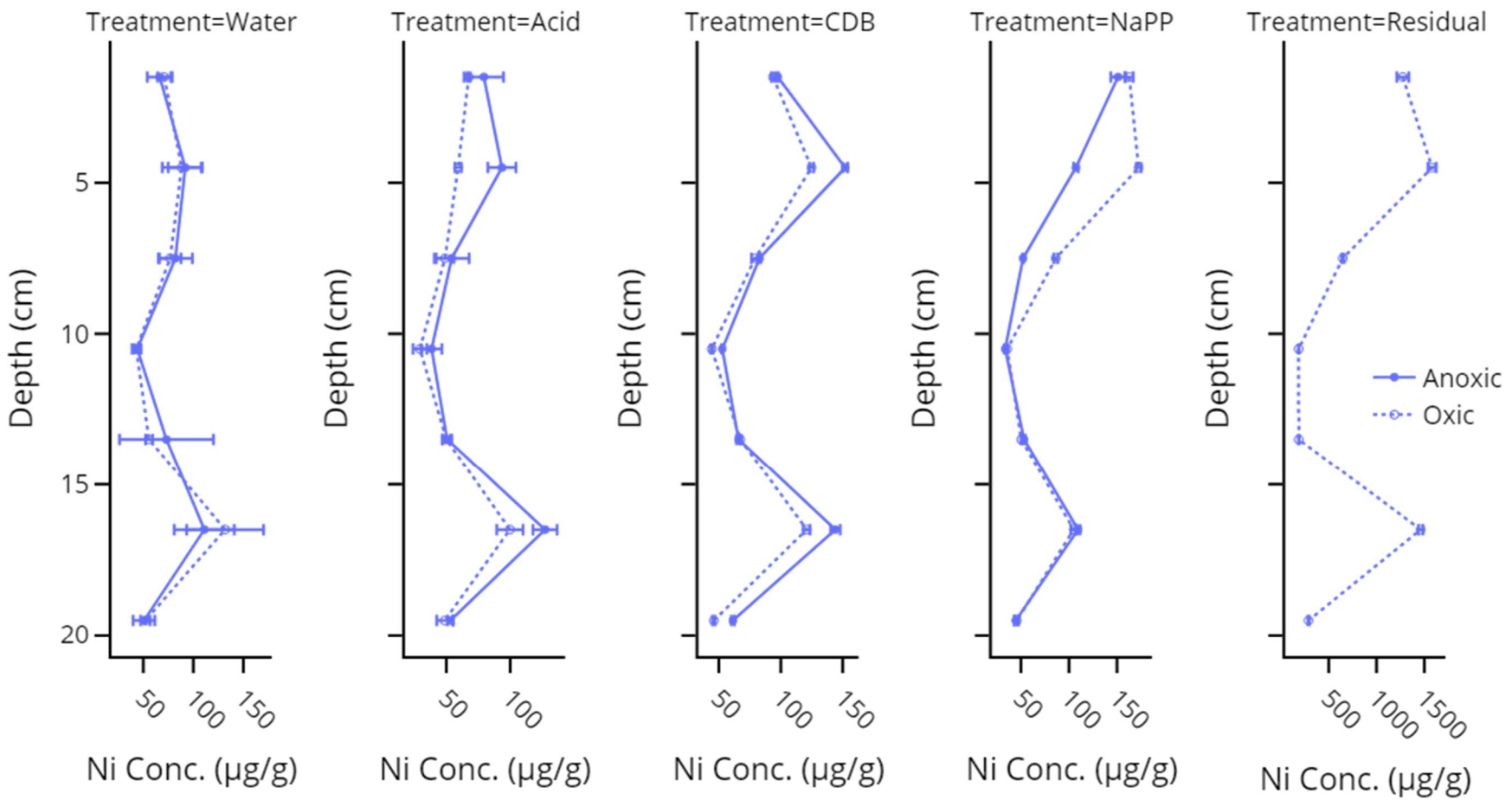

Figure B - 8: Concentrations of Ni in each extractant phase and under oxic and anoxic conditions at Steed Pond.

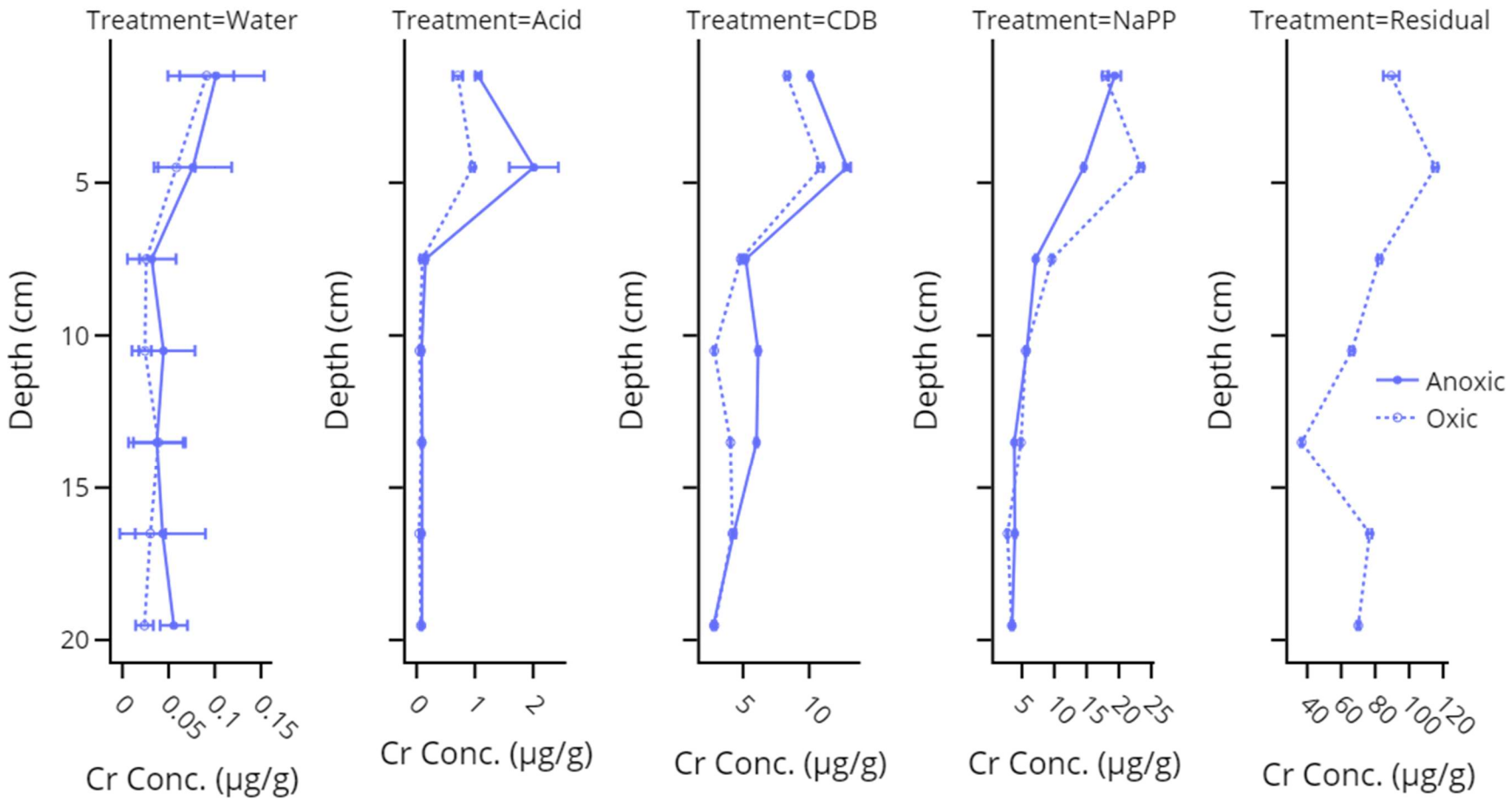

Figure B - 9: Concentrations of Cr in each extractant phase and under oxic and anoxic conditions at Steed Pond.

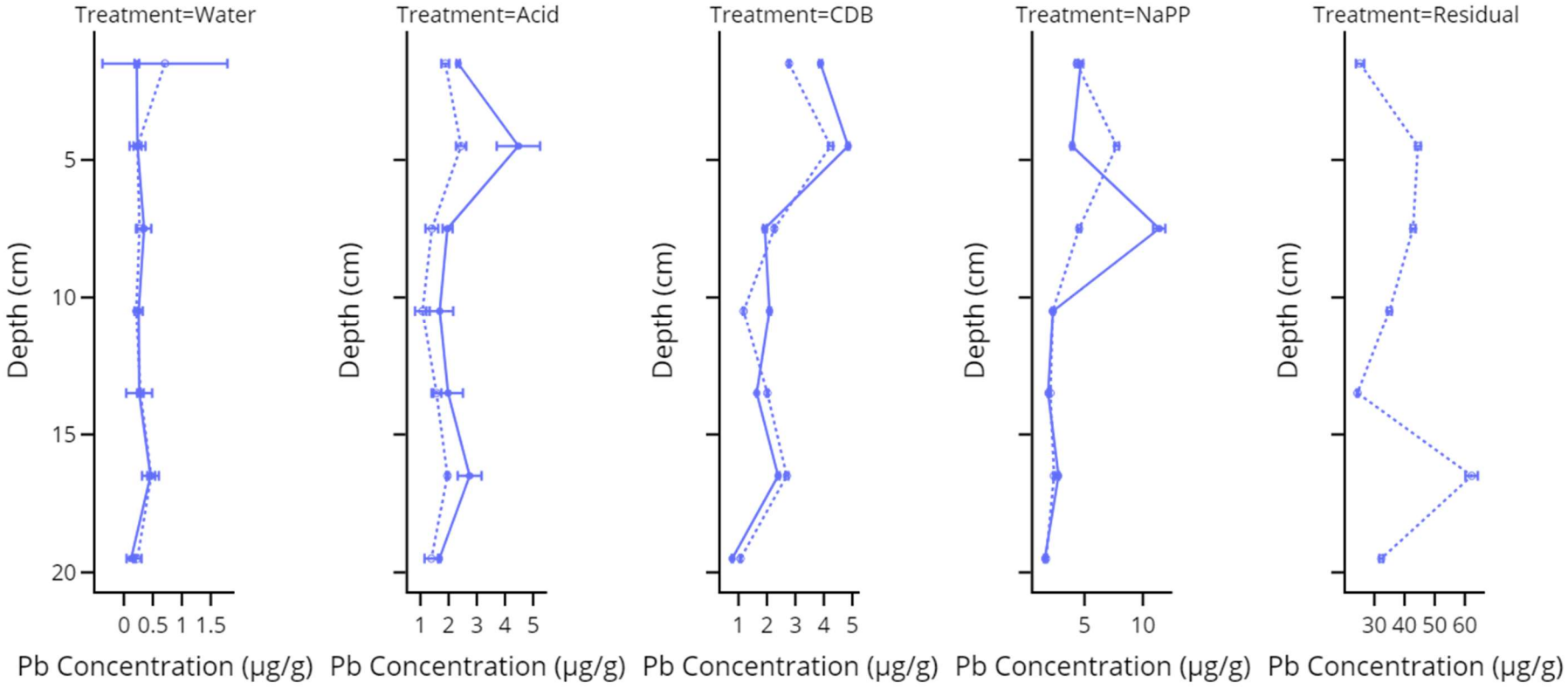

Figure B - 10: Concentrations of Pb in each extractant phase and under oxic and anoxic conditions at Steed Pond.

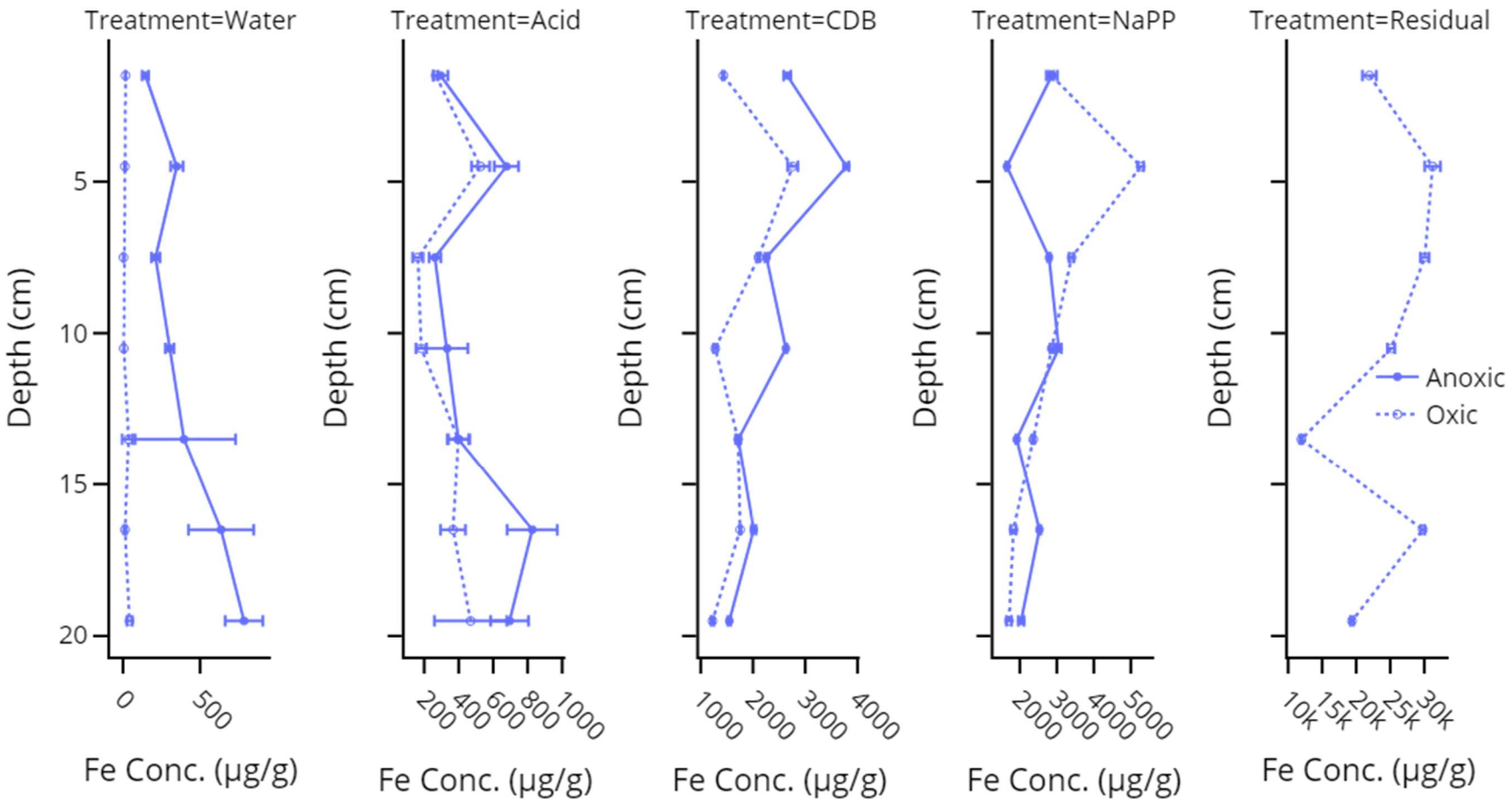

Figure B - 11: Concentrations of Fe in each extractant phase and under oxic and anoxic conditions at Steed Pond.

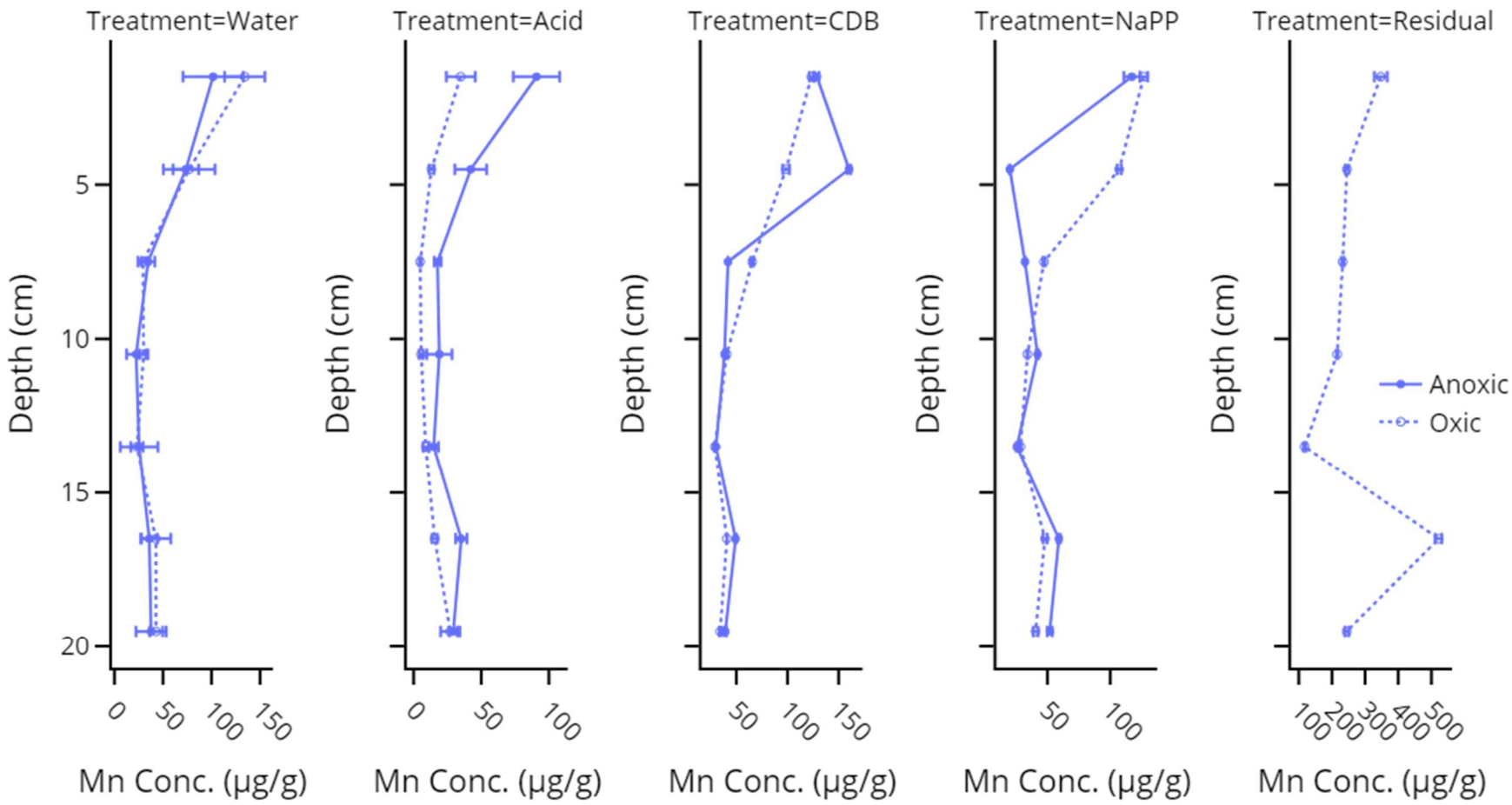

Figure B - 12: Concentrations of Mn in each extractant phase and under oxic and anoxic conditions at Steed Pond.

D. MOBILE URANIUM & NICKEL SOLIDS IN A CONTAMINATED WETLAND OVER THREE SEASONS: STREAMBANK EROSION MOVES MORE METAL THAN IRON-ORGANIC MATTER FLOCS

Figure C - 1: Beaver Pond sampling site, with piezometer (left pipe), stream gage (right pipe, protruding into stream channel), and rhizon sippers visible.

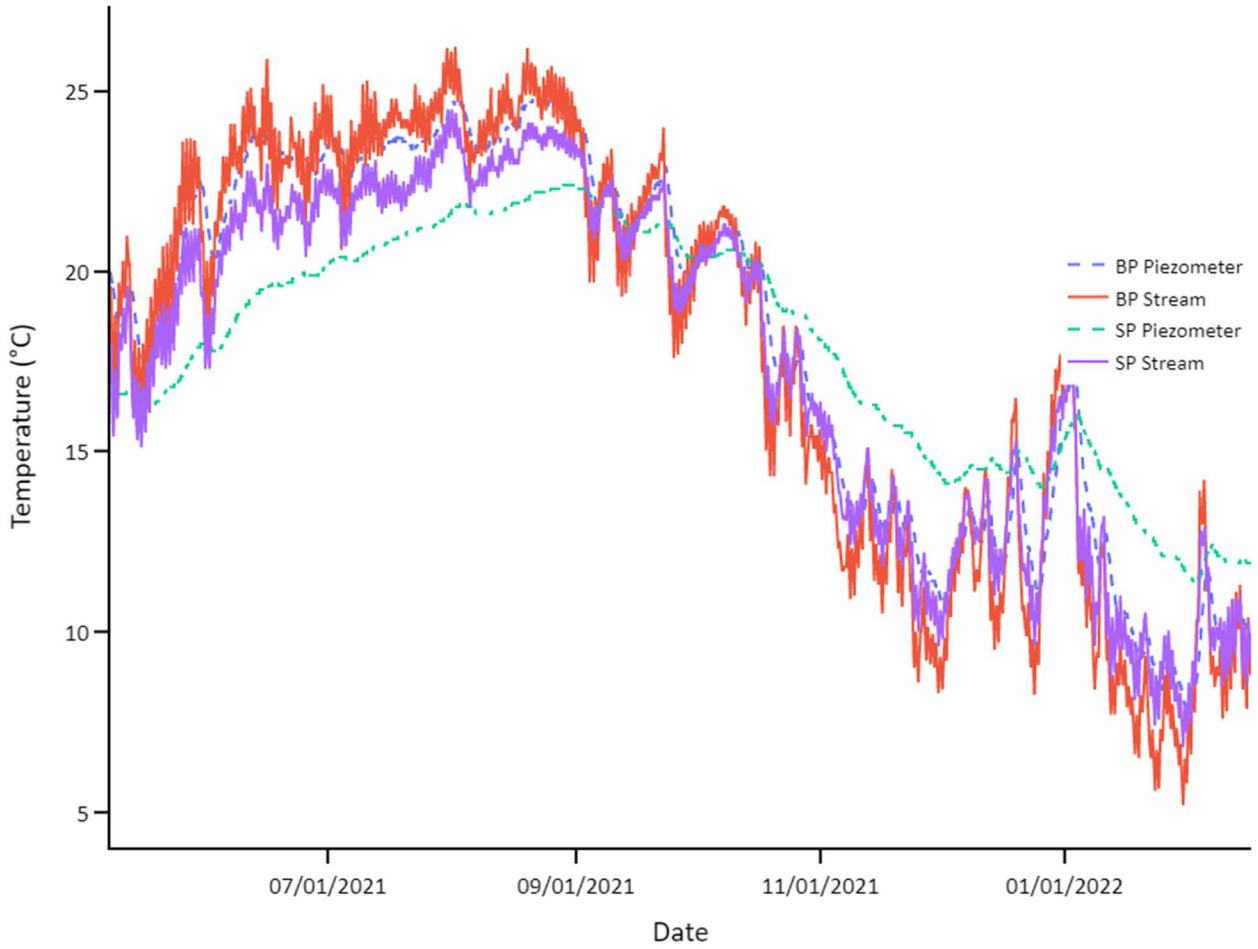

Figure C - 2: Temperatures in Beaver Pond and Steed Pond piezometers and stream gages.

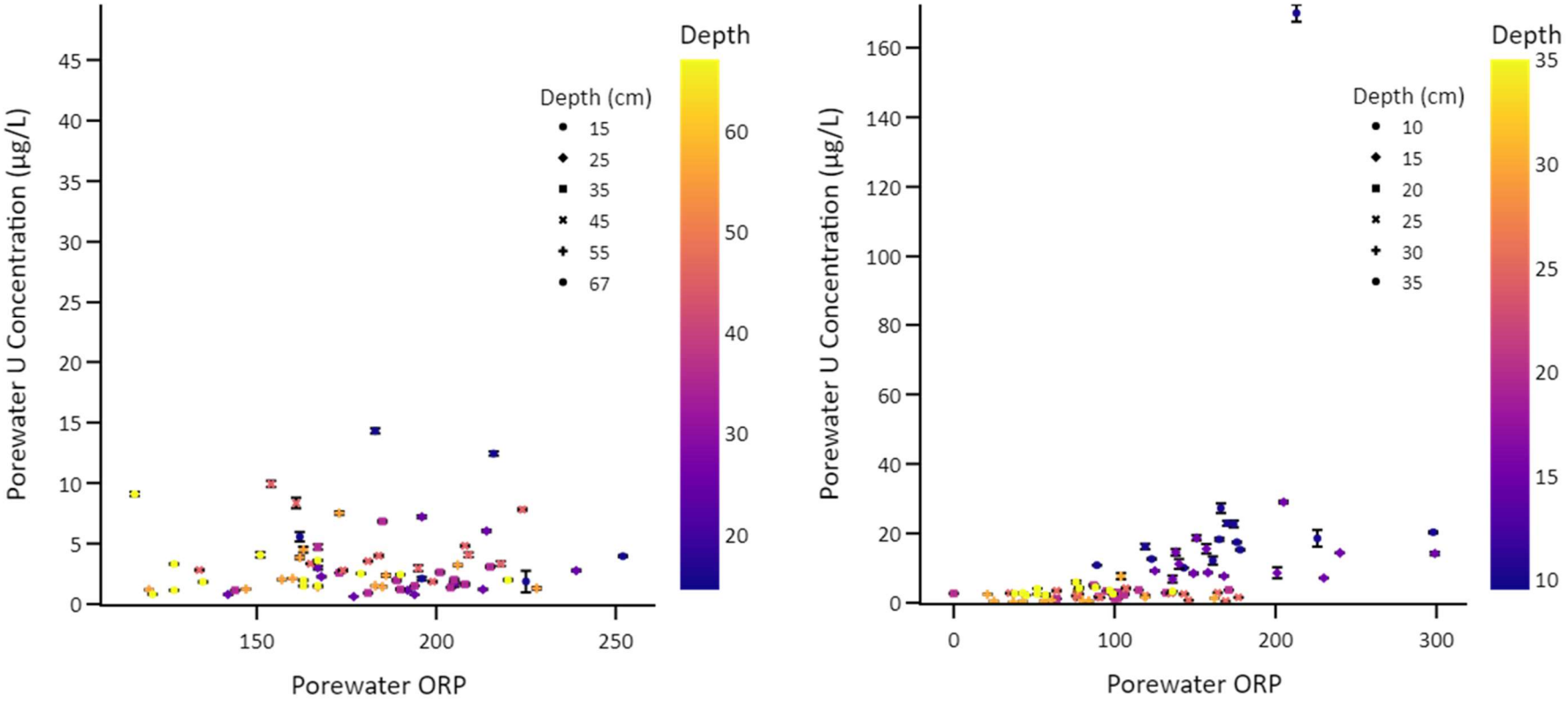

Figure C - 3: Uranium concentrations as a function of porewater ORP in Beaver Pond (left) and Steed Pond (right).

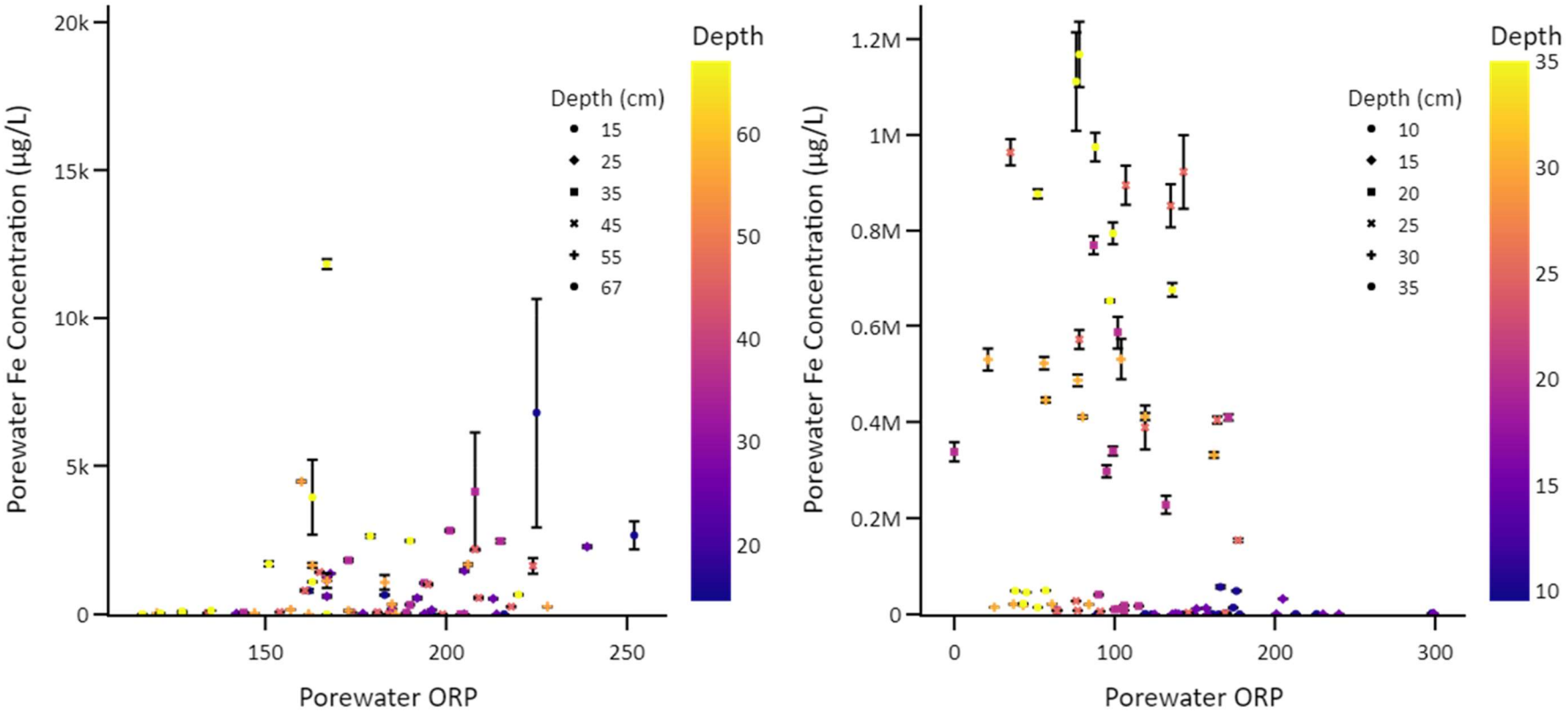

Figure C - 4: Iron concentrations as a function of porewater ORP in Beaver Pond (left) and Steed Pond (right).

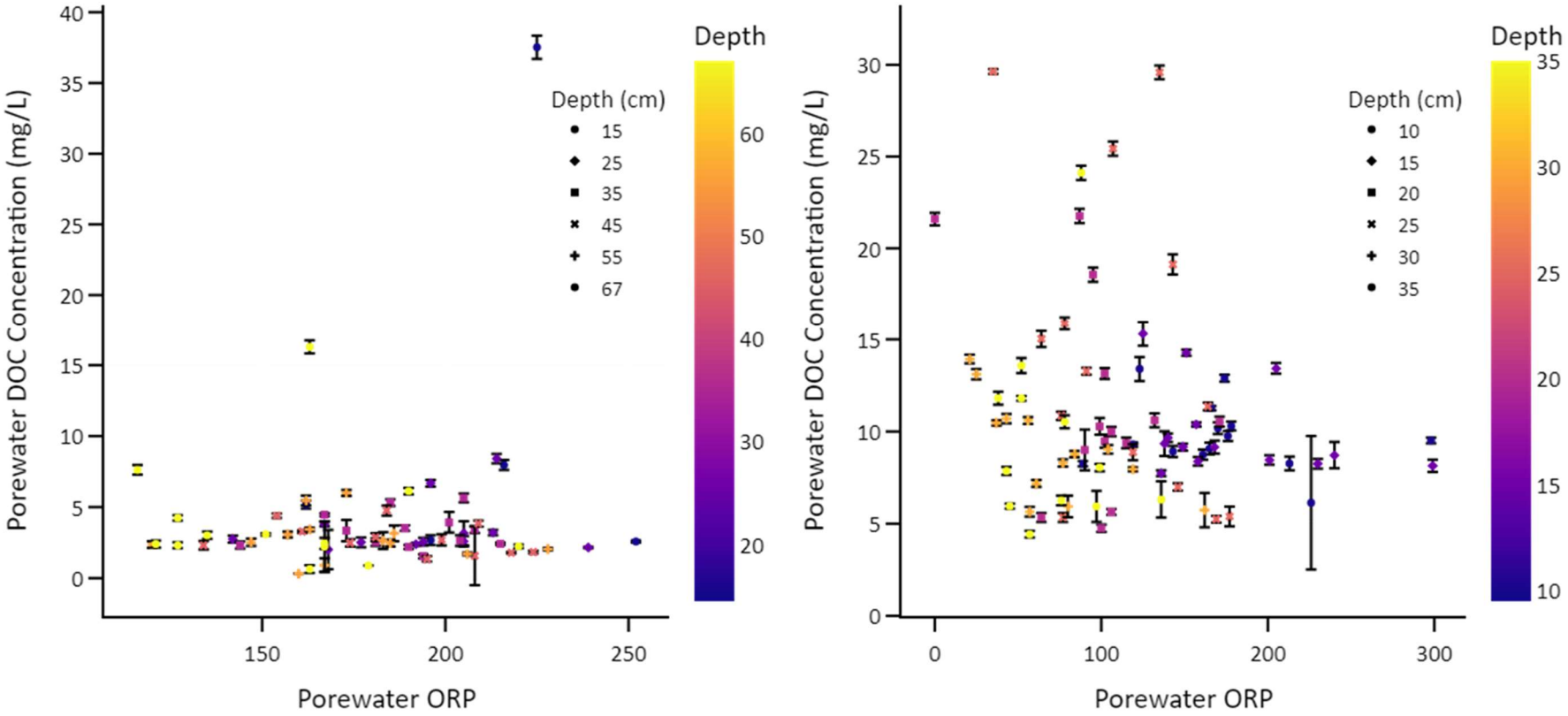

Figure C - 5: Dissolved organic carbon concentrations as a function of porewater ORP in Beaver Pond (left) and Steed Pond (right).

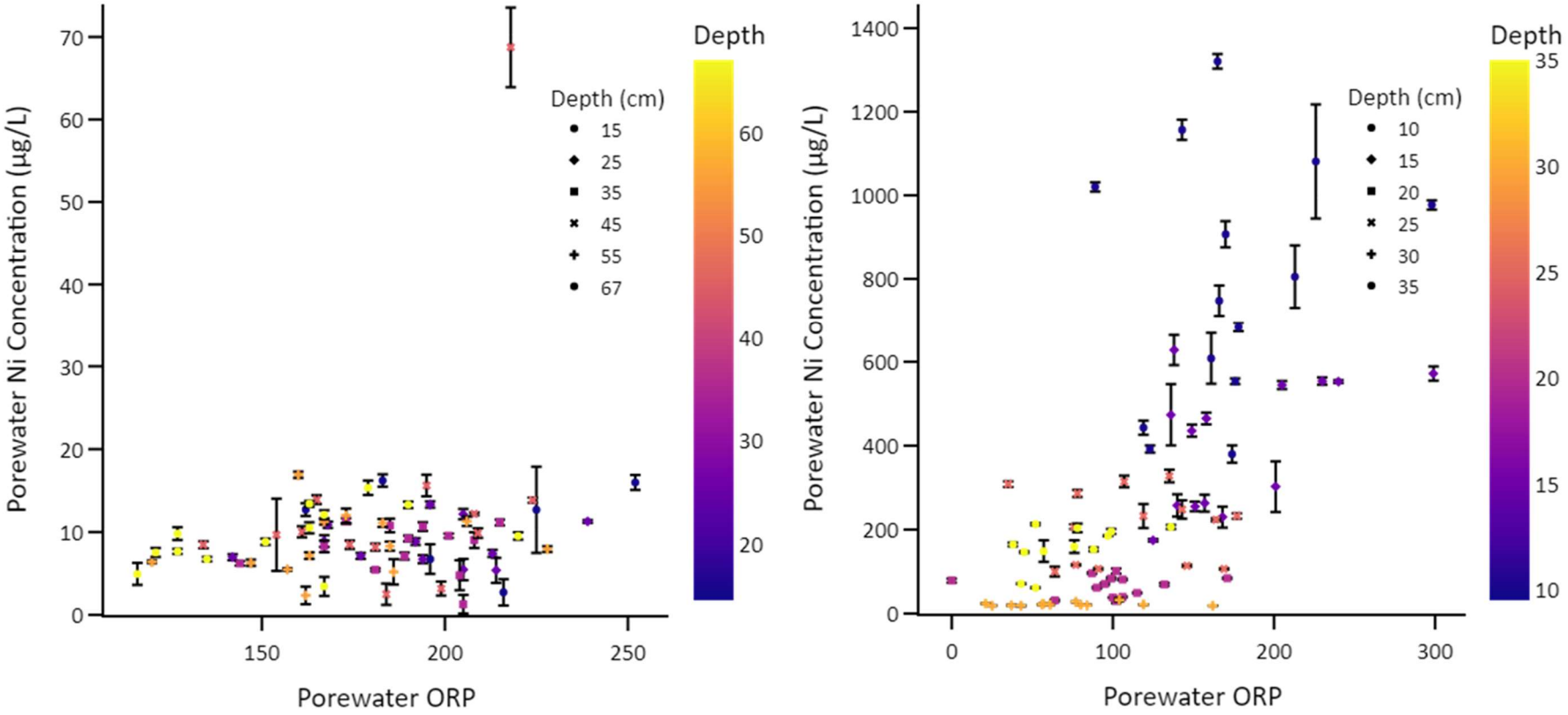

Figure C - 6: Nickel concentrations as a function of porewater ORP in Beaver Pond (left) and Steed Pond (right).

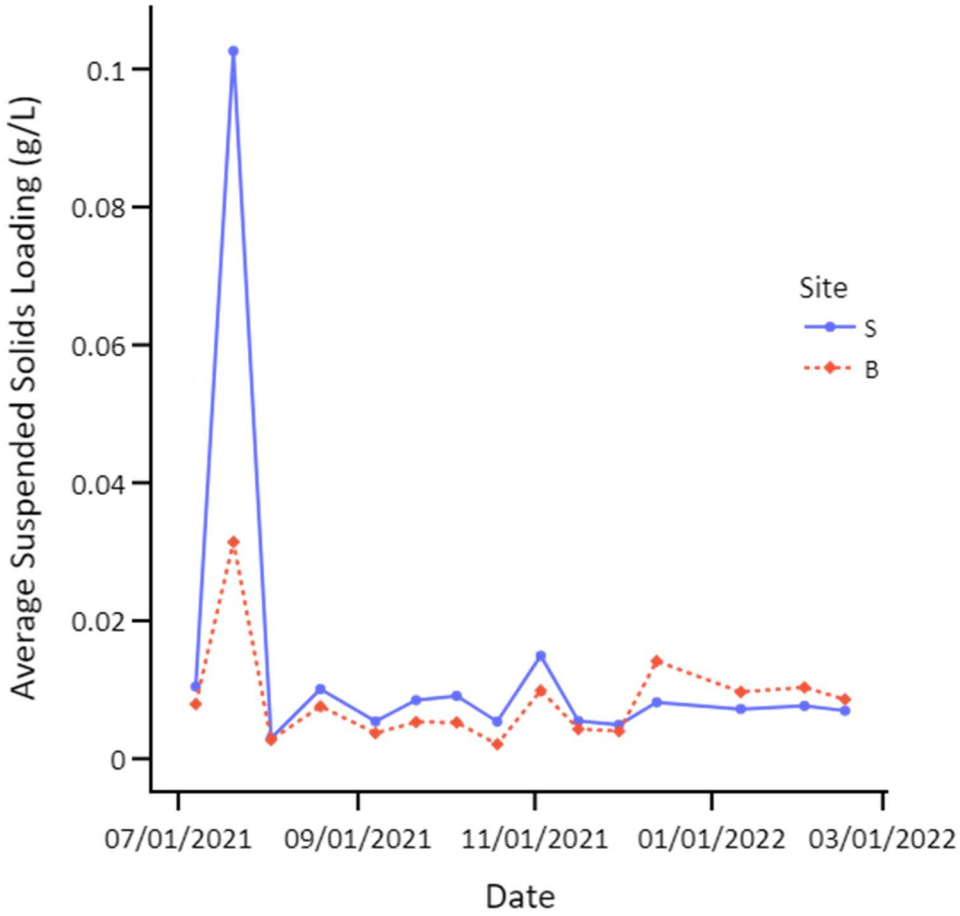

Figure C - 7: Suspended solids loading at Steed Pond and Beaver Pond over time.

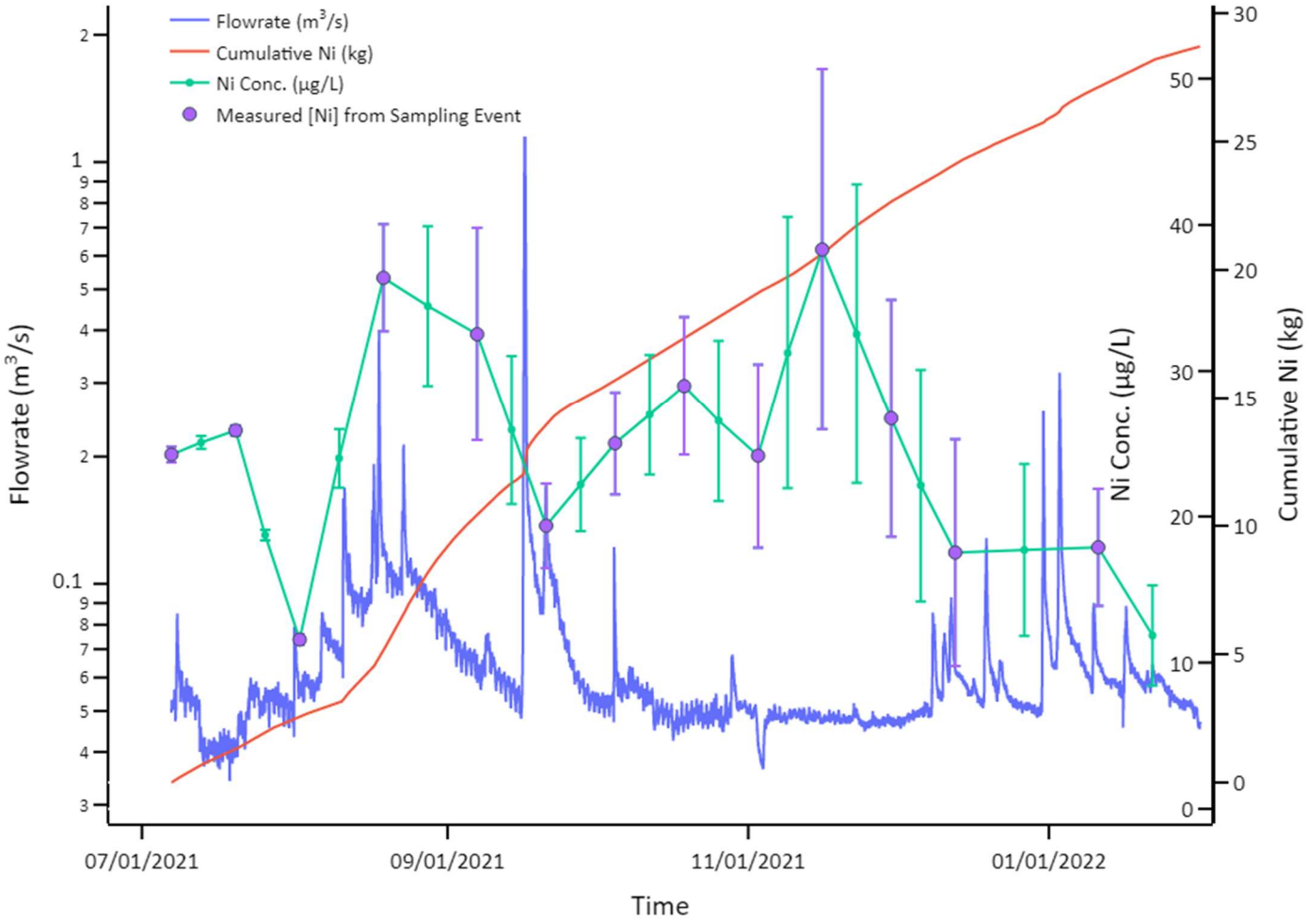

Figure C - 8: Cumulative Ni transport from Steed Pond.